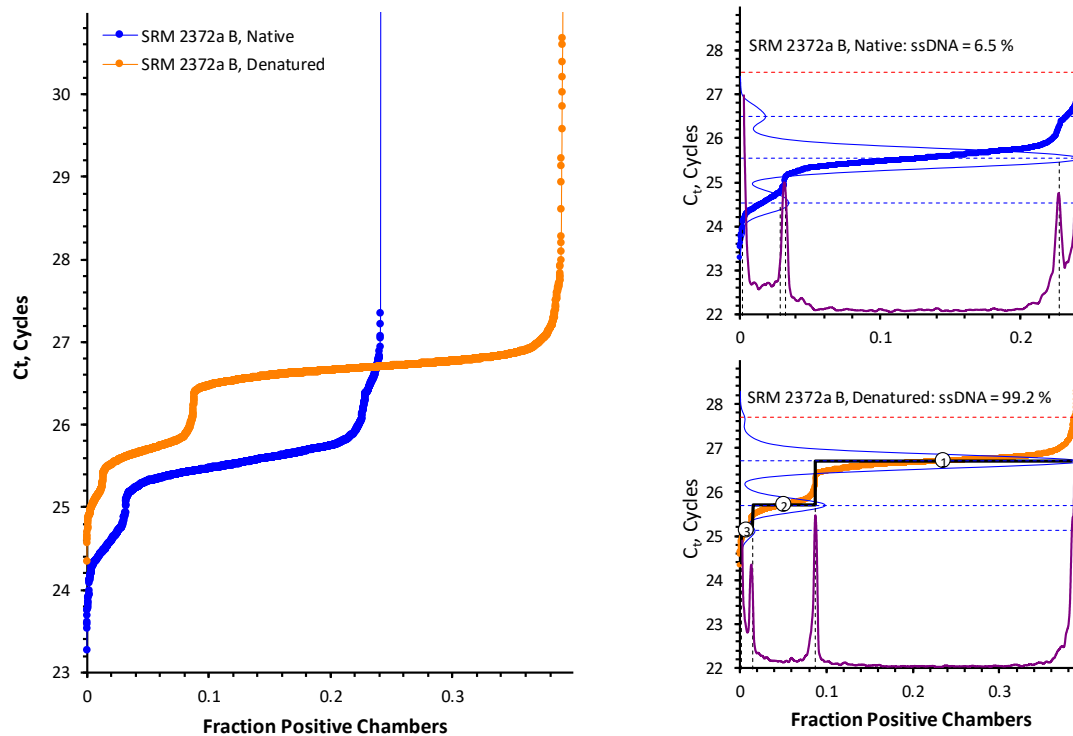


NIST Special Publication 1200-27

Evaluation of Methods for Assessing the Proportion of Single-Stranded Nuclear DNA in Human Blood Extracts

Margaret C. Kline
David L. Duewer

This publication is available free of charge from:
<https://doi.org/10.6028/NIST.SP.1200-27>



NIST Special Publication 1200-27

**Evaluation of Methods for Assessing the
Proportion of Single-Stranded Nuclear DNA
in Human Blood Extracts**

Margaret C. Kline
*Biomolecular Measurement Division
Material Measurement Laboratory*

David L. Duewer
*Chemical Sciences Division
Material Measurement Laboratory*

This publication is available free of charge from:
<https://doi.org/10.6028/NIST.SP.1200-27>

May 2019



U.S. Department of Commerce
Wilbur L. Ross, Jr., Secretary

National Institute of Standards and Technology
Walter Copan, NIST Director and Undersecretary of Commerce for Standards and Technology

Certain commercial entities, equipment, or materials may be identified in this document to describe an experimental procedure or concept adequately. Such identification is not intended to imply recommendation or endorsement by the National Institute of Standards and Technology, nor is it intended to imply that the entities, materials, or equipment are necessarily the best available for the purpose.

Publications in the SP 1200 subseries include written procedural methods in the design and implementation of experiments that ensure successful replication of results by others. Publications may include detailed procedures, lists of required equipment and instruments, information on safety precautions, the calculation of results and reporting standards.

National Institute of Standards and Technology Special Publication 1200-27
Natl. Inst. Stand. Technol. Spec. Publ. 1200-27, 84 pages (May 2019)
CODEN: NSPUE2

This publication is available free of charge from:
<https://doi.org/10.6028/NIST.SP.1200-27>

Abstract

This report documents our evaluation of three digital PCR (dPCR)-based methods for estimating the proportion, if any, of single-stranded DNA (ssDNA) in a sample that is believed to be mostly double-stranded DNA (dsDNA). These methods are: 1) a modification of a published real-time chamber-digital PCR (cdPCR) method, 2) comparing droplet-digital (ddPCR) results for native samples with those of an aliquot that has been gently heat-denatured, and 3) comparing ddPCR results for native samples with those of an aliquot in which dsDNA entities have been enzymatically rendered non-amplifiable. The cdPCR method requires use of exceptionally efficient PCR assays and appears to be insensitive to ssDNA proportions less than about 8 %. The denaturation/native comparison does not provide a unique estimate of ssDNA proportion but rather an upper limit. The enzymatic method requires careful choice and evaluation of restriction enzyme and PCR assay but has the potential to provide metrologically traceable estimates of the proportion of ssDNA.

Key words

chamber digital PCR (cdPCR); denaturation; deoxyribose nucleic acid (DNA) double-stranded DNA (dsDNA); droplet digital PCR (ddPCR); human nuclear DNA (nDNA); single-stranded DNA (ssDNA); Standard Reference Material (SRM); SRM 2372 Human DNA Quantitation Standard; SRM 2372a Human DNA Quantitation Standard.

Table of Contents

Abstract	i
Key words	i
Table of Contents	ii
List of Tables	iii
List of Figures	iv
Glossary	v
Symbols	v
1. Introduction	1
1.1. Materials	2
1.1.1. Safety.....	2
1.1.2. Processing.....	3
1.1.3. SRM 2372 Component B	3
1.1.4. SRM 2372a Component B	3
1.1.5. Why These Materials.....	3
1.2. Assays.....	5
1.3. dPCR	8
1.3.1. Chamber-Digital PCR (cdPCR)	8
1.3.2. Droplet-Digital PCR (ddPCR).....	14
1.4. Quantifying “Proportion”	15
1.5. Correcting DNA Mass Concentration Estimates.....	15
2. Heat Denaturation	16
2.1. Temperature and Duration.....	16
2.2. Choice of Conditions.....	18
2.2.1. Evolved Method for Heat-Denaturation.....	18
2.3. DNA Concentration.....	19
2.4. Renaturation	20
2.4.1. Evolved Method for Adding KCl.....	23
3. cdPCR Direct Assessment	24
3.1. Practicalities	25
3.1.1. Late Starters.....	25
3.1.2. One-Cycle Delayed Starts	25
3.1.3. Non-Ideal Target Dispersion.....	25
3.2. Staircase Analysis.....	26
3.3. Staircase Results for SRMs 2372 B and 2372a B	27
3.3.1. Quantitation	28
3.3.2. Uncertainty Analysis	28
3.4. Mixtures.....	31
3.4.1. Staircase Analysis for Mixtures of SRM 2372 B	31
3.4.2. Analysis of Mixtures of Native and Heat-Denatured Materials	33
3.4.3. Evolved Method for Preparing Mixtures.....	35
4. ddPCR Ratio Analysis	36
4.1. Limiting Values.....	36

4.1.1. Confounded Processes.....	38
4.2. Ratio Results for SRMs 2372 B and SRM 2372a B.....	38
4.3. Variability of the Heat-Denaturation Process	42
4.4. Correlations Between Measurement Results.....	42
4.5. SRM 2372 B Mixture	43
5. ddPCR Enzyme Analysis	46
5.1. Enzyme:Assay Combinations.....	46
5.1.1. Evolved Method for Preparing Restriction Enzyme Reactions.....	49
5.1.2. Loss of Entities Due to the Restriction Process	50
5.1.3. Evolved Method for Preparing Twice-Cut Reactions	54
5.1.4. Incubation Time	54
5.2. Enzyme:Assay Results	57
5.2.1. Performance Evaluation	62
5.2.2. Enzyme:Assay Design Considerations.....	64
5.3. SRMs 2372 B Mixture	65
5.4. Comparison of Enzyme:Assay Combinations.....	67
6. Comparison of Staircase with Enzyme Measurements.....	68
6.1. SRM 2372 B Mixture	68
6.2. Possible Platform Artifact	69
7. Summary	70
7.1. Method Evaluation	70
7.1.1. cdPCR Staircase Analysis	70
7.1.2. ddPCR Ratio Analysis.....	70
7.1.3. ddPCR Enzyme Analysis	70
7.2. Defining the Measurand	70
7.3. Adapting Methods for Other DNAs	70
8. Acknowledgements	72
9. References.....	72

List of Tables

Table 1. NIST-Developed Human nDNA Assays	7
Table 2. Changes in NEIF Assay with Salt Concentration and Time.....	22
Table 3. Recipe for Preparing 60 μ L of Samples in (0 to 400) mmol/L KCl	23
Table 4. cdPCR Analysis Results for SRM 2372 B.....	29
Table 5. cdPCR Analysis Results for SRM 2372a B.....	30
Table 6. cdPCR Staircase Results for SRM 2372 B Mixtures.....	33
Table 7. Recipe for Preparing 30 μ L each of (0, 20, 40, 80, 100) % Volumetric Mixtures ..	35
Table 8. ddPCR Ratio Analysis Results for Native and Heat-Denatured Samples	39
Table 9. ddPCR Ratio Results for SRM 2372 B Mixtures	44
Table 10. Nuclease Cut Sites for the Human nDNA dPCR Assays	47
Table 11. Restriction Enzymes.	48
Table 12. Recipe for 25 μ L Enzyme Reactions	49
Table 13. Size of Restriction Fragments Containing the Target Sequence of the Assay	51

Table 14. Enzyme Treatment Related Loss of Entities.....	53
Table 15. Changes with Enzyme Incubation Time.....	56
Table 16. ddPCR Analysis Results for Native and Heat-Denatured Samples a.....	60
Table 17. Summary of Enzyme:Assay Combinations Evaluated.....	64
Table 18. ddPCR Enzyme:Assay Results for SRM 2372 B Mixtures.....	66

List of Figures

Figure 1. Absorbance Spectra of SRM 2372 B and SRM 2372a B.....	4
Figure 2. Chromosomal Locations of NIST-Developed Human nDNA Assays.....	5
Figure 3. Relative Agreement Between NIST-Developed Human nDNA Assays.....	6
Figure 4. cdPCR Ogives for NIST Human nDNA Assays.....	10
Figure 5. Ogive Alignment.....	11
Figure 6. Summary Ogives for NIST Human nDNA Assays.....	11
Figure 7. Ogive Kernel Densities and First Derivatives.....	13
Figure 8. ddPCR Droplet Patterns for NIST Human nDNA Assays.....	14
Figure 9. Change in λ_1/λ_0 with Denaturation Temperature.....	17
Figure 10. Change in λ_1/λ_0 with Denaturation Duration.....	17
Figure 11. FlashGel of Native and Heat-Denatured SRM 2372 B and SRM 2372a B.....	18
Figure 12. Change in λ_0 , λ_1 , and λ_1/λ_0 with Dilution.....	19
Figure 13. Changes with Salt Concentration and Time for SRM 2372 B.....	20
Figure 14. Comparison of Observed and Idealized Ogives for SRM 2372 B.....	24
Figure 15. Exemplar Ogives for Native and Heat-Denatured B and aB.....	27
Figure 16. Staircase Analysis of Native and Heat-Denatured B and aB.....	28
Figure 17. Exemplar Ogives for Native SRM 2372 B Mixtures.....	31
Figure 18. Exemplar Staircase Analysis of SRM 2372 B Mixtures.....	32
Figure 19. Staircase Measured Vs Estimated Proportions of ssDNA.....	34
Figure 20. Limiting Values of $\varphi = f(p_0, \chi, \omega)$ Parameters as Functions of φ	37
Figure 21. p_0 As Functions of χ and ω when $\varphi = 1.75$	38
Figure 22. Summary of λ_0 , λ_1 , and φ	41
Figure 23. Correlations Between Materials Analyzed Together.....	43
Figure 24. Ratio Measured Vs Estimated Proportions of ssDNA.....	45
Figure 25. Effect of Restriction Conditions on ddPCR Results.....	50
Figure 26. FlashGels of Various Enzyme Treatments of SRM 2372 B.....	52
Figure 27. Effect of Incubation Time on Selected Enzyme:Assay Combinations.....	55
Figure 28. Summary of q_0 , ψ , and p_0 for B and aB.....	58
Figure 29. Correlation Between B and aB Values.....	59
Figure 30. Relationship Between p_0 and ψ	62
Figure 31. Rank-Ordered Mean(p_0 /Median) Values.....	63
Figure 32. Enzyme:Assay Vs Estimated Proportions of ssDNA.....	65
Figure 33. Comparison of two Enzyme:Assay Combinations Used in the Mixture Studies.....	67
Figure 34. ddPCR Enzyme Vs cdPCR Staircase Estimates.....	68
Figure 35. Effect of Restriction Without Cutting on cdPCR Results.....	69

Glossary

A	adenine, nucleic acid base
bp	basepair, two nucleic acid bases connected by hydrogen-bonds
cdPCR	chamber digital PCR
C	cytosine, nucleic acid base
CV	coefficient of variation (relative standard deviation, expressed in %)
ddPCR	droplet digital PCR
dPCR	digital PCR (platform independent)
DNA	deoxyribose nucleic acid
dsDNA	double-stranded DNA
EDTA	ethylenediaminetetraacetic acid
entity	an independently dispersing DNA fragment that contains one or more amplifiable target nucleotide sequences
G	guanine, nucleic acid base
nDNA	nuclear DNA
PCR	polymerase chain reaction
sham-restriction	enzyme digestion procedure using TE ⁻⁴ in place of the restriction enzyme
ssDNA	single-stranded DNA
T	thymine, nucleic acid base
TE ⁻⁴	10 mmol/L tris-HCl, 0.1 mmol/L EDTA, pH 8.0 buffer
tris-HCl	tris-(hydroxymethyl)aminomethane HCl

Symbols

0	designates a native sample
1	designates a heat-denatured sample
$C_{DNA,sample}$	desired concentration of DNA in sample, ng/ μ L
$C_{DNA,stock}$	concentration of DNA in stock material, ng/ μ L
$C_{KCl,sample}$	desired concentration of KCl in sample, mmol/L
$C_{KCl,stock}$	concentration of KCl in stock diluent, mmol/L
C_t	crossing threshold, the interpolated number of PCR amplification cycles required for a dPCR signal intensity to exceed a user-assigned level
e	total number of independently dispersing entities in a sample
e_0	e for a native sample
e_1	e for a heat-denatured sample
k	scalar constant
\ln	logarithm to the base e (2.71828...), “natural logarithm”
\log_2	logarithm to the base 2, “binary logarithm”
\log_{10}	logarithm to the base 10, “decadic logarithm”
Mean()	arithmetic mean of the set of values specified by the quantity within the ()
Median()	50 th percentile of the set of values specified by the quantity within the ()
N_d	number of dsDNA entities
N_e	number of entities (both dsDNA and ssDNA)
N_s	number of ssDNA entities
N_{tot}	the total number of available values

N_{use}	the number of values used to estimate a statistic
p	entity proportion of ssDNA in a sample, either as a fraction or percentage
p_0	p for a native sample
p_1	p for a heat-denatured sample,
q_0	$\lambda_0(\text{Enzyme})/\lambda_0$, a naïve estimate of the ssDNA entity fraction in a native sample without correcting for ssDNA loss during cutting
s	number of independently dispersing ssDNA entities in a sample
s_0	s for a native sample
s_1	s for a heat-denatured sample
v	volume fraction
v_0	v of a native sample
v_1	v of a heat-denatured sample
v_m	v of a mixture of m % heat-denatured with $(100-m)$ % native material
V_{DNA}	Volume of stock DNA material used to prepare sample, μL
V_{KCl}	Volume of KCl stock diluent used to prepare sample, μL
V_{TE}	Volume of TE^{-4} buffer used to prepare sample, μL
V_{total}	Desired sample volume, μL
x_i	i^{th} element of a vector of values
X	scalar constant
y_i	i^{th} element of a vector of transformed values
λ	copies per reaction vessel (chamber or droplet)
λ_0	λ of a native sample
$\lambda_0(\text{Enzyme})$	λ of an enzyme-treated native sample
λ_1	λ of a heat-denatured sample
$\lambda_1(\text{Enzyme})$	λ of an enzyme-treated heat-denatured sample
λ_v	λ of a $(1-v) + v$ volumetric mixture of native and heat-denatured samples
φ	λ_1/λ_0 , entity fraction of the number of entities in a sample after heat-denaturation
ψ	$\lambda_1(\text{Enzyme})/\lambda_1$, entity fraction of ssDNA in a heat-denatured sample that is rendered non-amplifiable by a restriction enzyme
χ	fraction of dsDNA converted to ssDNA by heat denaturation
ω	fraction of ssDNA entities rendered non-amplifiable or in-accessible by heat-denaturing

1. Introduction

The Digital Polymerase Chain Reaction (dPCR) has been asserted to be or to have the potential to be a “primary reference measurement procedure” (aka “primary method of measurement”) [1,2,3,4]. The international chemical metrology community has defined this concept as [1]:

“... a method having the highest metrological properties, whose operation can be completely described and understood, for which a complete uncertainty statement can be written down in terms of SI units”

where “SI” is the International System of Units, including the natural unit of enumeration (one) [5].

Beginning in 2013 we have evaluated dPCR-based assays for use in value-assigning the quantity of human nuclear DNA (nDNA) in blood extracts [6,7,8,9]. These studies established that, using multiple assays and both droplet dPCR (ddPCR) and real-time chamber dPCR (cdPCR) platforms, dPCR mass concentration results can be made metrologically traceable to the SI units of enumeration and volume. In 2018, we used dPCR methods to certify Standard Reference Material (SRM) 2372a Human DNA Quantitation Standard [10,11]. However, we recently became aware that our traceability model was incomplete: we and others have assumed that the DNA in our materials exists exclusively as double-stranded DNA (dsDNA) [12]. Establishing full metrological traceability for dPCR measurement values requires quantitative evaluation of this assumption. A reliable method for determining the presence of single-stranded DNA (ssDNA) in a predominantly dsDNA sample is needed to support the certification and stability monitoring of existing and future SRMs for DNA quantification.

In dPCR, DNA fragments are dispersed into separate reaction partitions (chambers or droplets). After PCR amplification to an assay’s terminal plateau phase, partitions with an above-threshold signal are considered “positive” while those below-threshold are considered “negative”. It is assumed that the positive partitions originally held at least one DNA fragment containing the assay’s target nucleotide sequence. While DNA in intact cells is (almost always) exclusively dsDNA, extraction processes and storage conditions have the potential to denature extracted dsDNA to ssDNA [13]. dsDNA fragments contain two target sequences that disperse as a single entity. If dsDNA fragments are converted to two ssDNA fragments, the number of independently dispersing entities will increase by a factor of two, biasing the dPCR results.

Optical absorbance at 260 nm is quantitatively related to the strength of interactions among the aromatic bonds of neighboring nucleotides [14], with minimum absorbance when the bases are tightly coiled and at maximum when the bases are completely disassociated. This phenomenon is known as hypochromism [15]. When stored “at physiological pH, the intra-strand repulsion between the negatively charged phosphate groups forces the double helix into more rigid rodlike conformation ... furthermore, the repulsion between phosphate groups on opposite strands tends to separate the complementary strands” [16]. While sometimes asserted to enable accurate quantitation of DNA [17], the quantity measured by

spectrophotometric methods is thus related to the tertiary structure of the entities but not necessarily their number.

Circular dichroism spectroscopy is sensitive to the conformational structures of DNA in solution [18], and different DNA configurations migrate differentially in agarose gel electrophoresis [19]. Both techniques have been used to qualitatively discriminate ssDNA from dsDNA in “pure” single-sequence materials, but neither technique has been demonstrated to quantify small proportions of ssDNA in a complex, multi-chromosome genomic material.

A real-time cdPCR technique has been described that can estimate the proportion of ssDNA entities in plasmid DNA from the distribution of the reaction curve crossing-thresholds (C_t) [12]. However, this method was not demonstrated to be applicable to complex genomic samples.

The following sections document the DNA extracts used in the studies, the spectrophotometric behavior of these materials, and three dPCR-based methods for estimating the proportion, if any, of ssDNA in a sample. These methods are: 1) a modification of the real-time cdPCR method, 2) comparing ddPCR results for native samples with those of an aliquot that has been gently denatured, and 3) comparing ddPCR results for native samples with those of an aliquot in which dsDNA entities have been enzymatically rendered non-amplifiable. The cdPCR method requires use of exceptionally efficient PCR assays and is currently insensitive to ssDNA proportions less than about 8 %. The denaturation/native comparison does not provide a unique estimate of ssDNA proportion but rather an upper limit. The enzymatic method requires careful choice and evaluation of restriction enzyme and PCR assay but has the potential to provide metrologically traceable estimates of ssDNA proportion.

1.1. Materials

Each unit of SRM 2372 and its replacement, SRM 2372a, delivered three human genomic extracts in aqueous solution. For both SRMs, these extracts are designated as components A, B, and C. The human DNA materials used in these studies, SRM 2372 component B (“B”) and SRM 2372a component B (“aB”), were extracted from the white blood cell component of human buffy coat cells using a modified “salting out” procedure [20]. These two materials were prepared from anonymized female donor tissues obtained from commercial sources. Both SRMs were developed after appropriate human subjects’ research determinations by NIST.

1.1.1. Safety

Every donor unit used in the preparation of B or aB was tested by FDA-licensed tests and found to be negative for all required tests available at the time of purchase. However, no known test method can offer complete assurance that infectious agents were absent. Accordingly, these materials were handled at the Biosafety Level 2. All solutions derived from these materials were handled at the Biosafety Level 1 and disposed of in accordance with local, state, and federal regulations.

1.1.2. Processing

The extracted DNAs were air-dried in a laminar flow hood and stored in perfluoroalkoxy fluoropolymer (PFA) containers at 4 °C prior to solubilization in 10 mmol/L tris-(hydroxymethyl)aminomethane HCl (Tris-HCl), 0.1 mmol/L ethylenediaminetetraacetic acid (EDTA), pH 8.0 (TE⁻⁴, also called 0.1X TE) buffer. The materials were equilibrated at 4 °C over a period of several weeks until visual inspection indicated that all solids had completely disappeared into solution. Subsets of these primary stocks were further diluted with TE⁻⁴ to provide suitable volumes of approximately 50 ng/μL DNA. Both the 50 ng/μL production materials and residual primary stocks were stored in PFA containers at 4 °C. Just prior to vialing, the production materials were brought to room temperature inside a laminar flow hood and gently mixed. See [10, 21] for further details.

1.1.3. SRM 2372 Component B

The DNA for the multi-donor B was isolated in 2006, prepared as described above, transferred in 110 μL aliquots into sterile polypropylene vials, and stored at 4 °C. Gel electrophoresis conducted in mid-2015 indicated that most of the DNA was sufficiently large to not migrate into the gel and the remainder had electrophoretic mobilities consistent with lengths greater than 10,000 bp [7].

About 50 vials of B were produced in excess and were available for study after the supplies of SRM 2372 Human DNA Quantitation Standard were exhausted in May 2017. In early 2018 measurements were made of the liquid volume in these vials. Over the more than 10 y storage (7.1 ± 0.3) % of the TE⁻⁴ buffer had evaporated. The remaining liquid in these vials was combined and stored in a PFA container at 4 °C and used as needed in our studies.

A relatively large volume of the primary stock used to produce SRM 2372 component B has been held in a PFA container at 4 °C since October 2006. This undiluted B (“UB”) material was used in place of B for studies that required large volumes of material.

1.1.4. SRM 2372a Component B

The DNA for the single-donor aB material was isolated in late 2016, prepared as described above, and in mid-2017 mostly transferred in 55 μL aliquots into sterile polypropylene vials. The aB extract solution was prepared in excess, with a small volume remaining after vialing. The excess solution was stored in a PFA container at 4 °C and used as needed in our studies.

1.1.5. Why These Materials

The certified values for the SRM 2372 components were the absorbance (technically, “decadic attenuation”) of the native materials at several wavelengths. By widely accepted convention, an aqueous DNA solution having an absorbance of 1.0 at 260 nm corresponds to a mass concentration of DNA of 50 ng/μL for dsDNA and (37 to 40) ng/μL for ssDNA [22]. By 2012 the absorbance in several units of SRM 2372 had somewhat variably increased outside of the uncertainty intervals certified in October 2006. After establishing that these changes likely resulted from changes in tertiary structure, in 2013 the SRM was re-certified based upon the absorbance of the materials after sodium hydroxide (NaOH) denaturing [23].

Figure 1 compares the native and NaOH-denatured absorbance spectra of B and aB between 220 nm and 320 nm. By late 2017 the absorbance of native B at 260 nm approached that of the NaOH-denatured material. The absorbance of the native aB had not appreciably increased after 10 months of storage at 4 °C.

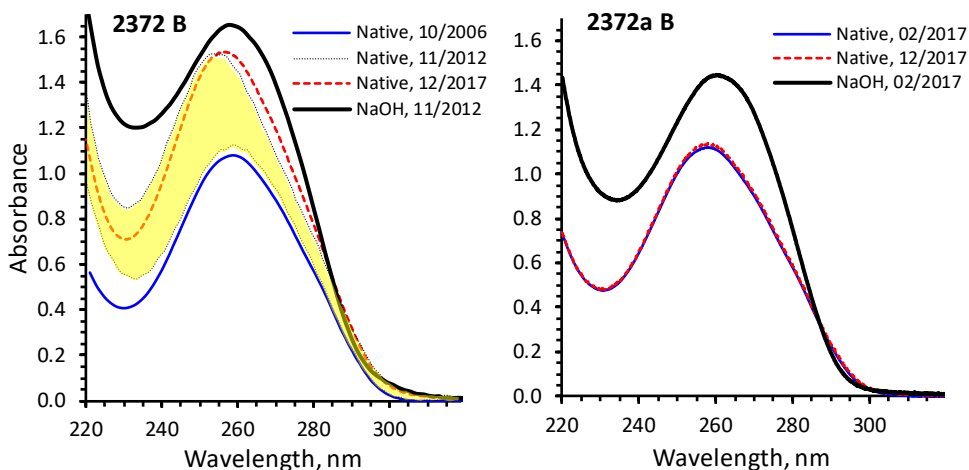


Figure 1. Absorbance Spectra of SRM 2372 B and SRM 2372a B

These plots display UV/vis absorption spectra for SRM 2372 Component B and SRM 2372a Component B. The solid black lines report the dilution-adjusted absorbance spectra of the NaOH-denatured materials; the blue lines report the spectra of the native materials shortly after extraction, and the red lines report the native spectra in 12/2017. In the subplot to the left, the yellow shading bracketed by thin dotted lines represents the range of spectra observed for individual units of SRM 2372 B in 11/2012. The SRM 2372 B spectrum of 12/2017 has been adjusted for the observed 10 % evaporation.

Shortly after extraction, the absorbances at 260 nm were 1.073 ± 0.031 for B and about 1.11 ± 0.04 for aB, giving a B/aB absorbance ratio of 0.97 ± 0.04 . In late 2017 the dilution-adjusted ddPCR entity per droplet was $(1.42 \pm 0.02)/(1.25 \pm 0.03)$, giving a B/aB entity ratio of 1.14 ± 0.03 [10]. If the initial 260 nm absorbance of the native materials is proportional to the dsDNA entity concentration, then the ratio should have been about $2 \times 0.97/1.11 = 1.7$ had B become mostly converted from dsDNA to ssDNA. This suggests that most entities in B disperse as dsDNA, but that some small proportion has denatured to ssDNA. If the initial absorbance is proportional to dsDNA concentration, then the ratio of the ratios suggests that the entity concentration of B has increased by a factor of about $(1.14 \pm 0.03)/(0.97 \pm 0.04) = 1.18 \pm 0.06$; i.e., that by this measure about 18 % of the B dsDNA has denatured.

The absence of appreciable spectrophotometric change in aB over the 10 months since extraction suggests that it contains little to no ssDNA.

These materials were therefore chosen for intensive study because: 1) they promised to contain different proportions of ssDNA, 2) adequate quantities were available, 3) SRM 2372a is NIST's current DNA quantitation standard, and 4) understanding the ddPCR behavior of these SRM-related materials contributes to the metrological characterization of future DNA quantitation certified reference materials.

1.2. Assays

We developed 10 human nDNA qPCR assays to enable confident assessment of nDNA concentration in the SRM 2372a component materials. As shown in Figure 2, three assays target nucleotide sequences at different locations on chromosome 2 (near the centromere, middle of the short arm, and at the tip of the short arm) to evaluate whether the target location impacts dPCR results. The other seven assays target locations on different chromosomes to check that results for individual chromosomes are in one-to-one correspondence with the number of genomes.

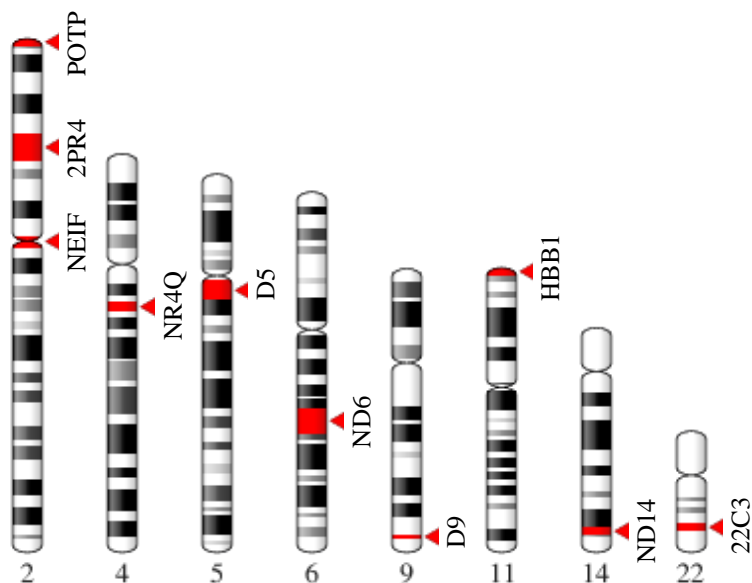


Figure 2. Chromosomal Locations of NIST-Developed Human nDNA Assays.

Figure 3 summarizes the relative performances of the assays for the SRM 2372a ddPCR certification measurements. Within measurement uncertainties, all 10 assays provided the same quantitative values.

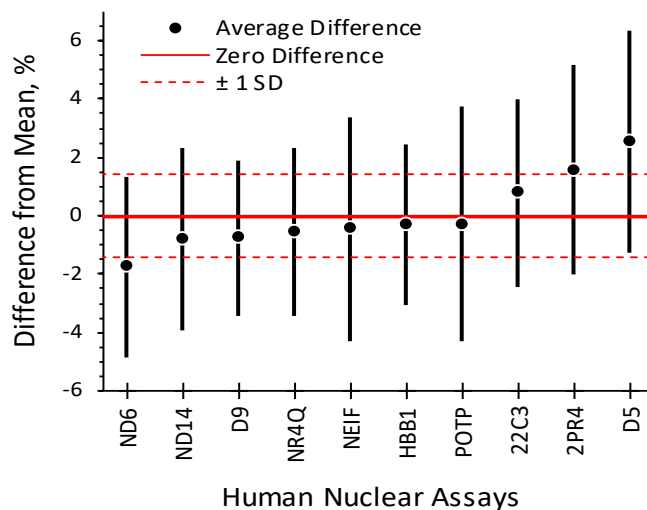


Figure 3. Relative Agreement Between NIST-Developed Human nDNA Assays

The dots denote mean relative differences among 10 assays averaged for the 3 SRM 2372a components, estimated as $\%d_i = 100(\sum_{j=1}^3(\lambda_{ij} - 1)/\bar{\lambda}_j)/3$, where λ_{ij} is the number of entities per droplet for the i^{th} assay of the j^{th} component and $\bar{\lambda}_j$ is the grand mean for the component. The vertical “bars” span ± 1 standard uncertainty about each difference. The thin red dashed horizontal lines bound an approximate 68 % confidence interval around the zero-difference line.

Table 1 details the name, location, primer and probe sequences, and amplicon length of the dPCR assays used in our studies.

Table 1. NIST-Developed Human nDNA Assays

Assay Target	Chromosome Band Accession #	Primers and Probe ^a	Amplicon Length, bp
NEIF Gene EIF5B	Chr 2 p11.1-q11.1 NC_000002.12	F GCCAAACTTCAGCCTTCTCTTC R CTCTGGCAACATTTCACTACA P ^{B+} TCATGCAGTTGTCAGAAGCTG	67
2PR4 Gene RPS27A	Chr 2 p16 NC_000002.12	F CGGGTTTGGGTTTCAGGTCTT R TGCTACAATGAAAACATTCAGAAAGTCT P ^B TTTGTCTACCACTTGCAAAGCTGGCCTTT	97
POTP STR TPOX	Chr 2 p25.3 NC_000002.12	F CCACCTTCCTCTGCTCACTTT R ACATGGGTTTTGCCTTTGG P ^T CACCAACTGAAATATG	60
NR4Q Gene DCK	Chr 4 q13.3-q21.1 NC_000004.12	F TGGTGGGAATGTTCTTCAGATGA R TCGACTGAGACAGGCATATGTT P ^{B+} TGTATGAGAAACCTGAACGATGGT	83
D5 STR D5S2500	Chr 5 q11.2 NC_000005.10	F TTCATACAGGCAAGCAATGCAT R CTTAAAGGGTAAATGTTTGAGTAATAGAT P ^T ATAATATCAGGGTAAACAGGG	75
ND6 STR D6S474	Chr 6 q21-22 NC_000006.12	F GCATGGCTGAGTCTAAGTTCAAAG R GCAGCCTCAGGGTTCTCAA P ^T CCCAGAACCAAGGAAGATGGT	82
D9 STR D9S2157	Chr 9 q34.2 NC_000009.12	F GGCTTTGCTGGGTTACTGCTT R GGACCACAGCACATCAGTCACT P ^T CAGGGCACATGAAT	60
HBB1 Gene HBB	Chr 11 p15.5 NC_000011.10	F GCTGAGGGTTTGAAGTCCAACCT R GGTCTAAGTGATGACAGCCGTACCT P ^T AGCCAGTGCCAGAAGAGCCAAGGA	76
ND14 STR D14S1434	Chr 14 q32.13C NC_000014.9	F TCCACCACTGGGTTCTATAGTTC R GGCTGGGAAGTCCCACAATC P ^{B+} TCAGACTGAATCACACCATCAG	109
22C3 Gene PMM1	Chr 22 q13.2 NC_000022.10	F CCCCTAAGAGGTCTGTTGTGTTG R AGGTCTGGTGGCTTCTCCAAT P ^B CAAATCACCTGAGGTCAAGGCCAGAACA	78

a) F = Forward primer, R = Reverse primer,
P^B = Blackhole quencher probe, P^{B+} = Blackhole Plus quencher probe, P^T = Taqman MGB probe.
A = adenine, C = cytosine, G = guanine, T = thymine

1.3. dPCR

dPCR technologies enable estimation of the proportion of independently dispersing entities that contain one or more target nucleotide sequences. All dPCR platforms partition the sample into multiple isolated reaction volumes, amplify target DNA until the signal from even single entities can be detected, and after the final amplification cycle determine the proportion of volumes with above threshold signal, $N_{\text{pos}}/N_{\text{tot}}$, where N_{pos} is the number of volumes with above-threshold signal and N_{tot} is the total number counted. When the entity concentration in a sample is such that N_{pos} is greater than zero and smaller than N_{tot} , then the average number of entities per reaction volume, λ , can be modeled with the Poisson relationship, $\lambda = -\ln(1 - N_{\text{pos}}/N_{\text{tot}})$, where “ln” is the natural logarithm. All else being equal, the greater the number of reaction volumes per sample the more precise the measurement.

The Poisson model may yield significantly biased estimates when λ is large [12]. While the definition of “large” apparently depends on the platform used and the DNA evaluated, for human nDNA we have observed the onset of non-linearity at λ greater than about 0.8 entity per reaction volume [10]. In the studies reported here we use dilutions of native samples designed to give λ in the range of (0.2 to 0.4) entities per volume.

This report presents results from two dPCR platforms: 1) ddPCR and 2) real-time cdPCR. ddPCR systems disperse an aqueous sample into many thousands to millions of droplets suspended in a body of oil, amplify the sample through a set number of cycles, then measure fluorescence intensity of a large subset of droplets having a desired size. Evaluating large numbers of droplets provides excellent measurement precision, but at the cost of only evaluating the droplet signals after amplification is complete. (There are experimental ddPCR systems that follow the development of fluorescence signal in individual droplets, but such systems were not available to us.) In contrast, cdPCR systems disperse a sample into a relatively small number of reaction chambers having fixed locations. This enables following the growth of fluorescence signals as functions of amplification cycle, at the cost of limited measurement precision.

1.3.1. Chamber-Digital PCR (cdPCR)

We use a Fluidigm BioMark (South San Francisco, CA USA) real time cdPCR system with BioMark 48.770 digital arrays. Each analysis uses a disposable microfluidic device (“chip”) that has 48 panels of 770 reaction chambers, each chamber of nominal volume 0.85 nL. For our studies, samples were amplified using a temperature ramp of 2 °C/s, an initial hold at 95 °C for 10 min then 60 cycles of 95 °C for 15 s with annealing at 61 °C for 60 s.

This real-time cdPCR system monitors fluorescence intensity in all the chip’s reaction chambers at the completion of each amplification cycle. This enables characterization of the amplification curves for the individual chambers, which in turn can (with very efficient PCR assays) enable direct enumeration of the proportion of chambers that contain (0, 1, 2, 3, ...) entities.

We previously documented that the empirical cumulative distribution function (ogive) of the C_t values can reveal the proportion of chambers originally containing the same number of amplification targets [6]. Ideally, chambers containing only one ssDNA entity will cross the

signal threshold one cycle later than chambers containing one dsDNA or two ssDNA entities. However, observing this structure requires that virtually all entities in all chambers start to amplify at the same time: a chamber containing a single dsDNA entity that begins to amplify one cycle late will generate the same reaction curve as a chamber containing a single ssDNA entity that amplified in the initial cycle. Observing the structure also requires that all entities and their amplification progeny amplify efficiently so that all chambers originally containing the same number and type of entity have virtually the same C_t .

Figure 4 displays the ogives for the technical replicates of the 10 human nDNA assays in one cdPCR chip. The figure also displays the summary ogive for each assay, created by combining the C_t results of all the technical replicates into a single vector and re-sorting.

Occasionally, the ogives for some of the technical replicates (each a panel of 770 chambers in the 48-panel cdPCR chip) will be systematically offset from one another. Such offsets introduce uninformative “noise” structure into the summary ogive. This can be largely eliminated by aligning each of the replicate ogives to have the same consensus C_t value at some characteristic fraction of positive chambers. The alignment is illustrated in Figure 5.

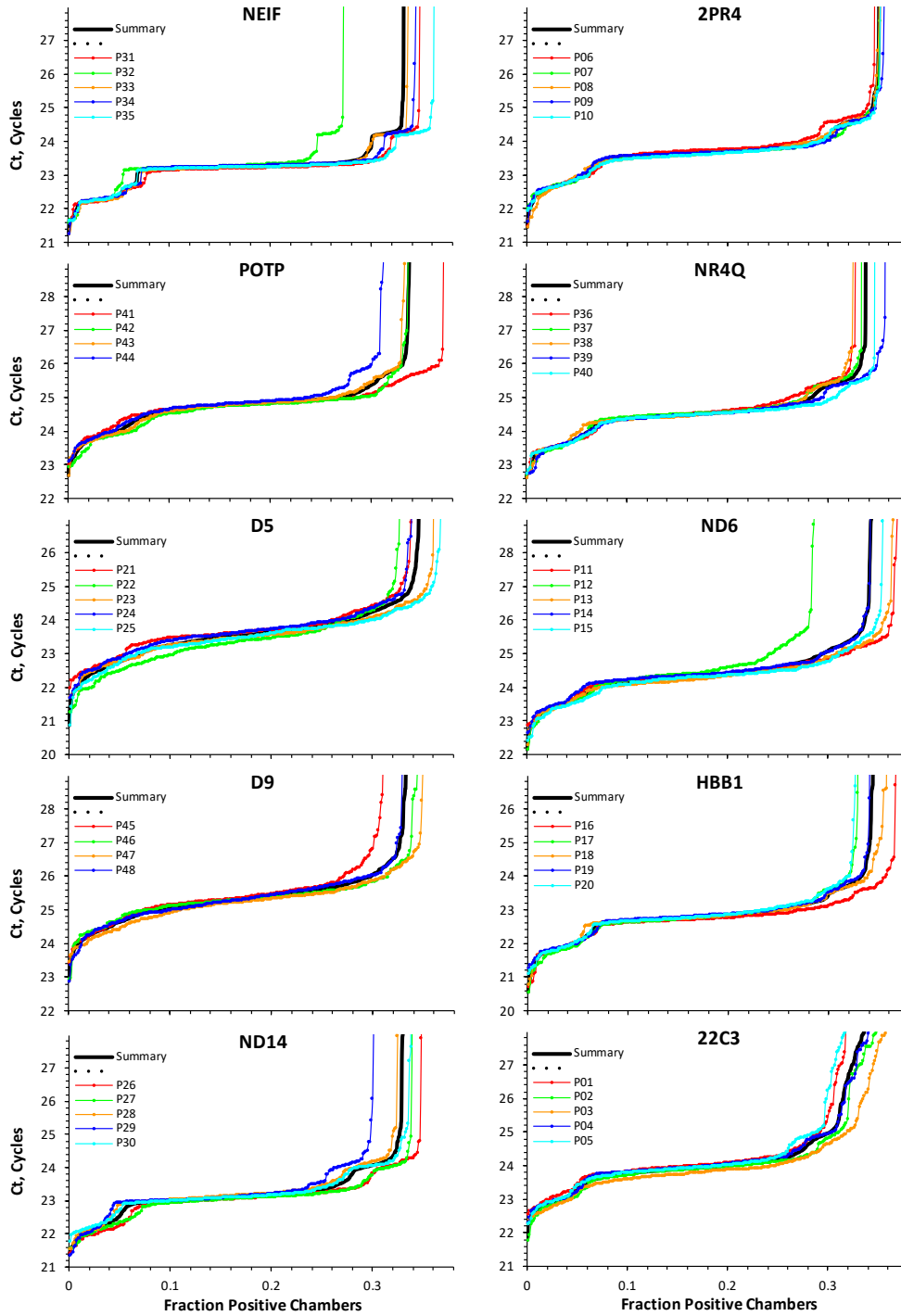


Figure 4. cdPCR Ogives for NIST Human nDNA Assays.

Each subplot displays a section of the cumulative Ct distributions (ogives) for the same DNA extract of one of the 10 NIST-developed dPCR assays used to certify the concentration of human nDNA in SRM 2372a. Each thin line in a subplot is the ogive for one of the four or five replicate panels of the given assay, identified as “Pxx” where “xx” is the chip panel number. The thick black line combines the results from all replicates. These data were obtained for a dilution of 2372 Component B with chip 1670089148, using the linear derivative analysis mode.

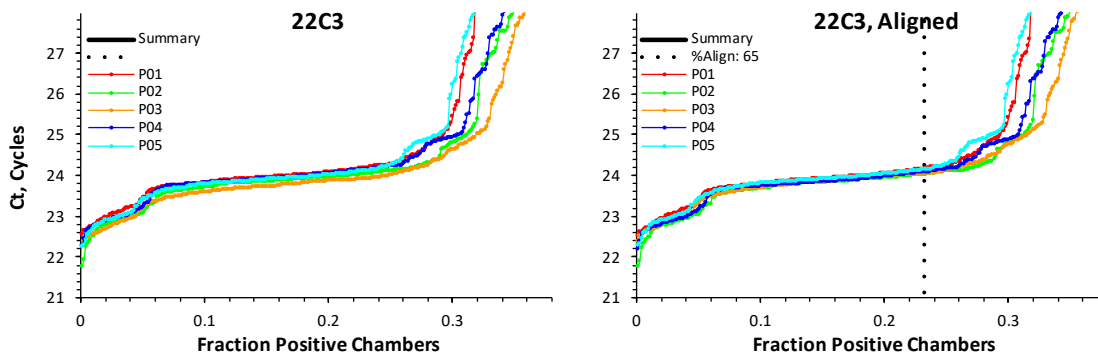


Figure 5. Ogive Alignment

The subplot to the left displays the 22C3 assay’s five replicate ogives before alignment, the subplot to the right displays them after aligning them to have the consensus 65th percentile C_t . The dotted vertical line marks the approximate fraction positive location of this one-point alignment.

Figure 6 compares the summary ogives for the assays. All assays give about the same 0.32 fraction of positive chambers after 60 amplification cycles, but there is considerable variation in the ogive shapes. While the initial C_t values differ among the assays by about three cycles, this does not necessarily reflect amplification efficiency but rather the relative fluorescence of the assay probes.

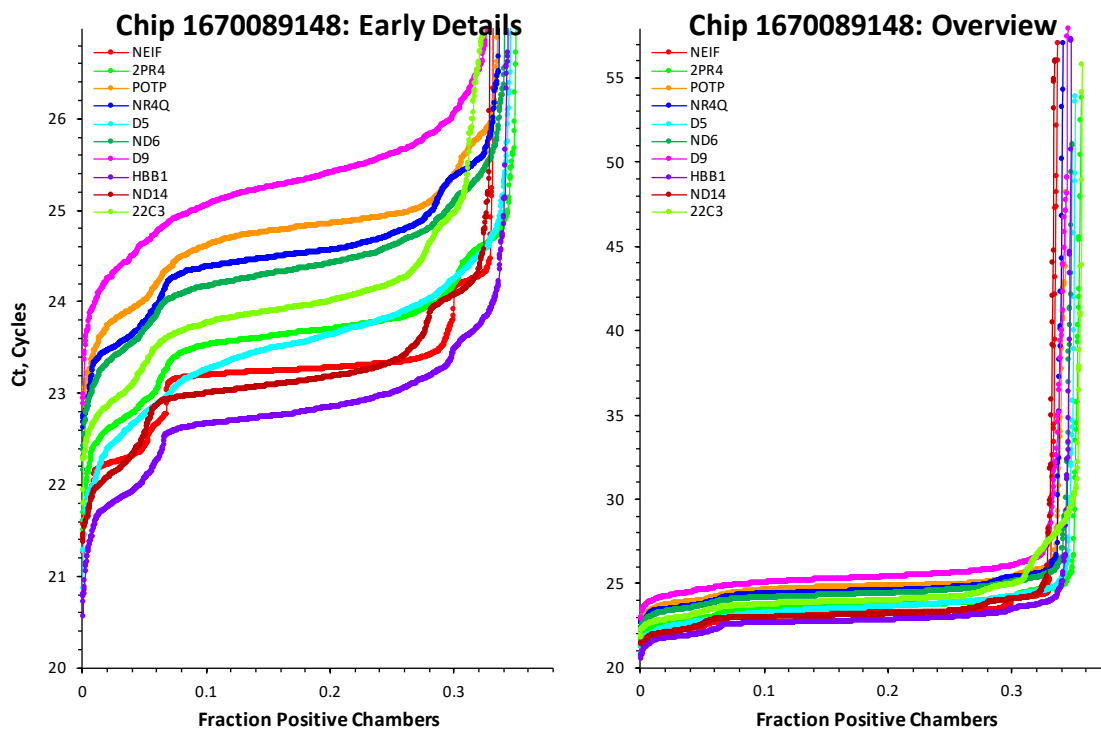


Figure 6. Summary Ogives for NIST Human nDNA Assays.

The subplot to the left displays the average ogives for the 10 nDNA dPCR assays displayed at the same graphical resolution used in Figure 4. The subplot to the right displays the complete average ogives. While the ogives displayed in the higher-resolution section have different shapes, all assays reach a similar final fraction of positive chambers.

Since fluorescence intensity should nominally double with each cycle, the C_t values for each assay will ideally be no more than about five cycles larger than the earliest C_t values: if the intensity for a chamber originally containing a single target sequence crosses the threshold at cycle n , then chambers with two should cross at cycle $n-1$, with four at $n-2$, eight at $n-3$, and 16 at $n-4$. At sample dilutions where the average number of entities is less than one, the probability of chambers originally containing even 16 sequences is very low. However, the fluorescence in a few chambers cross the intensity threshold many tens-of-cycles late. The reaction curves in these “late starter” chambers generally do not differ in shape from their earlier siblings, only in when the entities started to efficiently amplify. We have shown that most of the ddPCR “fog” between the background and majority bands (see Figure 8) come from delayed initiation of amplification [8].

Figure 7 displays the summary ogives, their kernel densities (the derivative of the ogive with respect to C_t), and their derivatives with respect to fraction positive.

A kernel density is an estimate of the probability density function of the distribution, computed by summing Gaussian “kernel” distributions that are centered on every C_t . All kernels are assigned the same empirically defined standard deviation, just large enough to generate a smooth curve without losing significant structure. These kernel densities document the relative number of chambers that provide very similar C_t values.

How the C_t values vary as a function of the fraction of positive chambers is computed as the first derivative of sliding quadratic boxcar least squares fits to the data. Every boxcar includes the same number of C_t values; the number of values determined empirically to provide a relatively smooth curve without loss of structure.

Only the NEIF assay approaches ideal behavior.

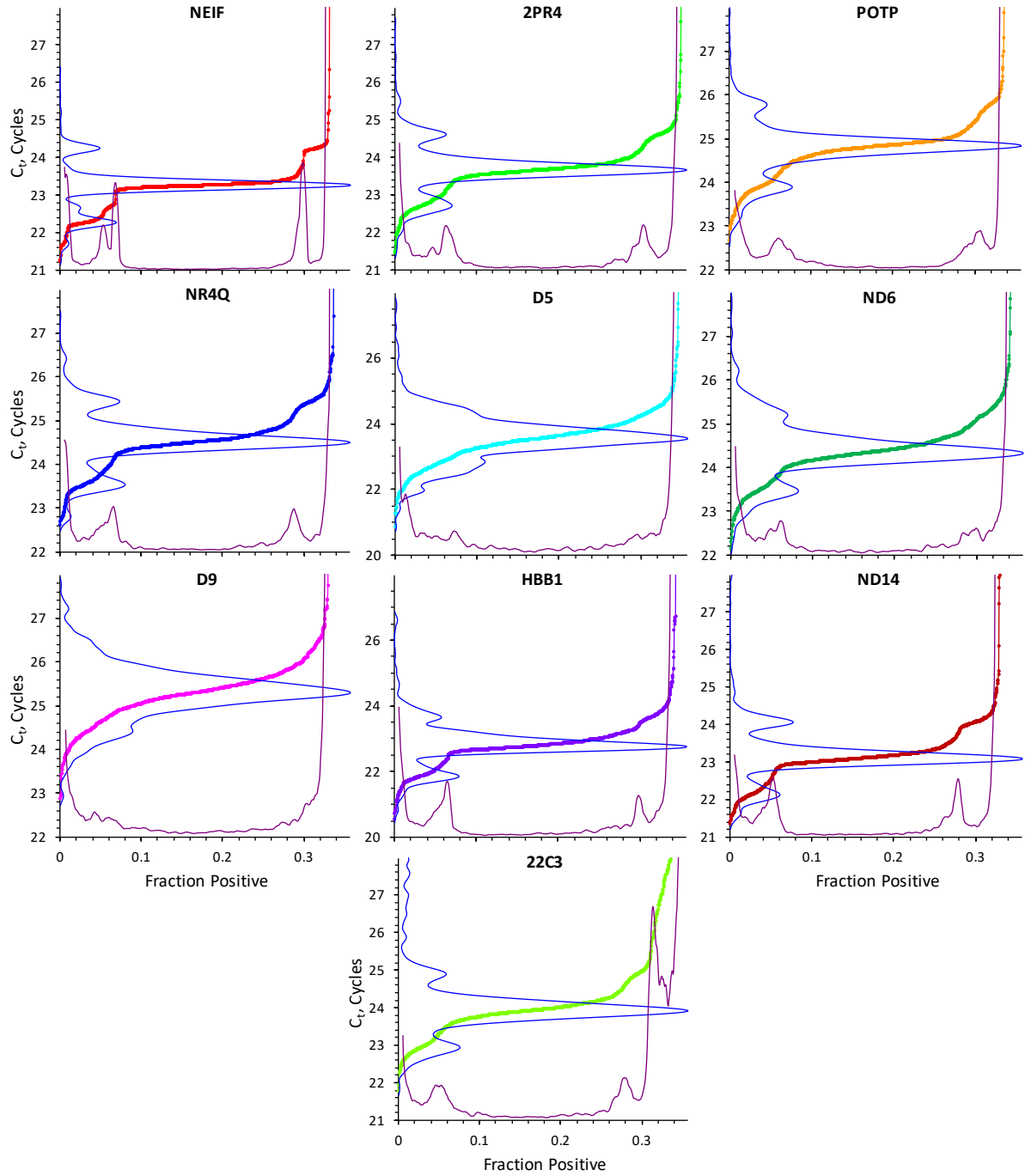


Figure 7. Ogive Kernel Densities and First Derivatives.

The thick line in each subplot is the average ogive for one of the 10 human nDNA assays. The thin blue curve plotted along the left axis of each subplot is the ogive's kernel density function (essentially a smoothed histogram) showing the relative number of chambers with given C_i as a function of C_i ; the curve's horizontal-axis is scaled to have its maximum at the right-edge of the subplot. The thin purple curve plotted along the bottom edge of each subplot is the ogive's first derivative showing the rate of change in C_i values as a function of fraction positive chambers.

1.3.2. Droplet-Digital PCR (ddPCR)

We use QX100 and QX200 ddPCR systems (Bio-Rad, Hercules, CA USA) where droplets are formed in a disposable microfluidic cartridge that mixes droplet generating oil with the DNA in a vacuum/pressure-operated droplet generator. Generated droplets from each sample are transferred to one well of a 96-well plate. After all samples are transferred, the plate is heat-sealed with foil and PCR amplified using a well-calibrated thermal cycler. For the current studies, samples were amplified using a temperature ramp of 2.5 °C/s, an initial hold at 95 °C for 10 min then 60 cycles of 94 °C for 30 s with annealing at 61 °C for 60 s, a hold at 98 °C for 10 min to harden the droplets and a final hold at 4 °C until the samples were removed. After amplification, the 96-well plate is transferred to the droplet reader which counts the number of valid droplets in each well and measures their fluorescence intensities. The manufacturer states 10,000 droplets as a lower bound necessary for reliable results; there typically are about 15,000 droplets.

Figure 8 displays exemplar droplet patterns for the 10 human nDNA assays. While the threshold fluorescence signal varies among the assays, the gap between the negative threshold and most of the positive signals is adequately wide for all assays.

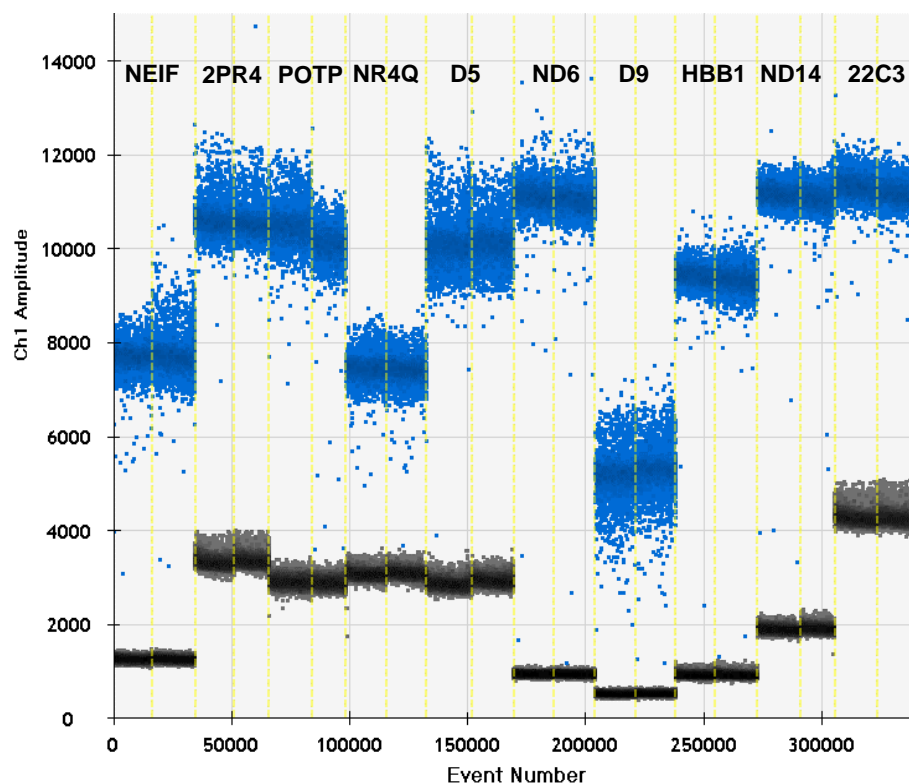


Figure 8. ddPCR Droplet Patterns for NIST Human nDNA Assays.

This plot displays representative droplet fluorescence patterns for two technical replicates each of the 10 NIST-developed human nDNA assays after 60 amplification cycles. Every dot represents the signal intensity of one droplet. The black dots denote the background fluorescence of (negative) droplets that did not contain an amplifiable entity. The blue dots denote (positive) droplets that contained at least one amplifiable entity. Blue dots between the upper edge of the population of negative and the lower edge of the main population of positive droplets are analogous to the cdPCR “late starters.” These results were obtained for a dilution of SRM 2372a Component B.

Transforming the entities per droplet measurements to have units of entities per volume requires knowledge of the mean droplet volume [9]. Droplet volumes for the reagents we use are about 0.74 nL [24]. However, droplet volume is sensitive to the exact composition of the ddPCR system’s proprietary reagents and can vary from batch to batch. While accurate knowledge of droplet volume was not required for the studies described here, changes in droplet volume would complicate comparing results over time. The same reagent batch was used throughout the studies described in this report.

1.4. Quantifying “Proportion”

The following discussions express measurements of proportion (a part in relation to the whole) as either “fraction” (that is, proportion on a scale of 0 to 1) or “percent” (proportion on a scale of 0 to 100). Fractions are more convenient for use in mathematical relationships, percentages are more easily interpreted (contrast “0.01 entity fraction” vs “1 %”).

However, sometimes the choice of scale is for purely mundane considerations:

- Four significant-digit fractions require six characters (0.1234) while percentages require just five (12.34). This space-saving can make real differences in the width of tables and clarity of axis labels.
- History. We’ve been working on this stuff since 2014 and some habits die hard.

Regardless of which scale is used, we have attempted to make the value of all proportions clear through textual context, table headers and footnotes, and figure captions.

1.5. Correcting DNA Mass Concentration Estimates

Given that separating one dsDNA fragment containing the target sequence for a PCR assay creates two ssDNA fragments that contain the target, one-half of the daughter ssDNA entities will exceed the number of their dsDNA parents. That is, assuming all target-containing entities are dsDNA will generate estimates of ng/μL mass concentration that are biased high by one-half of the ssDNA proportion.

The corrected mass concentration estimate is:

$$[\text{nDNA}]_{\text{corrected}} = \left(1 - \frac{p_0}{2}\right) [\text{nDNA}] \frac{\text{ng}}{\mu\text{L}} \quad [1]$$

where p_0 is the measured fraction of ssDNA in the sample and $[\text{DNA}]$ is estimated using Equation 6 in [9]. The corrected standard uncertainty is:

$$u([\text{nDNA}]_{\text{corrected}}) = \sqrt{u^2([\text{nDNA}]) + \left(\frac{u(p_0)}{2}\right)^2} \frac{\text{ng}}{\mu\text{L}} \quad [2]$$

where $u(p_0)$ is the estimated standard uncertainty for p_0 and $u([\text{DNA}])$ is estimated using Equation 7 in [9].

2. Heat Denaturation

Developing methods for evaluating the proportion of ssDNA in samples containing both dsDNA and ssDNA entities required access to materials containing known proportions of the two forms. Producing such mixtures requires a mechanism for converting the mostly dsDNA of the study samples into predominantly ssDNA without otherwise modifying the samples. Any sort of chemical modification (e.g., addition of NaOH or dimethyl sulfoxide) irreversibly changes the composition of the sample solution. Of the two widely used physical methods, sonication and heating, sonication randomly shears DNA as well as separating strands and thereby potentially reduces the number of amplifiable entities. Heat denaturation appears to be the only practical mechanism for denaturation.

Since PCR amplification proceeds by cycling between denaturation and renaturation conditions, there is considerable literature on optimizing temperature and timing for samples mixed with PCR reagents. However, to our knowledge there have been few studies on optimizing dsDNA heat-denaturation for samples in just TE⁻⁴ buffer – although one study found that heat-denaturation using a “boil for 5 min and snap cool” recipe yielded poorly reproducible results [13]. We therefore investigated denaturing conditions for our B and aB study materials.

Our optimization studies use the metric

$$\varphi = \lambda_1/\lambda_0 \quad [3]$$

where λ_0 is the measured copies per droplet of a native sample and λ_1 the copies per droplet of an aliquot of the sample after heat-denaturation. Since denaturation of a dsDNA entity can produce at most two accessible, amplifiable ssDNA entities, the maximum value for φ is 2.0. Values below this limit could arise from incomplete denaturation, partial renaturation, damage that renders entities inaccessible or non-amplifiable, or the presence of ssDNA entities in the native material.

2.1. Temperature and Duration

In previously described studies we established that 1) the maximum observed φ with our human nDNA assays was about 1.9 rather than the 2.0 limit, 2) the number of accessible, amplifiable entities after heat-denaturing declined with increasing temperature and increasing time at that temperature, and 3) the B and aB materials responded quite differently to the denaturation conditions [10]. Our focus thus became determination of the lowest temperature and shortest time that would reliably maximize φ for both materials.

Figure 9 summarizes the effect of denaturation temperature on single treatments of (15, 30, and 60) s of the B and aB materials. The φ values for both materials reach their plateaus only at 94 °C and between 30 s and 60 s treatment duration. We believe that the differences in the response of the B and aB DNA is, like their spectrophotometric behavior, related to their tertiary structure. The strands in the dsDNA entities in the older B material are more easily denatured than are those in the more recently extracted aB.

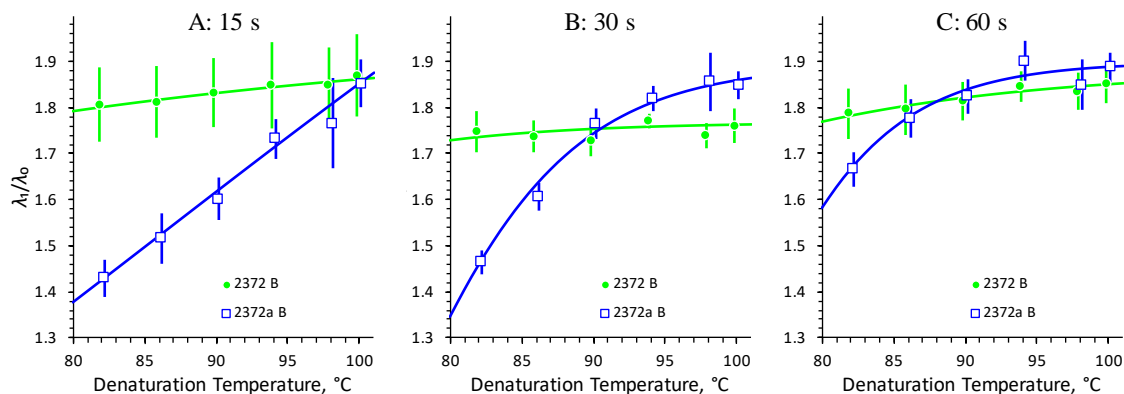


Figure 9. Change in λ_1/λ_0 with Denaturation Temperature

The symbols represent the mean measured entities per droplet in heat-denatured samples relative to the corresponding values of the native materials; the bars span ± 1 standard uncertainty. The lines are empirical fits to the three-parameter sigmoidal model, $\varphi = \lambda_1/\lambda_0 = \alpha/(1+e^{-\beta(T-\gamma)})$, where T is the denaturation temperature. The time at maximum temperature was A) 15 s, B) 30 s, and C) 60 s.

Figure 10 summarizes the effect of the duration of denaturation at 94 °C and 96 °C for the B and aB materials. As expected, φ for both materials are highest at the shortest duration studied. Prolonged exposure at these temperatures reduces the accessibility and/or amplifiability of ssDNA.

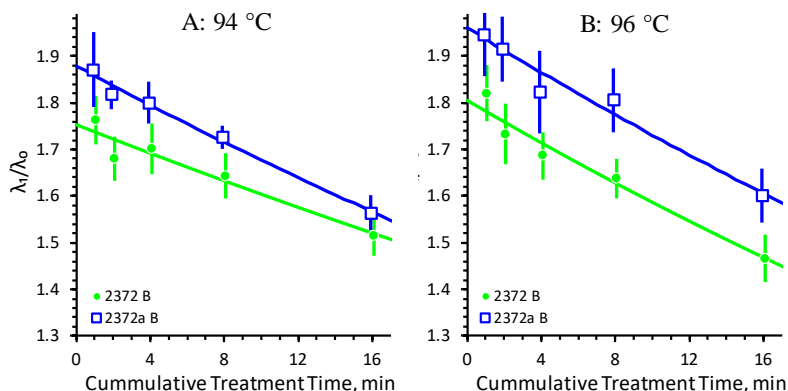


Figure 10. Change in λ_1/λ_0 with Denaturation Duration

The symbols represent the mean measured entities per droplet in heat-denatured samples relative to the corresponding values of the native materials; the bars span ± 1 standard uncertainty. The lines denote regression fits to the linear function, $\varphi = \lambda_1/\lambda_0 = a + bD$, where D is the length of time that the samples were held at the denaturation temperature. The denaturation temperatures were A) 94 °C and B) 96 °C.

2.2. Choice of Conditions

As shown in Figure 9C, at 60 s treatment duration there were only small differences between denaturing at 94 °C and 98 °C. However, the slope of the relationships between ϕ and duration are approximately equal only at 96 °C. To better ensure complete denaturation of other DNA extracts, we chose to use 96 °C for 60 s as our standard heat-denaturation method.

Figure 11 is image of a FlashGel (Lonza, Rockland, ME USA) that compares the native and heat-denatured forms of B and aB at 96 °C for 60 s. The intercalating dye used in this gel system binds much more strongly to dsDNA than to ssDNA. In both B and aB, the native and heat-denatured DNA consists almost entirely of fragments considerably larger than 4000 basepair (bp), the largest of the ladder markers. There is little to no evidence for dsDNA in either of the heat-denatured materials.

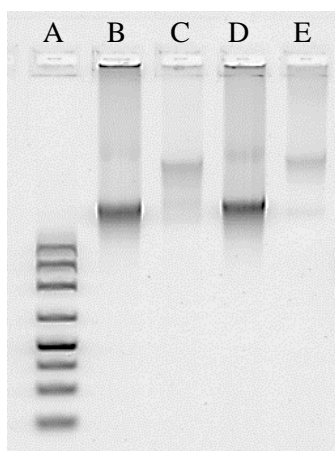


Figure 11. FlashGel of Native and Heat-Denatured SRM 2372 B and SRM 2372a B

A) FlashGel DNA Marker. The bands, from low to high, are at (100, 200, 300, 500, 800, 1250, 2000, and 4000) bp. B) native SRM 2372 B. C) heat-denatured SRM 2372 B. D) Native SRM 2372a B. E) heat-denatured SRM 2372a B.

2.2.1. Evolved Method for Heat-Denaturation

The following is the heat-denaturation recipe adopted for use in these studies. For DNA samples having a mass concentration of about 10 ng/ μ L, 15 μ L of sample is enough volume for at least five ddPCR technical replicates.

- 1) Transfer 30 μ L of DNA sample into one PCR tube, thoroughly mix by vortexing then microcentrifuge until all solution is at the bottom of the tube.
- 2) Transfer 15 μ L of the just-mixed sample into a second PCR tube.
- 3) Place one of the tubes in a water/ice storage block and the other into a well-calibrated thermocycler with a lid heated to 105 °C.
- 4) Bring the thermocycler temperature to 25 °C and hold for 30 s.
- 5) Raise the temperature at 6 °C/s (or as quickly as the thermocycler allows) from 25 °C to 96 °C.
- 6) Hold at 96 °C for 1 min.
- 7) Drop the temperature at 6 °C/s (or as quickly as the thermocycler allows) from 96 °C to 4 °C and hold at 4 °C.

- 8) Remove the tube from the thermocycler, gently finger-flick the solution to ensure uniform mixing then briefly microcentrifuge until all liquid is at the bottom of the tube.
- 9) Transfer the tube to a water/ice storage block. Keep the tubes with the 15 μL of native sample and the 15 μL of its heat-denatured sibling in this block until ready to perform the dPCR analyses.
- 10) Just prior to use, remove the tubes containing the native and heat-denatured samples from storage and allow to warm to room temperature. Briefly microcentrifuge the tubes until all liquid is at the bottom.

2.3. DNA Concentration

We evaluated whether the λ_1/λ_0 ratio depends on the DNA concentration in a sample. Samples were prepared from the B and aB stocks to provide λ_0 values of (0.40, 0.20, 0.10, and 0.05) copies per droplet. These samples were independently prepared by direct dilution of the stock materials with TE⁻⁴ buffer, not by serial dilution. Figure 12 summarizes the analysis results.

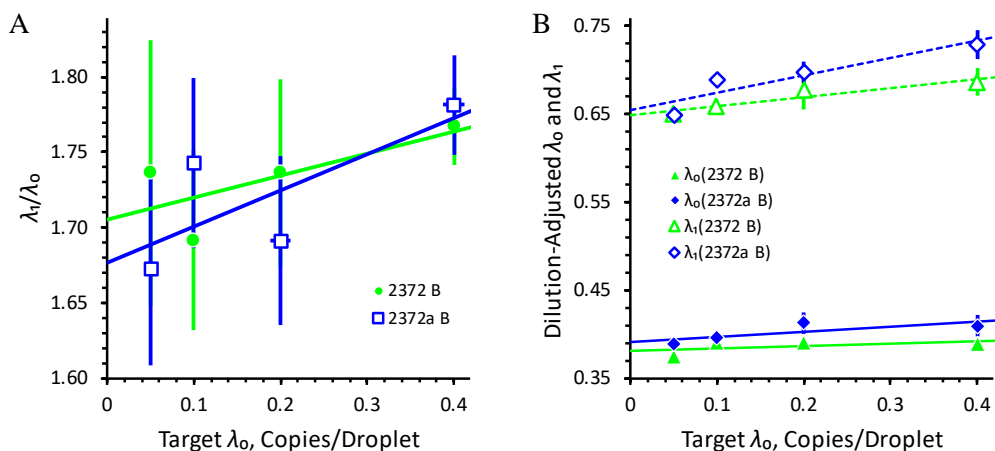


Figure 12. Change in λ_0 , λ_1 , and λ_1/λ_0 with Dilution

The symbols represent the mean results as a function of the target λ_0 (1-to-4, 1-to-8, 1-to-16, and 1-to-32 dilutions of the stock materials) for each sample; the bars span ± 1 standard uncertainty. The lines are empirical linear fits. A) displays λ_1/λ_0 . B) displays dilution-adjusted λ_0 and λ_1 values.

The λ_1/λ_0 appear to decrease with the lower DNA concentrations provided by greater dilution. While the dilution-adjusted λ_0 decrease slightly with the lower concentration, the slope of the λ_1 decrease for both materials is about four-fold that of λ_0 . We speculate that these declines may be related to entities binding to the container walls, where a small constant loss causes proportionally greater decline at lower DNA concentrations.

Regardless of the true cause(s) for the observed declines, the results suggest that studies be performed using samples of roughly the same, relatively high DNA concentration. Given that we have observed loss of assay linearity with λ_0 above 0.8 entities per droplet [10], for native samples we target λ_0 in the range of (0.2 to 0.4) dsDNA entities per droplet to keep the λ_1 of heat-denatured materials within the linear range of our assays.

2.4. Renaturation

Renaturation, the recombination of two ssDNA entities back into one dsDNA entity, is a plausible cause for the apparent limiting value for $\phi = \lambda_1/\lambda_0$ being less than 2. Renaturation is facilitated by storage in buffer with relatively high salt content [25]. Figure 13 summarizes results for B in TE⁻⁴ and TE⁻⁴ with additional (40, 80, 160, 320, and 400) mmol/L KCL, immediately after sample preparation and after 4 d (≈ 96 h) storage at 4 °C. These solutions were prepared using a commercial pH 8 PCR buffer containing 500 mmol/L KCl and 150 mmol/L Tris-HCl.

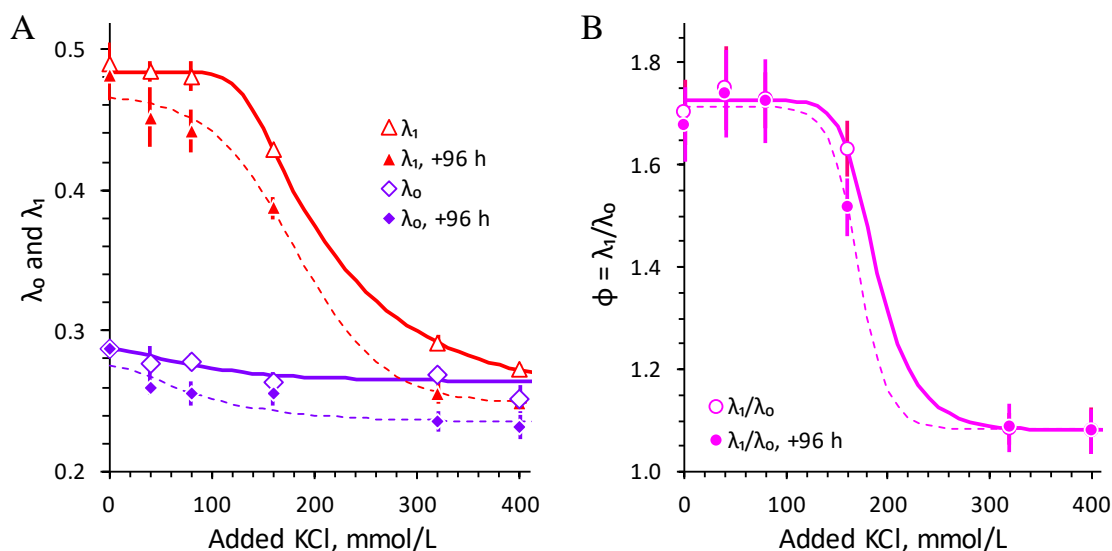


Figure 13. Changes with Salt Concentration and Time for SRM 2372 B

The symbols represent the mean results of the NEIF assay for a series of samples prepared at different concentrations of KCl; the bars span ± 1 standard uncertainty. The solid lines connecting open symbols are empirical sigmoidal fits to results obtained immediately after sample preparation; the dashed lines connecting solid symbols are empirical fits to results obtained for the same samples after 4 d storage at 4 °C. A) The purple diamonds represent λ_0 of native SRM 2372 B; the red triangles represent λ_1 of the heat-denatured materials. B) The circles represent the $\phi = \lambda_1/\lambda_0$ ratios.

Subplot A) of Figure 13 shows that the λ_0 and λ_1 results for native B samples evaluated immediately after preparation are slightly smaller in the samples in (40 and 80) mmol/L KCl. In the higher KCl concentration samples the λ_0 values decline slowly but the λ_1 decline precipitously. On re-evaluation after storage, the λ_0 of the sample in TE⁻⁴ is unchanged but λ_1 is reduced in all the KCl samples. This suggests that 1) adding KCl to the TE⁻⁴ buffer promotes renaturation, 2) the PCR reaction appears to be uninhibited by even 320 mmol/L added KCL, but 3) heat-denaturation at 96 °C is inhibited in samples stored in TE⁻⁴ with more than 80 mmol/L added KCl.

Subplot B) of Figure 13 shows that ϕ for the (40 and 80) mmol/L added KCl samples is slightly higher than in the un-augmented TE⁻⁴. This increase in ϕ results from the decline in λ_0 being proportionally greater than the decline in λ_1 , suggesting that there may be some “almost-but-not-quite” separated strands in the native material that renature quickly in addition to completely separated strands [26]. The ϕ of the un-augmented TE⁻⁴ is slightly lower after 4 d storage while being unchanged in the (40 and 80) mmol/L added KCl

materials. This suggests that renaturation of completely separated strands proceeds at the same slow rate in native and heat-denatured solutions containing up to about 80 mmol/L KCl.

Table 2 lists the numeric values for the results displayed in Figure 13 along with confirmatory results contrasting both B and aB materials in TE⁻⁴ and TE⁻⁴ with 40 mmol/L added KCl. The solutions used for the confirmatory results were prepared from reagent-grade KCl dissolved in TE⁻⁴.

The confirmatory results for the aB material provided in Table 2 indicate that 40 mmol/L KCl in the aB solutions has little effect. However, the ϕ values for the 40 mmol/L aB are slightly smaller than for the untreated sample while they are slightly larger with material B. This is compatible with the spectrophotometric evidence that little to none of the aB DNA has denatured to ssDNA: in the absence of ssDNA in the native material, only the heat-denatured solution can renature.

Table 2. Changes in NEIF Assay with Salt Concentration and Time

		SRM 2372 B ^a						SRM 2372a B ^a									
Date ^b	KCl ^c	#	λ_0	$s(\lambda_0)$	#	λ_1	$s(\lambda_1)$	φ	$u(\varphi)$	#	λ_0	$s(\lambda_0)$	#	λ_1	$s(\lambda_1)$	φ	$u(\varphi)$
19-Apr-18	0	4	0.2871	0.0057	3	0.4888	0.0152	1.70	0.06								
19-Apr-18	40	4	0.2764	0.0123	3	0.4838	0.0075	1.75	0.08								
19-Apr-18	80	4	0.2784	0.0059	4	0.4808	0.0110	1.73	0.05								
19-Apr-18	160	4	0.2628	0.0085	4	0.4289	0.0037	1.63	0.05								
19-Apr-18	320	4	0.2689	0.0057	4	0.2917	0.0056	1.09	0.03								
19-Apr-18	400	3	0.2517	0.0102	4	0.2721	0.0040	1.08	0.05								
23-Apr-18	0	3	0.2873	0.0062	4	0.4820	0.0181	1.68	0.07								
23-Apr-18	40	4	0.2594	0.0042	4	0.4514	0.0211	1.74	0.09								
23-Apr-18	80	4	0.2561	0.0086	3	0.4415	0.0152	1.72	0.08								
23-Apr-18	160	4	0.2552	0.0077	4	0.3871	0.0081	1.52	0.06								
23-Apr-18	320	4	0.2353	0.0075	4	0.2556	0.0079	1.09	0.05								
23-Apr-18	400	3	0.2312	0.0087	4	0.2495	0.0036	1.08	0.04								
20-Nov-18	0	5	0.2620	0.0060	5	0.4249	0.0077	1.62	0.05	5	0.2386	0.0058	5	0.4047	0.0086	1.70	0.05
20-Nov-18	40	5	0.2505	0.0122	5	0.3981	0.0120	1.59	0.09	5	0.2106	0.0079	5	0.3617	0.0084	1.72	0.08
23-Nov-18	0	5	0.2241	0.0057	5	0.4111	0.0110	1.83	0.07	5	0.2214	0.0076	5	0.4042	0.0050	1.83	0.07
23-Nov-18	40	5	0.2197	0.0080	5	0.3808	0.0103	1.73	0.08	5	0.2086	0.0046	5	0.3412	0.0053	1.64	0.04

^a # = number technical replicates, λ_0 = mean of native sample replicates in units of entities per droplet, $s()$ = standard deviation of the quantity within the (), λ_1 = mean of heat-denatured sample replicates in units of entities per droplet, $\varphi = \lambda_1/\lambda_0$; $u()$ = standard uncertainty of the quantity within the ().

^b Date of ddPCR analysis

^c KCl concentration, mmol/L.

2.4.1. Evolved Method for Adding KCl

Achieving our target λ_0 value of ≈ 0.3 entities per droplet requires use of samples with DNA concentration of ≈ 10 ng/ μ L. Given stock materials of substantially higher mass concentration, the desired DNA and KCl concentrations can be achieved by using a combination of TE⁻⁴ and a solution of KCl dissolved in TE⁻⁴ using the following formulae

$$\begin{aligned} V_{\text{DNA}} &= V_{\text{total}}(C_{\text{DNA,sample}}/C_{\text{DNA,stock}}) \\ V_{\text{KCl}} &= V_{\text{total}}(C_{\text{KCl,sample}}/C_{\text{KCl,stock}}) \\ V_{\text{TE}} &= V_{\text{total}} - V_{\text{DNA}} - V_{\text{KCl}} \end{aligned} \quad [4]$$

where:

- $C_{\text{DNA,sample}}$... Desired concentration of DNA in sample, ng/ μ L;
- $C_{\text{DNA,stock}}$ Concentration of DNA in stock material, ng/ μ L;
- $C_{\text{KCl,sample}}$ Desired concentration of KCl in sample, mmol/L;
- $C_{\text{KCl,stock}}$ Concentration of KCl in stock diluent, mmol/L;
- V_{DNA} Volume of stock DNA material used to prepare sample, μ L;
- V_{KCl} Volume of KCl stock diluent used to prepare sample, μ L;
- V_{TE} Volume of TE⁻⁴ buffer used to prepare sample, μ L;
- V_{total} Desired sample volume, μ L.

For example, the concentration of the B and aB materials used in this study is ≈ 50 ng/ μ L. To achieve the desired 10 ng/ μ L samples they need to be diluted 1-to-5 (one-part DNA plus four-parts diluent). Using a stock KCl solution of 500 mmol/L, Table 3 lists the volumes needed to produce 60 μ L each of the samples in Figure 13.

Table 3. Recipe for Preparing 60 μ L of Samples in (0 to 400) mmol/L KCl

$C_{\text{KCl,sample}}$	V_{DNA}	V_{KCl}	V_{TE}	V_{total}	$C_{\text{DNA,sample}}$
0	12	0	48	60	10
40	12	4.8	43.2	60	10
80	12	9.6	38.4	60	10
160	12	19.2	28.8	60	10
320	12	38.4	9.6	60	10
400	12	48	0	60	10

Since pipetting small volumes can be problematic, samples of lower KCl concentration should be used to prepare a more dilute KCl stock. For example, for 60 μ L of a 40 mmol/L KCl sample, first prepare 100 μ L of a 150 mmol/L KCl solution (e.g., combine 15 μ L of a 1000 mmol/L KCl stock with 85 μ L of TE⁻⁴) then combine 16 μ L this solution with 12 μ L of 50 ng/ μ L stock DNA and 32 μ L of TE⁻⁴.

3. cdPCR Direct Assessment

As discussed in Section 1.3.1, ideally the reaction curves for all cdPCR chambers that contain the same number of target sequences will cross the fluorescence threshold at the same cycle, i.e., they will all have the same C_t value. The resulting ogive will then resemble a staircase with vertical risers and horizontal treads [6]. Figure 14 compares an idealized “staircase” with an observed ogive.

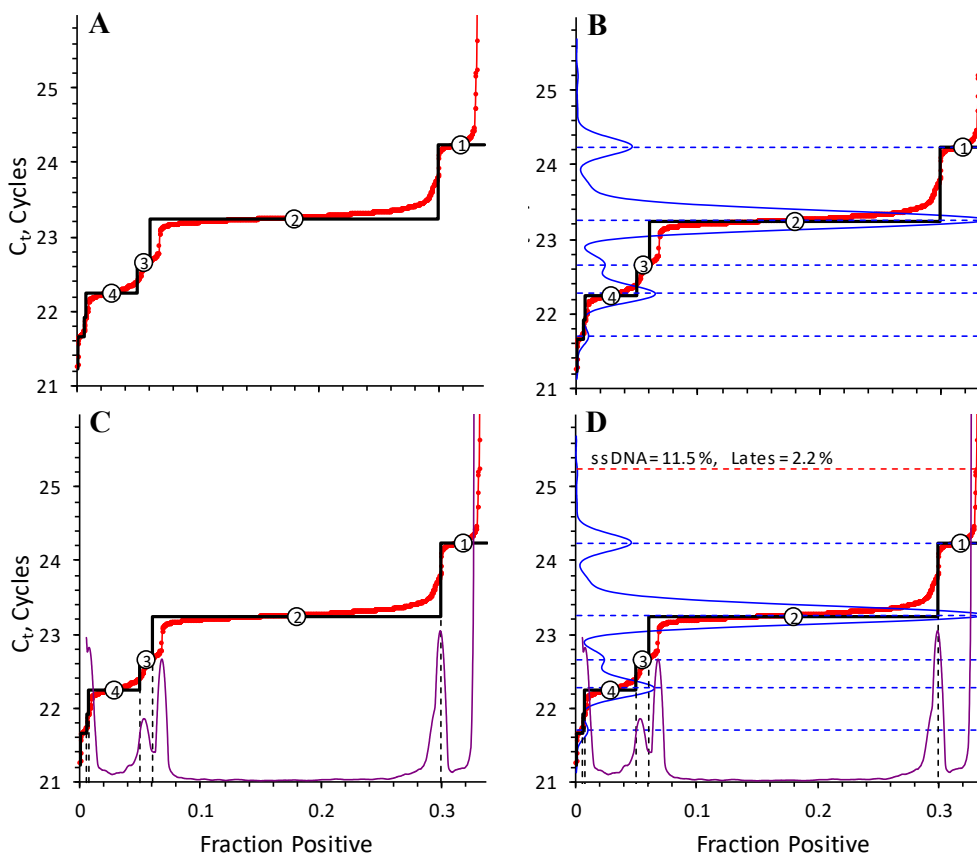


Figure 14. Comparison of Observed and Idealized Ogives for SRM 2372 B

A) The red curve is the observed ogive for the NEIF assay of SRM 2372 B in chip 1670089148. The thick black “staircase” curve is the ideal ogive for a given percentage of single-stranded DNA (ssDNA), here 11.5 %, in a DNA extract that is otherwise double-stranded DNA (dsDNA). The middle of each tread is labeled with the number of entities per chamber that produce the tread. B) The horizontal blue dotted lines mark the location of the kernel density peak maxima. The C_t location of the staircase is defined by alignment of the uppermost tread and the kernel density function’s uppermost peak. C) The black vertical lines connect the location of the stair risers with the horizontal axis; ideally, they bisect a derivative peak. D) The horizontal red dotted line is one C_t above the one-entity tread; C_t values above this line are considered “late starters.” The text above this line reports the estimated percentage of ssDNA and “late starters” in the sample.

3.1. Practicalities

The risers of the staircase mark the transition between chambers containing increasing numbers of targets; their height is proportional to the \log_2 of the number of entries per chamber of the lower tread divided by the number for the upper tread. The width of a tread is proportional to the number of chambers originally containing the same number of targets. Given an assay that is extremely efficient at amplifying all original target sequences and the resulting amplicons, estimating the percentage of ssDNA entities in the sample is equivalent to determining the width of the top tread of a best-fit ideal staircase relative to the fraction of positive chambers. However, this analysis has practical limitations even with the very efficient NEIF assay.

3.1.1. Late Starters

Regardless of assay, often several percent of the chambers become positive many amplification cycles later than expected for chambers containing a single target sequence. For all 10 of our nDNA dPCR assays the ogives become essentially vertical after 30 amplification cycles (see Figure 6), yet even at 60 cycles there are still a few chambers that become positive. These late starts may result from dsDNA or ssDNA entities with accessibility or amplifiability issues that are overcome only after many cycles.

Since the shape of the ogive does not contain information on the number of target sequences originally in these late-start chambers, we chose to analyze only the portion of the ogive with Ct values no larger than one cycle beyond the single-target tread.

3.1.2. One-Cycle Delayed Starts

Chambers containing a single dsDNA entity that does not start to amplify until the second amplification cycle will have the same C_t as chambers containing a single ssDNA entity that amplifies in the first cycle. The regular observation of a small peak in the kernel density function one cycle above the one-entity ssDNA tread in heat-denatured samples confirms the reality of this delay: there is no plausible mechanism for amplifying one-half of a single target sequence.

The width of the top tread confounds the proportion of ssDNA with the proportion of one-cycle amplification delay.

3.1.3. Non-Ideal Target Dispersion

The microfluidic lines connecting samples to panels vary in length in a systematic pattern. Particularly with λ values larger than about 0.8 entity per chamber, we occasionally observe sets of replicate ogives where the ratios among the tread widths vary in concert with the lengths of the plumbing. Depending on the number and location of the panels used for the technical replicates, the proportions of the number of entities per chamber may not accurately reflect the proportions of dsDNA and ssDNA in the samples.

Even with the summary ogive displayed in Figure 14, while the single-target tread of the staircase matches the relevant first derivative peak, the risers for the two- and three-target treads are somewhat offset from their first derivative peaks. This may reflect imperfect

modeling or, as suggested in [12], a not-strictly Poisson distribution of the dsDNA and ssDNA entities.

We believe that the impact of this issue can be minimized by using many technical replicates per sample and distributing the replicates to evenly sample panels over the different plumbing lengths.

3.2. Staircase Analysis

The Poisson distribution describes the expected result when a given number of entities are independently and randomly dispersed into given number of chambers. An ideal ogive can then be estimated using a random number generator that provides uniformly distributed values given three input parameters: 1) the proportion of ssDNA entities in a mixture of dsDNA and ssDNA entities, p_0 ; the average number of entities per chamber, λ ; and the number of chambers, k . The total number of entities in the sample is $N_e = k\lambda$, the number of ssDNA entities is $N_s = p_0N_e$ (with rounding to the nearest integer), and the number of dsDNA entities is $N_d = N_e - N_s$.

Staircase estimation proceeds as follows:

- 1) Establish a vector x of length k . Set every x_i to have the value 0.
- 2) Randomly distribute N_s ssDNA entities into the vector. That is, generate an integer index, i , of value 1 to k where every integer over that range is equally likely; add 1 to x_i ; repeat N_s times.
- 3) Randomly distribute N_d dsDNA entities into the vector. That is, generate an integer index, i , of value 1 to k where every integer over that range is equally likely; add 2 to x_i ; repeat N_d times.
- 4) Sort the x_i into decreasing order. That is, sort x so that the elements containing the largest values come first.
- 5) For all x_i having value greater than 0, store the value $X - \log_2(x_i)$, where X is the Ct of the single entity tread of the experimentally observed ogive.
- 6) Repeat steps 1 through 5 as many times as you have time and patience for.
- 7) Define a summary vector y where every y_i element is the median of the array of the stored (sorted and transformed) x_i .
- 8) If 95 % confidence intervals are desired, define bounding interval vectors from the 2.5th and 97.5th percentiles of the array of the stored (sorted and transformed) x_i .
- 9) Plot the median (and bounding interval) y_i as a function of i/k .

For a given summary ogive, k is just 770 times the number of technical replicates and λ can be estimated from the measured fraction of positive chambers and the estimated number of late starters. “Best estimates” for p_0 can be established by iteratively comparing the staircase for trial p_0 values with the observed ogive until the riser locations approximately match those of the first derivative peaks. More sophisticated matching rules could be established, but eyeball estimation is robust to irregularities and provides estimates of p_0 that are reproducible within about 1 % across multiple independent trials by different analysts.

The staircase analyses in this report were accomplished using the Poisson module of the Excel-based cdPCR_OgiveMaker.xlsm system. This system was developed by the authors in

Microsoft Visual Basic as an exploratory tool and, while available on request, was not designed for routine use by others.

3.3. Staircase Results for SRMs 2372 B and 2372a B

Figure 15 displays summary ogives for dilutions of the native B and aB materials, identified with the “0” subscript, and after heat-denaturing, designated with the subscript “1”. The fraction of positive chambers for B₀ and aB₀ are nearly identical while the fraction for B₁ is notably less than for aB₁. Perhaps counter-intuitively, this indicates that the proportion of ssDNA in the B material is significantly higher than in aB: since the proportion of dsDNA in B is lower, heat-denaturation produces relatively fewer new ssDNA entities.

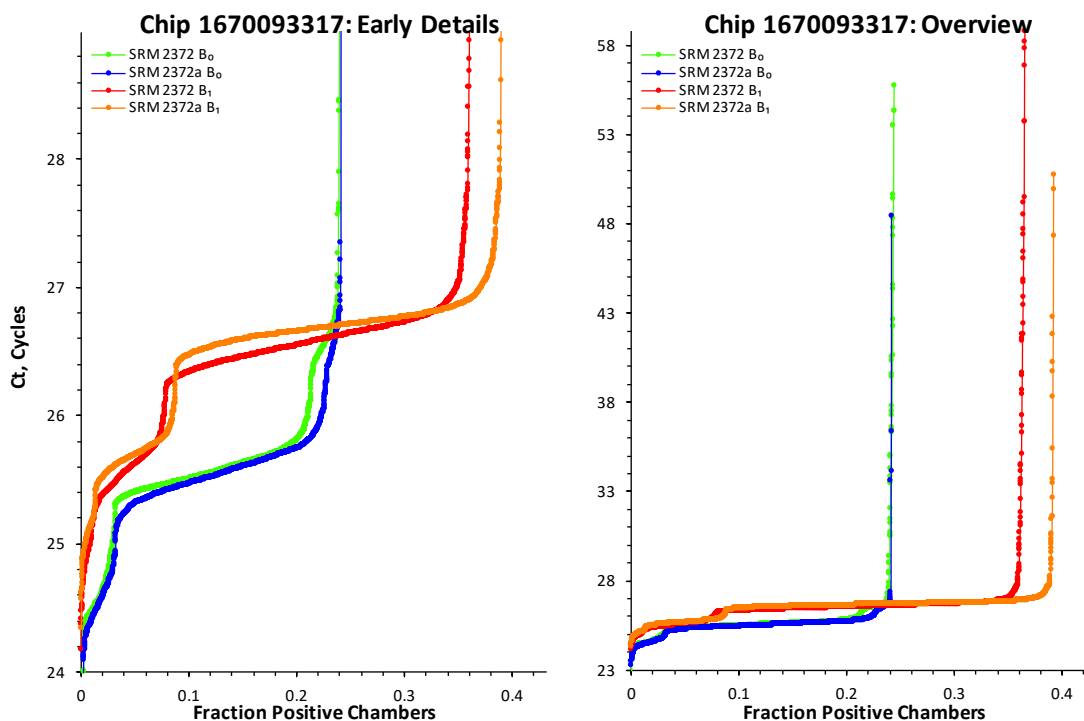


Figure 15. Exemplar Ogives for Native and Heat-Denatured B and aB.

The subplot to the left displays at high graphical resolution the average ogives for native and heat-denatured SRM 2372 B and SRM 2372a B samples. The subplot to the right displays the complete ogives. These ogives were obtained with the NEIF assay using chip 1670093317.

Figure 16 displays the staircase analysis of these B₀, B₁, aB₀, and aB₁ summary ogives.

Note: These summaries represent “best case” rather than “typical” performance; however, (almost) all our cdPCR evaluations with the NEIF assay have provided interpretable summary ogives. The few outright failures resulted from various hardware performance issues that were corrected following maintenance. However, we believe that occasional within-chip chamber volume variability contributes to chip-to-chip differences in ogive structure.

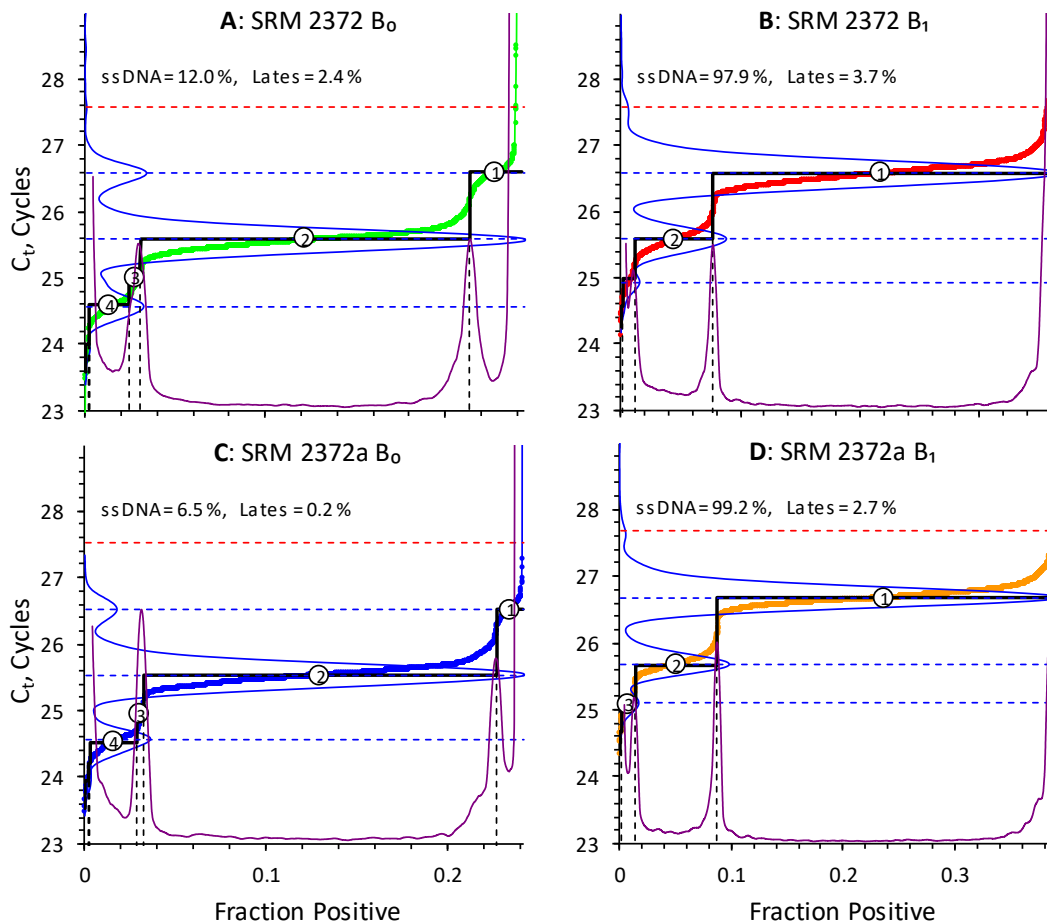


Figure 16. Staircase Analysis of Native and Heat-Denatured B and aB.

A) Native SRM 2372 B. B) Heat-denatured SRM 2372 B. C) Native SRM 2372a B. D) Heat-denatured SRM 2372a B. These exceptionally clear ogives were obtained with the NEIF assay using chip 1670093317.

3.3.1. Quantitation

Table 4 and Table 5 summarize independent estimates of percent late starters, L , and ssDNA entities, p , for B_0 , B_1 , aB_0 , and aB_1 . The value of each estimate is the staircase evaluation of the summary ogive formed by combining all technical replicates for the given material.

These estimates appear stable with respect to chip batch, date, and the number of entities per chamber.

3.3.2. Uncertainty Analysis

In addition to the full summary ogive used to estimate the values of L and p , two partial summaries were evaluated and used in estimating the uncertainties in the proportions, $u(L)$ and $u(p)$. These summaries were formed by combining the half of technical replicates having the fewest number of positive chambers and the half having the greatest number of positive chambers. When the number of replicates was not evenly divisible, the replicate with the median number of positive chambers was not used in either summary. The uncertainties were then estimated as the standard deviation of the three determinations.

Table 4. cdPCR Analysis Results for SRM 2372 B

Chip	Date	SRM 2372 B, Native ^{a,b}						SRM 2372 B, Heat Denatured ^{a,b}									
		#	λ_0	$u(\lambda_0)$	L_0	$u(L_0)$	p_0	$u(p_0)$	#	λ_1	$u(\lambda_1)$	L_1	$u(L_1)$	p_1	$u(p_1)$	λ_0/λ_1	$u(\lambda_0/\lambda_1)$
1670093317	04/04/18	12	0.280	0.024	2.4	0.1	12.0	0.0	12	0.455	0.025	3.7	1.0	97.0	1.7	1.63	0.17
1670093314	04/23/18	12	0.374	0.024	2.4	0.3	15.0	2.1	12	0.610	0.046	4.1	1.0	98.5	0.3	1.63	0.16
1670093313	05/07/18	12	1.885	0.065	0.8	0.1	12.0	0.0									
1670098065	07/12/18	12	0.336	0.025	2.2	0.3	10.0	0.6	12	0.573	0.029	4.5	0.3	95.0	2.8	1.71	0.15
1670098075	07/12/18	12	0.498	0.021	1.9	0.1	10.0	0.3									
1670098075	07/12/18	12	0.508	0.027	1.6	0.1	11.0	0.0									
1670098101	08/09/18	12	0.646	0.027	1.7	0.1	12.0	0.0									
1670098122	08/17/18	8	0.364	0.024	2.7	0.5	11.0	0.9									
1670098185	08/29/18	12	0.261	0.013	2.3	0.8	11.0	0.6									
1670098207	08/31/18	12	0.280	0.017	2.3	0.1	10.0	0.3									
1670099184	08/31/18	12	0.328	0.024	2.4	0.4	11.0	2.0									
1670100132	09/20/18	15	0.350	0.031	1.8	0.1	12.0	0.6									
					<i>N</i> :	12		12			<i>N</i> :	3		3		3	
					\bar{x} :	2.0		11.4			\bar{x} :	4.1		96.8		1.65	
					<i>s</i> :	0.5		1.4			<i>s</i> :	0.4		1.8		0.05	
					\bar{u} :		0.3		0.9		\bar{u} :		0.8		1.9		0.16
					$u(\bar{x})$:	0.2		0.5			$u(\bar{x})$:	0.5		1.5		0.10	

- a* # = number technical replicates, λ_0 = entities per chamber in native sample, L_0 = percent late starters in native sample, p_0 = percent ssDNA entities in native sample, λ_1 = entities per chamber in heat-denatured sample, L_1 = percent late starters in heat-denatured sample, p_1 = percent ssDNA entities in heat-denatured sample, $u()$ = standard uncertainty of the quantity within the ().
- b* N = number of independent results, \bar{x} = mean; s = standard deviation, \bar{u} = pooled standard uncertainty, $u(\bar{x})$ = standard uncertainty of the mean.

Table 5. cdPCR Analysis Results for SRM 2372a B

Chip	Date	SRM 2372 B, Native ^{a,b}						SRM 2372 B, Heat Denatured ^{a,b}									
		#	λ_0	$u(\lambda_0)$	L_0	$u(L_0)$	p_0	$u(p_0)$	#	λ_1	$u(\lambda_1)$	L_1	$u(L_1)$	p_1	$u(p_1)$	λ_0/λ_1	$u(\lambda_0/\lambda_1)$
1670093317	04/04/18	12	0.276	0.017	0.2	0.1	7	0.3	12	0.498	0.027	2.7	0.5	99	1	1.80	0.15
1670093316	04/09/18	9	0.327	0.023	0.3	0.2	6	1.7									
1670093313	05/07/18	12	1.520	0.188	0.3	0.1	9	3	12	2.799	0.1	0.8	0.1	97	1.7	1.84	0.24
1670098006	05/23/18	12	1.453	0.059	0.2	0.1	6	0.5	12	2.781	0.1	0.7	0.2	95	4	1.91	0.10
1670098077	07/20/18	12	0.591	0.039	1.5	0.1	10.5	0.3									
1670100105	09/17/18	16	0.285	0.027	0.8	0.2	8.5	0.9									
					$N:$	6		6				$N:$	3		3		3
					$\bar{x}:$	0.6		7.8				$\bar{x}:$	1.4		97.0		1.85
					$s:$	0.5		1.8				$s:$	1.1		2.0		0.06
					$\bar{u}:$		0.1		1.5			$\bar{u}:$		0.3		2.6	0.17
					$u(\bar{x}):$	0.2		1.0				$u(\bar{x}):$	0.7		1.9		0.10

- a* # = number technical replicates, λ_0 = entities per chamber in native sample, L_0 = percent late starters in native sample, p_0 = percent ssDNA entities in native sample, λ_1 = entities per chamber in heat-denatured sample, L_1 = percent late starters in heat-denatured sample, p_1 = percent ssDNA entities in heat-denatured sample, $u()$ = standard uncertainty of the quantity within the ().
- b* N = number of independent results, \bar{x} = mean; s = standard deviation, \bar{u} = pooled standard uncertainty, $u(\bar{x})$ = standard uncertainty of the mean.

3.4. Mixtures

The results for the native and heat-denatured samples presented in Table 4 and Table 5 confirm that 1) there is a larger proportion of ssDNA in native B than in native aB and 2) heat-denaturing converts all to nearly all dsDNA in the B and aB materials to ssDNA. While these results establish the precision of staircase estimates, they do not address their trueness (lack of bias).

In the absence of suitable reference materials or recognized reference measurement procedures, establishing the trueness of staircase estimation is at best complicated. However, it is relatively straightforward to evaluate whether the process provides estimates that are linearly related to the proportion of ssDNA in a sample.

3.4.1. Staircase Analysis for Mixtures of SRM 2372 B

Figure 17 displays the summary ogives for one set of mixtures for material B. Figure 18 displays the staircase analysis of these ogives. Note that the width of the one-sequence per chamber tread increases (as the width of the two-sequences per chamber tread decreases) as the proportion of heat-denatured material increases.

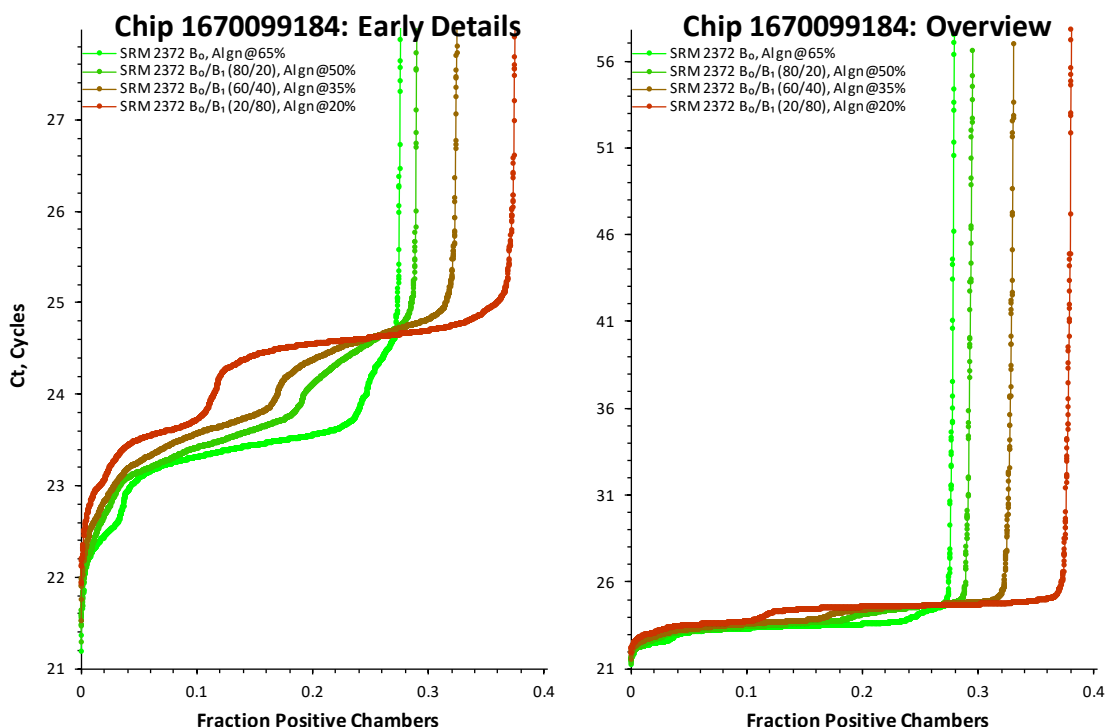


Figure 17. Exemplar Ogives for Native SRM 2372 B Mixtures.

The subplot to the left displays at high graphical resolution the average ogives for native and (80 % native, 20 % heat-denatured), (60 % native, 40 % heat-denatured), and (20 % native, 80 % heat-denatured) mixtures of SRM 2372 B. The subplot to the right displays the complete ogives. These ogives were obtained with the NEIF assay using chip 1670099184.

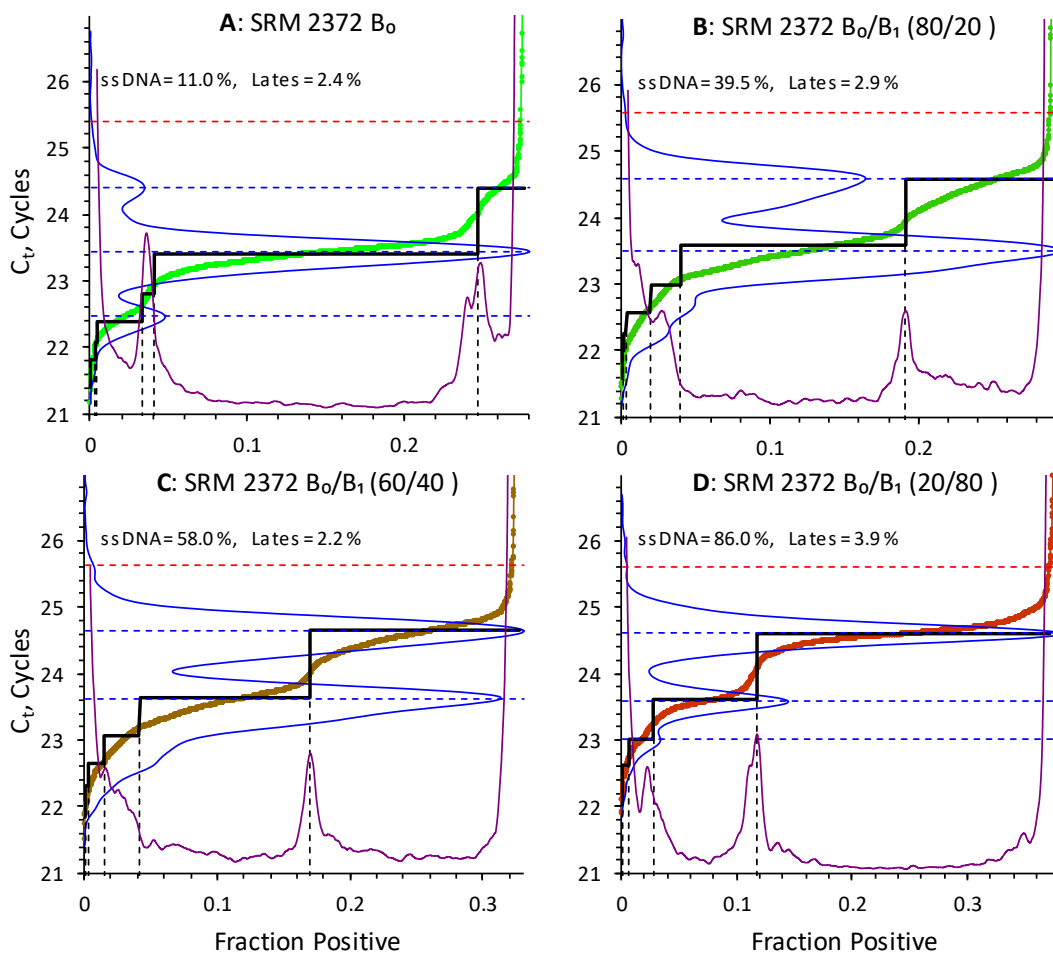


Figure 18. Exemplar Staircase Analysis of SRM 2372 B Mixtures.

A) Native SRM 2372 B. B) Volumetric mixture of 80 % native and 20 % heat-denatured SRM 2372 B. C) Volumetric mixture of 60 % native and 40 % heat-denatured SRM 2372 B. D) Volumetric mixture of 20 % native and 80 % heat-denatured SRM 2372 B. These more typical ogives were obtained with the NEIF assay using chip 1670099184.

Table 6 summarizes the results for three independent mixture preparations.

Table 6. cdPCR Staircase Results for SRM 2372 B Mixtures

			Volume % of Heat-Denatured Sample ^a							
Mtrl ^b	Date	Assay	$v_m = 0 \%$		$v_m = 20 \%$		$v_m = 40 \%$		$v_m = 80 \%$	
			p_0	$u(p_0)$	p_{20}	$u(p_{20})$	p_{40}	$u(p_{40})$	p_{80}	$u(p_{80})$
UB	08/29/18	HBB1	11.0	0.6	39.0	1.0	57.5	1.0	86.0	1.0
UB	08/31/18	POTP	10.0	0.3	37.0	2.5	56.0	0.3	88.0	0.3
B	09/04/18	POTP	11.0	2.0	39.0	2.0	57.0	0.1	85.5	1.0
Summaries ^c			N :		3		3		3	
			\bar{x} :		10.7		38.3		56.8	
			s :		0.6		1.2		0.8	
			\bar{u} :		1.2		1.9		0.006	
			$u(\bar{x})$:		0.3		0.7		0.4	
									0.8	

- a* v_m = mixture by volume of $m \%$ heat-denatured with $(100-m) \%$ native material,
 p_0 = percent ssDNA entities per chamber in native sample,
 p_{20} = percent ssDNA entities per chamber in mixture of 80 % native and 20 % heat-denatured sample,
 p_{40} = percent ssDNA entities per chamber in mixture of 60 % native and 40 % heat-denatured sample,
 p_{80} = percent ssDNA entities per chamber in mixture of 20 % native and 80 % heat-denatured sample,
 $u()$ = standard uncertainty of the quantity within the ().
- b* Material used to prepare mixture. UB is the undiluted stock material used to prepare SRM 2372 B in 2006.
- c* N = number of independent results, \bar{x} = mean, s = standard deviation, \bar{u} = pooled standard uncertainty, $u(\bar{x})$ = standard uncertainty of the mean.

3.4.2. Analysis of Mixtures of Native and Heat-Denatured Materials

Since a native DNA extract may contain some proportion of ssDNA and its heat-denatured sibling may not be entirely converted to ssDNA, estimating the percentage of ssDNA in a mixture of the two materials requires quantitative estimates for four parameters: 1) the entity proportion of ssDNA in the native material, p_0 ; 2) the entity proportion of ssDNA in its heat-denatured sibling, p_1 ; 3) the ratio of entities in the heat-denatured material relative to those in the native material, $\varphi = \lambda_1/\lambda_0$; and 4) the volume fraction of the heat-denatured material in the mixture, v_1 .

The entity fraction of ssDNA in a sample is:

$$p = s/e \quad [5]$$

where s is the number of ssDNA entities and e is the total number of entities (ssDNA and dsDNA).

The number of entities in the native and heat-denatured materials are, respectively:

$$e_0 = k \lambda_0 \quad [6]$$

$$e_1 = k \lambda_1 = k \lambda_0 \varphi \quad [7]$$

where k is the number of chambers. The number of ssDNA entities in the native and heat-denatured materials are, respectively:

$$s_0 = p_0 e_0 = p_0 k \lambda_0 \quad [8]$$

$$s_1 = p_1 e_1 = p_1 k \lambda_0 \varphi. \quad [9]$$

The total number of entities and the number of ssDNA entities in a two-component mixture are, respectively:

$$e_m = v_0 e_0 + v_1 e_1 \quad [10]$$

$$s_m = v_0 s_0 + v_1 s_1 \quad [11]$$

where the subscript “m” designates the mixture. In a two-component mixture of native and heat-denatured materials, the volume fraction of the native sample is:

$$v_0 = 1 - v_1 . \quad [12]$$

For $v_m = v_1$, the entity fraction of ssDNA in the mixture is then:

$$\begin{aligned} p_m &= s_m/e_m \\ &= [(1 - v_m)p_0 k \lambda_0 + v_m p_1 k \lambda_0 \varphi]/[(1 - v_m)k \lambda_0 + v_m k \lambda_0 \varphi] \\ &= [k \lambda_0((1 - v_m)p_0 + v_m p_1 \varphi)]/[k \lambda_0((1 - v_m) + v_m \varphi)] \\ &= [p_0 - v_m p_0 + v_m p_1 \varphi]/[1 - v_m + v_m \varphi] \\ &= [p_0 + v_m(p_1 \varphi - p_0)]/[1 + v_m(\varphi - 1)] . \end{aligned} \quad [13]$$

From Table 6: $p_0 = 0.114 \pm 0.005$, $p_1 = 0.968 \pm 0.015$, and $\varphi = 1.65 \pm 0.10$. Figure 19 compares the measured and calculated values for the $v_m = (0.20 \pm 0.02, 0.40 \pm 0.02, 0.80 \pm 0.02)$ mixtures of native and heat-denatured B summarized in Table 6.

Within the measurement uncertainties, the staircase measurements appear linearly related to the entity proportion of ssDNA in a sample.

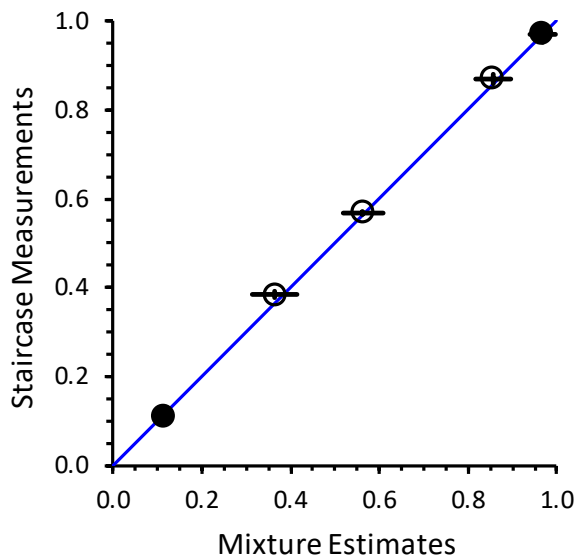


Figure 19. Staircase Measured Vs Estimated Proportions of ssDNA.

The solid black circles represent the staircase-measured fraction of ssDNA in the native and the heat-denatured SRM 2372 B. The open circles represent the staircase-measured and mixture estimated fraction of ssDNA in binary mixtures of the native and heat-denatured materials. The error crosses inside the open circles represent approximate standard uncertainties. The diagonal blue line represents equality between the staircase and mixture estimates.

3.4.3. Evolved Method for Preparing Mixtures

To prepare mixtures from a 10 ng/ μ L stock material:

- 1) Determine the number of mixtures to be made and what ratios are desired.
- 2) Determine the volume of the native DNA stock required and the volume of the heat denatured stock required.
- 3) Increase the volume prepared for the native and heat denatured materials by about 20 % to assure that you will have enough volume for the mixtures. Table 7 illustrates the volumes required for preparing 30 μ L of each DNA sample. As described in section 2.2.1, 30 μ L is enough for at least five ddPCR technical replicates each of native and heat-denatured stocks.

Table 7. Recipe for Preparing 30 μ L each of (0, 20, 40, 80, 100) % Volumetric Mixtures

ssDNA, %	V_0 , μ L	V_1 , μ L	V_{total} , μ L	C_{DNA} ng/ μ L
0	30	0	30	10
20	24	6	30	10
40	18	12	30	10
80	6	24	30	10
100	0	30	30	10
Totals	78	72	150	10
Prepare	90	90	180	10

- 4) Transfer 180 μ L of 10 ng/ μ L stock into a PCR tube.
 - a. Mix by vortexing then microcentrifuge.
- 5) Transfer 90 μ L of the native DNA into a labeled PCR tube; e.g., “B0”.
 - a. Transfer the tube to a water/ice storage block.
- 6) Transfer 30 μ L of the native DNA into multiple labeled PCR tubes; e.g., “B100”.
Note: Heat denaturing in aliquots of 30 μ L enables efficient and reproducible thermal transfer.
 - a. Heat-denature the DNA in these tubes. See Section 2.2.1 for the denaturation procedure.
 - b. Combine the tubes of denatured DNA into one of the tubes.
 - c. Mix by vortexing then microcentrifuge.
 - d. Transfer the tube to a water/ice storage block.
- 7) Label PCR tubes for the mixtures desired.
 - a. Pipet the pre-determined volumes of the Native DNA and the heat denatured DNA into each labeled tube.
 - b. Mix by vortexing then microcentrifuge.

4. ddPCR Ratio Analysis

As discussed in Section 1.3.2, the entity ratio $\varphi = \lambda_1/\lambda_0$ is a quantitative metric with proven utility for optimizing heat-denaturation conditions. We originally hoped that φ could also be used to estimate the absolute proportion of ssDNA entities in native samples. However, at least three factors may influence φ :

- p_0 , the proportion of ssDNA entities in the native sample at the time of measurement;
- χ , the fraction of dsDNA entities that are converted to ssDNA by heat-denaturation; and
- ω , the fraction of ssDNA entities that are rendered non-amplifiable or inaccessible by heat-denaturation.

For an ideal material and measurement process: $p_0 = 0$, $\chi = 1$, and $\omega = 0$. The ω term is required because, as demonstrated in Figure 9 and Figure 10, φ decreases with increasing treatment temperature and duration. Even an optimized heat-denaturation process may render some proportion of the entities inaccessible or non-amplifiable.

Let λ_0 be the total number of dsDNA and ssDNA entities that contain amplifiable and accessible target sequences in a native sample. The observable number of entities in its heat-denatured sibling, λ_1 , will be the sum of:

- $\lambda_0(1 - \chi)(1 - p_0)$, the number of dsDNA entities in the native sample that are not converted to ssDNA;
- $\lambda_0 2\chi(1 - \omega)(1 - p_0)$, twice the number of dsDNA entities that are converted to ssDNA, adjusted for the fraction of ssDNA that will not amplify; and
- $\lambda_0(1 - \omega)p_0$, the number of ssDNA entities in the native sample, adjusted for the fraction of ssDNA that will not amplify.

That is:

$$\begin{aligned}\lambda_1 &= \lambda_0(1 - \chi)(1 - p_0) + \lambda_0 2\chi(1 - \omega)(1 - p_0) + \lambda_0(1 - \omega)p_0 \\ &= \lambda_0(1 + \chi - \chi p_0 - \omega p_0 - 2\chi\omega + 2\chi\omega p_0) .\end{aligned}\quad [14]$$

Therefore:

$$\begin{aligned}\varphi &= \lambda_1/\lambda_0 \\ &= \lambda_0(1 + \chi - \chi p_0 - \omega p_0 - 2\chi\omega + 2\chi\omega p_0)/\lambda_0 \\ &= 1 + \chi - \chi p_0 - \omega p_0 - 2\chi\omega + 2\chi\omega p_0 .\end{aligned}\quad [15]$$

4.1. Limiting Values

Since φ is a function of three variables, $\varphi = f(p_0, \chi, \omega)$, φ by itself cannot provide unique estimates for the unknown quantities. However, any one of the three can be estimated given estimates for the other two:

$$p_0 = (\varphi - 1 - \chi + 2\chi\omega)/(2\chi\omega - \chi - \omega) ,\quad [16]$$

$$\chi = (\varphi - 1 + \omega p_0)/(1 - p_0 - 2\omega + 2\omega p_0) ,\quad [17]$$

$$\omega = (\varphi - 1 - \chi + \chi p_0)/(2\chi p_0 - p_0 - 2\chi) .\quad [18]$$

Values for φ can range from 0 to 2; that is from complete inactivation of all entities to complete denaturation without any inactivation of an entirely dsDNA native material. Values between 0 and 2 can be achieved by different combinations of values for p_0 (range 0 to 1), χ (range 0 to 1), and ω (range 0 to 1). Unique values for any of the three parameters can be estimated only when values of the other two are known.

However, upper limits on the possible values for each parameter can be established for a given φ value by fixing the other parameters at their ideal values: $p_0 = 0$, $\chi = 1$, and $\omega = 0$. For example, if $\varphi = 1.75$, then the maximum values for p_0 , χ , and ω are:

$$p_0 = (1.75 - 1 - 1 + 2 \cdot 1 \cdot 0) / (2 \cdot 1 \cdot 0 - 1 - 0) = -0.25 / (-1) = 0.25,$$

$$\chi = (1.75 - 1 + 0 \cdot 0) / (1 - 0 - 2 \cdot 0 + 2 \cdot 0 \cdot 0) = 0.75 / 1 = 0.75,$$

$$\omega = (1.75 - 1 - 1 + 1 \cdot 0) / (2 \cdot 1 \cdot 0 - 0 - 2 \cdot 1) = -0.25 / (-2) = 0.125.$$

Figure 20 displays these limits for φ from 0 to 2. As φ approaches its limit of 2, the values for the three parameters become increasingly constrained. At $\varphi = 2$ the parameter values become uniquely fixed at the ideal values. That is, the entities in the native material would need to be entirely dsDNA, denaturation must completely convert the dsDNA to ssDNA entities and must not inactivate any potentially amplifiable target sequence.

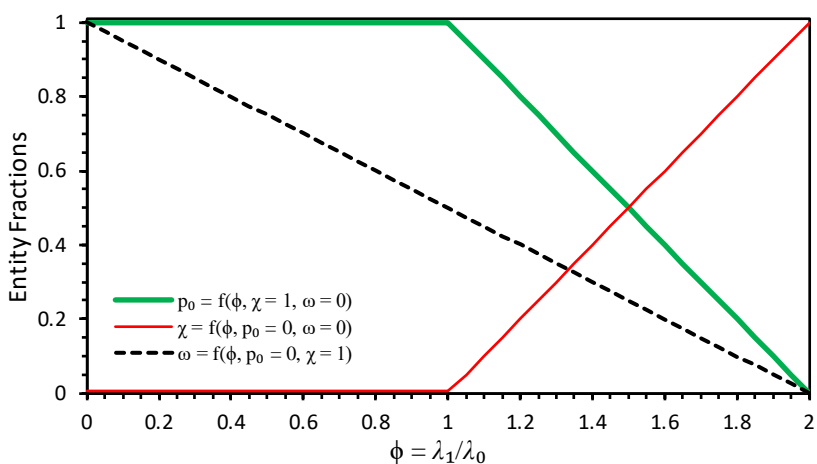


Figure 20. Limiting Values of $\varphi = f(p_0, \chi, \omega)$ Parameters as Functions of φ

The thick green curve represents the maximum value of p_0 compatible with a given φ value. The thin red line represents the minimum compatible value of χ . The dashed black line represents the maximum compatible value of ω .

Figure 21 displays the limiting values for p_0 at $\varphi = 1.75$ as functions of χ and ω when the other parameter is set to its ideal value (solid lines) and to a value slightly offset from the ideal (dashed lines). For the same 0.02 entity fraction change, the limiting value of p_0 is more sensitive to changes in ω than in χ .

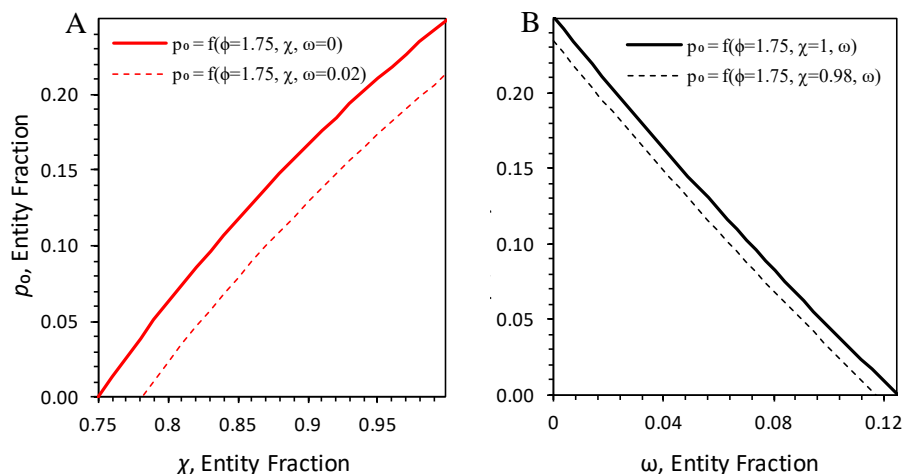


Figure 21. p_0 As Functions of χ and ω when $\phi = 1.75$

A) p_0 as a function of χ . The solid line is the relationship when $\omega = 0$; the dashed line when $\omega = 0.02$.
 B) p_0 as a function of ω . The solid line is the relationship when $\chi = 1$; the dashed line when $\chi = 0.98$.

4.1.1. Confounded Processes

The p_0 , χ , and ω parameters model the proportion of ssDNA in the native material, the efficiency of denaturation of dsDNA to ssDNA, and the inactivation of ssDNA. There are at least two other processes that are not explicitly addressed: 1) the proportion of ssDNA in the heat-treated material that renatures to dsDNA and 2) the proportion of dsDNA that is rendered non-amplifiable by the heat-denaturation process.

Renaturation combines two ssDNA entities containing target sequences back into one independently dispersing dsDNA entity. This is indistinguishable from one dsDNA entity failing to separate into two ssDNA entities. Therefore, renaturation is confounded with denaturation efficiency and contributes to the χ parameter.

Denaturation making one or both target sequences in a dsDNA entity non-amplifiable is indistinguishable from the process making one or two ssDNA entities non-amplifiable. Therefore, any target sequence becoming non-amplifiable during denaturation is confounded with inactivation of ssDNA entities and contributes to the ω parameter.

4.2. Ratio Results for SRMs 2372 B and SRM 2372a B

Table 8 lists ϕ estimates and the entities per droplet measurements they are derived from for the B and aB samples. These measurements were made over a period of almost seven months and with all 10 of the human nDNA dPCR assays.

The 95 % confidence intervals for B and aB are $\phi = 1.756 \pm 0.018$ and $\phi = 1.839 \pm 0.018$, respectively. From Equation 16, the limiting values for the proportion of ssDNA in the native materials are 0.244 ± 0.018 for B and 0.161 ± 0.018 for aB.

Figure 22 summarizes the λ_0 , λ_1 , and ϕ results in dot-and-bar format.

Table 8. ddPCR Ratio Analysis Results for Native and Heat-Denatured Samples

Date	Assay	SRM 2372 B ^a						SRM 2372a B ^a									
		#	λ_0	$u(\lambda_0)$	#	λ_1	$u(\lambda_1)$	φ	$u(\varphi)$	#	λ_0	$u(\lambda_0)$	#	λ_1	$u(\lambda_1)$	φ	$u(\varphi)$
04/13/18	NEIF									5	0.2417	0.0029	5	0.4521	0.0032	1.871	0.026
04/16/18	NEIF	5	0.2897	0.0049	5	0.5114	0.0038	1.765	0.033								
04/25/18	NEIF	5	0.2842	0.0046	5	0.5218	0.0037	1.836	0.033								
04/26/18	NEIF									5	0.2465	0.0023	5	0.4527	0.0057	1.836	0.029
04/30/18	NEIF	5	0.2871	0.0048	5	0.5034	0.0090	1.754	0.043	5	0.2348	0.0023	4	0.4426	0.0035	1.885	0.024
05/01/18	HBB1	5	0.2898	0.0033	5	0.5139	0.0055	1.773	0.028	5	0.2295	0.0019	5	0.4175	0.0045	1.819	0.024
05/02/18	HBB1	5	0.2774	0.0017	5	0.5091	0.0035	1.835	0.017	5	0.2384	0.0017	5	0.4427	0.0017	1.857	0.015
05/07/18	HBB1	5	0.2771	0.0017	5	0.4988	0.0044	1.800	0.019	5	0.2260	0.0020	5	0.4257	0.0037	1.884	0.024
05/08/18	2PR4	5	0.2769	0.0033	5	0.5015	0.0055	1.811	0.029	5	0.2264	0.0010	5	0.4313	0.0055	1.905	0.025
05/09/18	2PR4	5	0.2910	0.0035	5	0.5010	0.0042	1.722	0.025	5	0.2347	0.0022	5	0.4316	0.0052	1.839	0.028
05/10/18	2PR4	4	0.2866	0.0023	4	0.5088	0.0050	1.775	0.022	5	0.2311	0.0029	5	0.4335	0.0044	1.876	0.030
05/14/18	NEIF	5	0.2809	0.0039	5	0.5024	0.0027	1.789	0.027	5	0.2285	0.0029	5	0.4229	0.0032	1.851	0.028
05/17/18	ND6	5	0.2674	0.0024	5	0.4739	0.0054	1.772	0.026	5	0.2221	0.0020	5	0.4083	0.0034	1.838	0.022
05/21/18	2PR4	5	0.2873	0.0022	5	0.4912	0.0043	1.710	0.020	5	0.2284	0.0020	4	0.4153	0.0040	1.818	0.024
05/22/18	HBB1	5	0.2866	0.0017	5	0.5102	0.0077	1.780	0.029	5	0.2372	0.0011	5	0.4308	0.0051	1.816	0.023
05/23/18	NEIF									5	0.2417	0.0033	5	0.4404	0.0021	1.822	0.026
05/24/18	2PR4	5	0.2913	0.0016	5	0.4845	0.0051	1.664	0.020	5	0.2338	0.0027	5	0.4298	0.0051	1.838	0.030
05/25/18	ND6	4	0.2773	0.0013	5	0.4915	0.0040	1.773	0.016	5	0.2292	0.0020	5	0.4527	0.0030	1.975	0.021
05/29/18	ND6	4	0.2798	0.0033	5	0.4963	0.0047	1.774	0.027	5	0.2319	0.0014	5	0.4280	0.0036	1.846	0.019
05/30/18	POTP	5	0.2841	0.0014	5	0.4981	0.0025	1.753	0.012				4	0.4329	0.0028		
06/04/18	22C3	5	0.2931	0.0036	5	0.5017	0.0041	1.712	0.025	5	0.2300	0.0020	4	0.4417	0.0045	1.920	0.026
06/05/18	22C3	5	0.2871	0.0030	5	0.4839	0.0073	1.685	0.031	5	0.2303	0.0023	5	0.4180	0.0029	1.815	0.022
06/06/18	22C3	5	0.2912	0.0015	5	0.5239	0.0041	1.799	0.017	5	0.2396	0.0011	5	0.4357	0.0064	1.819	0.028
06/08/18	2PR4	5	0.2870	0.0012	5	0.5151	0.0055	1.795	0.021	5	0.2340	0.0033	5	0.4376	0.0066	1.870	0.039
06/08/18	NEIF	4	0.2934	0.0022	5	0.5210	0.0040	1.776	0.019	5	0.2366	0.0031	5	0.4417	0.0046	1.867	0.032
06/11/18	NR4Q	5	0.2844	0.0034	5	0.4969	0.0045	1.747	0.026	5	0.2373	0.0031	5	0.4476	0.0054	1.886	0.033
06/12/18	2PR4	5	0.2937	0.0019	5	0.5082	0.0017	1.731	0.013								
06/12/18	NEIF	5	0.2846	0.0026	5	0.5182	0.0054	1.821	0.025								
06/14/18	2PR4	7	0.2860	0.0026	7	0.4931	0.0025	1.724	0.018								
06/18/18	2PR4	7	0.2905	0.0021	7	0.5402	0.0052	1.859	0.022								
06/19/18	POTP	5	0.2856	0.0027	5	0.5018	0.0029	1.757	0.019	5	0.2302	0.0027	5	0.4375	0.0051	1.900	0.031
06/20/18	ND6	5	0.2859	0.0043	5	0.4960	0.0038	1.735	0.029	5	0.2395	0.0025	5	0.4264	0.0025	1.780	0.021
06/20/18	NR4Q	5	0.2945	0.0028	5	0.5080	0.0018	1.725	0.018	5	0.2376	0.0015	5	0.4328	0.0041	1.821	0.021
06/21/18	ND6	5	0.2890	0.0026	5	0.4880	0.0075	1.689	0.030	5	0.2338	0.0029	5	0.4242	0.0042	1.814	0.029

		SRM 2372 B ^a						SRM 2372a B ^a									
Date	Assay	#	λ_0	$u(\lambda_0)$	#	λ_1	$u(\lambda_1)$	φ	$u(\varphi)$	#	λ_0	$u(\lambda_0)$	#	λ_1	$u(\lambda_1)$	φ	$u(\varphi)$
06/22/18	ND14	5	0.2784	0.0023	2	0.4955	0.0030	1.780	0.018	5	0.2304	0.0018	5	0.4353	0.0070	1.889	0.034
06/25/18	ND14	5	0.2710	0.0026	5	0.5050	0.0034	1.864	0.022	5	0.2411	0.0016	5	0.4519	0.0042	1.874	0.021
06/26/18	D9	5	0.2806	0.0016	5	0.5163	0.0042	1.840	0.018	5	0.2361	0.0019	5	0.4405	0.0047	1.866	0.025
07/09/18	ND6	5	0.2879	0.0033	4	0.5010	0.0032	1.740	0.023	5	0.2371	0.0025	5	0.4260	0.0063	1.797	0.033
07/10/18	D5	5	0.2891	0.0020	5	0.4775	0.0038	1.652	0.017	3	0.2313	0.0017	4	0.4141	0.0041	1.790	0.022
07/16/18	ND14	5	0.2847	0.0039	5	0.4759	0.0065	1.672	0.032	5	0.2327	0.0010	5	0.4249	0.0085	1.826	0.037
08/07/18	2PR4	5	0.2752	0.0039	4	0.4758	0.0060	1.729	0.033	5	0.2330	0.0030	5	0.4139	0.0075	1.776	0.040
08/09/18	POTP	5	0.2793	0.0031	5	0.4788	0.0043	1.714	0.025	5	0.2240	0.0036	4	0.4129	0.0080	1.844	0.046
08/14/18	2PR4	4	0.2743	0.0039	4	0.4750	0.0065	1.732	0.034								
08/14/18	2PR4									5	0.2443	0.0020	5	0.4271	0.0063	1.749	0.030
08/14/18	HBB1									5	0.2428	0.0030	5	0.4305	0.0052	1.773	0.031
08/17/18	NEIF	4	0.2771	0.0045	4	0.4927	0.0030	1.778	0.031								
08/21/18	NEIF	4	0.2709	0.0012	4	0.4999	0.0032	1.845	0.014								
09/17/18	HBB1									5	0.2447	0.0048	5	0.4526	0.0072	1.850	0.047
09/18/18	HBB1	5	0.2689	0.0052	5	0.4772	0.0064	1.775	0.042								
10/30/18	ND14	5	0.2746	0.0028	5	0.4628	0.0024	1.685	0.020	5	0.2363	0.0017	4	0.4034	0.0062	1.708	0.029
10/31/18	D5	5	0.2952	0.0014	5	0.4966	0.0076	1.682	0.027	5	0.2432	0.0013	4	0.4346	0.0106	1.788	0.045
11/05/18	D5									5	0.2408	0.0025	4	0.4310	0.0055	1.790	0.029
11/06/18	ND14	5	0.2801	0.0032	5	0.4594	0.0039	1.640	0.024	5	0.2267	0.0024	5	0.4226	0.0036	1.864	0.026
Summaries ^b		<i>N</i> :	46		46		46			42		43		42			
		\bar{x} :	0.2836		0.4979		1.756			0.2346		0.4315		1.839			
		<i>s</i> :	0.0072		0.0166		0.056			0.0060		0.0124		0.049			
	\bar{u} :		0.0030		0.0048		0.025			0.0024		0.0052		0.029			
		$u(\bar{x})$:	0.0012		0.0026		0.009			0.0010		0.0021		0.009			
		$U_{95}(\bar{x})$:	0.0023		0.0051		0.018			0.0020		0.0041		0.018			

- a* # = number of technical replicates, λ_0 = entities per droplet in the native sample, $u()$ = standard uncertainty of the quantity within the (), λ_1 = entities per droplet in the heat-denatured sample, $\varphi = \lambda_1/\lambda_0$.
- b* *N* = number of independent results, \bar{x} = mean, *s* = standard deviation, \bar{u} = pooled standard uncertainty, $u(\bar{x})$ = standard uncertainty of the mean, $U_{95}(\bar{x})$ = expanded uncertainty. The true value of the measurand is, with about a 95 % level of confidence, expected to be within the interval $\bar{x} \pm U_{95}(\bar{x})$.

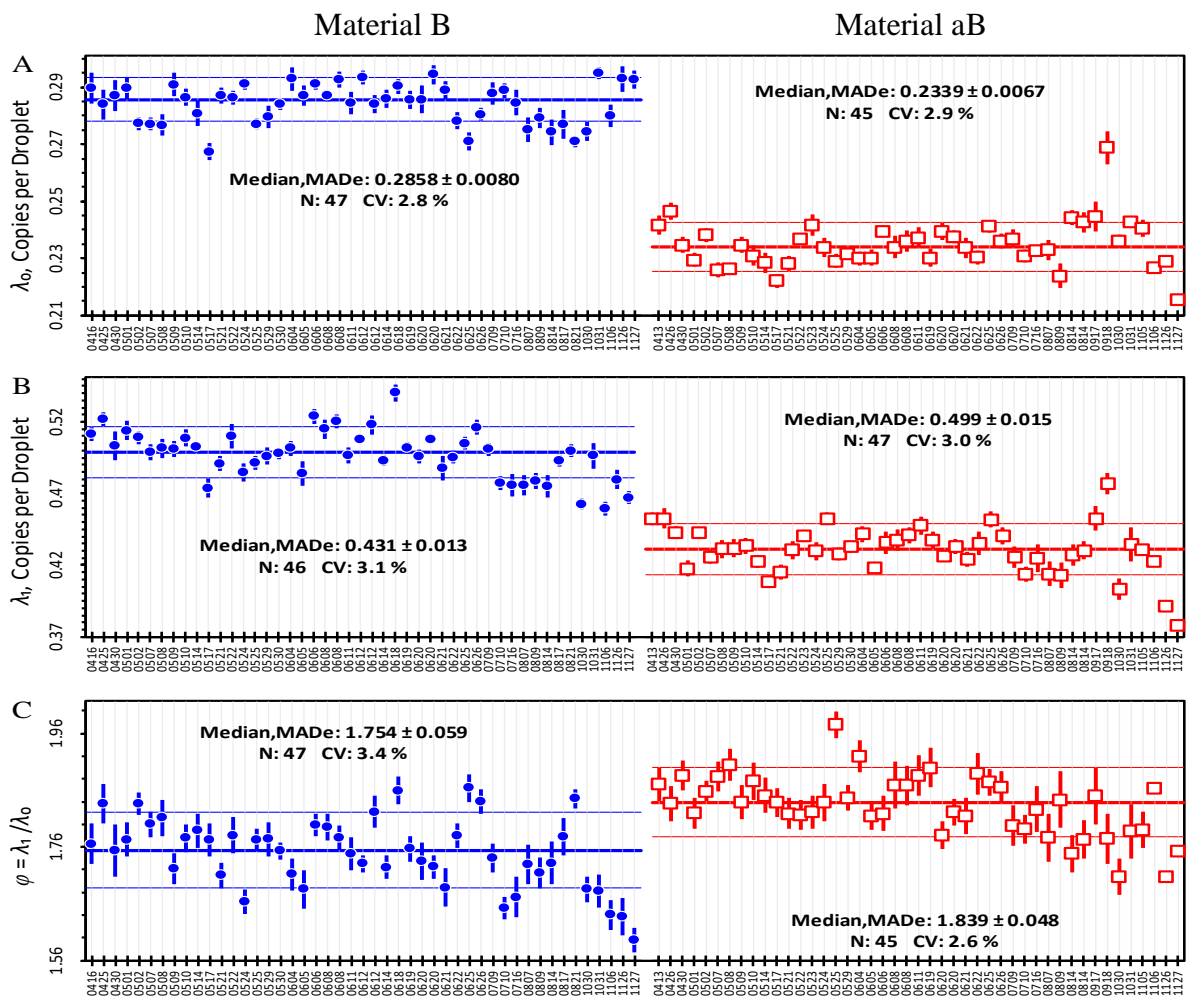


Figure 22. Summary of λ_0 , λ_1 , and φ

These dot-and-bar plots display λ_0 , λ_1 , and φ results for independent 1→5 volumetric dilutions of SRMs 2372 B and 2372a B. Each dot-and-bar represents the mean \pm 1 standard uncertainty of four to seven technical replicates. The data are presented in order of increasing date, indicated as month and day of 2018. The results to the left (blue) of each subplot are SRM 2372 B; those to the right (red) are SRM 2372a B. The horizontal lines represent estimates of the average \pm standard uncertainty for each population. Subplot A) displays the λ_0 results for the native samples, B) the λ_1 heat-denatured sample, and C) the $\varphi = \lambda_1/\lambda_0$ ratios.

4.3. Variability of the Heat-Denaturation Process

We previously estimated our ddPCR repeatability precision, expressed as a relative standard deviation (coefficient of variation, CV), to be 2.6 % [6, Table S6]. The variability of the λ_0 measurements for native B and aB are close to this limiting value, with robust CV estimates of 2.8 % for B and 2.9 % for aB. The robust CVs for the λ_1 measurements of the heat-denatured materials are slightly larger: 3.1 % for B and 3.0 % for aB. Since the native and heat-denatured materials are evaluated at the same time using the same equipment and reagents, the CV for the denaturation process variability component is $\sqrt{3.1^2 - 2.8^2} = 1.3$ % for the B material and $\sqrt{3.0^2 - 2.9^2} = 0.8$ % for aB. We speculate that the slightly greater variability of the B material may be, like the increased 260 nm absorbance, related to a looser tertiary structure.

The 95 % confidence intervals for the B and aB measurements of λ_0 and λ_1 do not overlap; however, the populations of the φ values are not well separated. This indicates that individual determinations of φ must be interpreted with great caution, even when the dPCR process itself is in excellent statistical control.

4.4. Correlations Between Measurement Results

Figure 23 examines the relationships between the results for the B and aB materials when the measurements were made in the same ddPCR run. To keep extreme values from dominating the evaluation, the square of the Pearson's correlation (R^2) between the paired (B, aB) λ_0 , λ_1 , and φ results is calculated using just the central 75 % of the available pairs. Since the results for every (B, aB) pair are for independent samplings of the two materials, whatever correlation between the results of the two materials must reflect factors that influence both materials: dPCR assay, parallel changes in the materials with time (e.g., evaporation), differences in the measurement process, differences in the reagents (e.g., composition of the reaction mixture), or environmental factors (e.g., laboratory temperature, humidity, barometric pressure).

The low correlation between the λ_0 results for the native materials, $R^2 = 0.08$ (see Figure 23 A), reflects the absence of systematic differences among the 10 dPCR assays: the differences among the highly repeated NEIF results are essentially as large as those between all assays (see Figure 22 A). Likewise, the λ_0 results do not appear to trend with analysis date for either material.

The strong correlation between the λ_1 results for the B and aB heat-treated materials, $R^2 = 0.59$ (see Figure 23 B), appears to be related to small differences in the heat-denaturation process. Since heating and cooling was accomplished for all the (B, aB) pairs using the same thermocycler and program, the correlation is most plausibly related to small variations in sample mixing and storage.

The modest correlation between the φ results, $R^2 = 0.34$ (see Figure 23 C), suggests that there are some in-common influence factors in the processing of the native and heat-denatured samples.

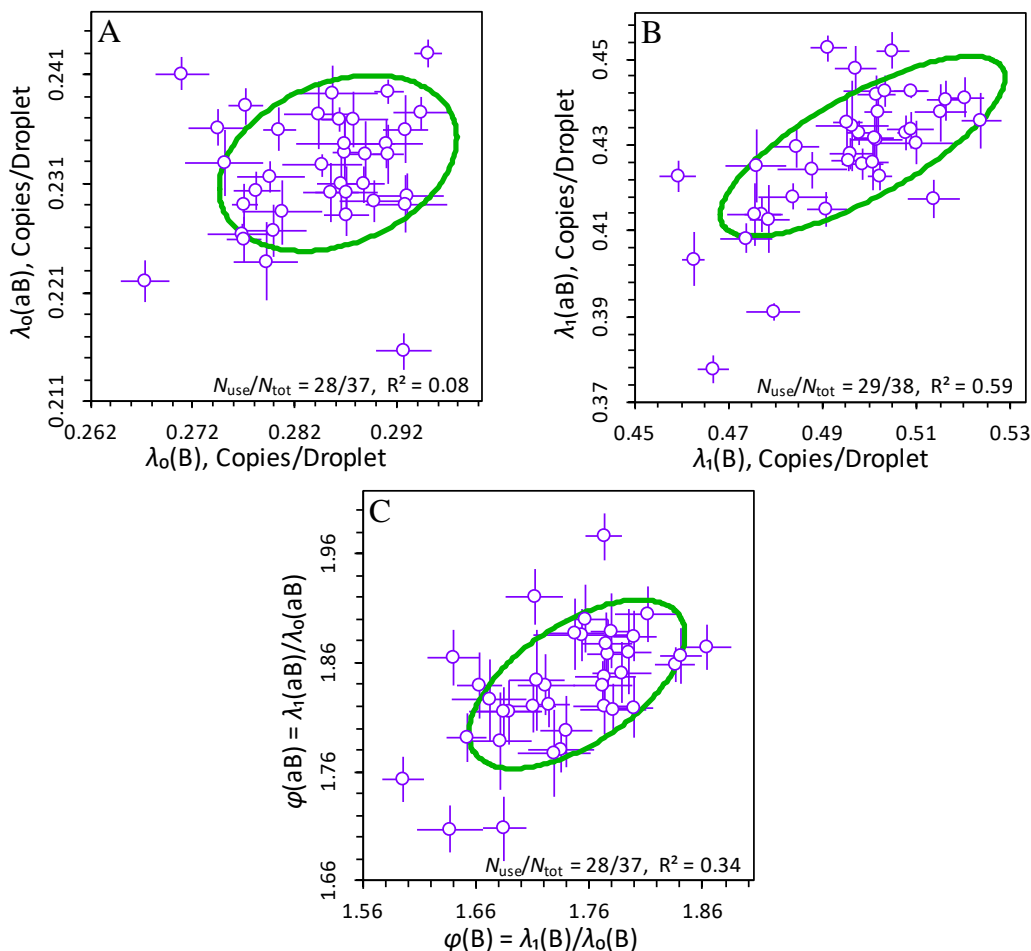


Figure 23. Correlations Between Materials Analyzed Together

These scatterplots compare the λ_0 , λ_1 , and $\varphi = \lambda_1/\lambda_0$ results for SRM 2372a B relative to those for SRM 2372 B when the two materials were evaluated in the same ddPCR session. Each dot-and-cross represents the mean \pm standard deviation of the mean of four to seven technical replicates of each material. Each ellipse (green) encloses the central 75 % of the bivariate distribution. The legend within each scatterplot identifies the total number of (B, aB) pairs, N_{tot} ; the number of pairs in the central 75 %, N_{use} ; and the square of the correlation among the N_{use} pairs. Subplot A) displays the λ_0 results for the native samples, B) the λ_1 heat-denatured samples, and C) the $\varphi = \lambda_1/\lambda_0$ ratios.

4.5. SRM 2372 B Mixture

Table 9 lists the ddPCR φ values for the three sets of mixtures discussed in Section 3.4 and the corresponding limiting proportion of ssDNA estimated from Equation 16 assuming the ideal values for χ and ω : 1 and 0.

Table 9. ddPCR Ratio Results for SRM 2372 B Mixtures

Mtrl ^b Date Assay			Volume % of Heat-Denatured Sample ^a															
			$v_m = 0\%$				$v_m = 20\%$				$v_m = 40\%$				$v_m = 80\%$			
			φ_0	$u(\varphi_0)$	\hat{p}_0	$u(\hat{p}_0)$	φ_{20}	$u(\varphi_{20})$	\hat{p}_{20}	$u(\hat{p}_{20})$	Φ_{40}	$u(\varphi_{40})$	\hat{p}_{40}	$u(\hat{p}_{40})$	Φ_{80}	$u(\varphi_{80})$	\hat{p}_{80}	$u(\hat{p}_{80})$
UB	08/29/18	HBB1	1.789	0.052	21.1	5.2	1.617	0.041	38.3	4.1	1.413	0.032	58.7	3.2	1.183	0.029	81.7	2.9
UB	08/31/18	POTP	1.717	0.068	28.3	6.8	1.577	0.068	42.3	6.8	1.433	0.065	56.7	6.5	1.135	0.048	86.5	4.8
B	09/04/18	POTP	1.745	0.083	25.5	8.3	1.587	0.058	41.3	5.8	1.385	0.044	61.5	4.4	1.157	0.039	84.3	3.9
Summaries ^c			N :	3	3		3	3	3	3	3	3	3	3				
			\bar{x} :	1.750	25.0		1.594	40.6	1.410	59.0	1.159	84.1						
			s :	0.037	3.7		0.021	2.1	0.024	2.4	0.024	2.4						
			\bar{u} :		0.069	6.9		0.057	5.7		0.049	4.9		0.040	4.0			
			$u(\bar{x})$:	0.045	4.5		0.035	3.5	0.031	3.1	0.027	2.7						

- ^a v_m = mixture by volume of $m\%$ heat-denatured with $(100-m)\%$ native material,
 φ_0 = ratio of entities in the heat-denatured sample to the entities in the native sample,
 \hat{p}_0 = estimated upper limit on the percent ssDNA in the native sample,
 φ_{20} = ratio of entities in the heat-denatured sample to the entities in the volumetric mixture of 80% native and 20% heat-denatured sample,
 \hat{p}_{20} = estimated upper limit on the percent ssDNA in the 80% native and 20% heat-denatured mixture
 φ_{40} = ratio of entities in the heat-denatured sample to the entities in the volumetric mixture of 60% native and 40% heat-denatured sample,
 \hat{p}_{40} = estimated upper limit on the percent ssDNA in the 60% native and 40% heat-denatured mixture
 φ_{80} = ratio of entities in the heat-denatured sample to the entities in the volumetric mixture of 20% native and 80% heat-denatured sample
 \hat{p}_{80} = estimated upper limit on the percent ssDNA in the 20% native and 80% heat-denatured mixture,
 $u()$ = standard uncertainty of the quantity within the ().
- ^b material used to prepare mixture. UB is the high-concentration primary (“undiluted”) stock material used to prepare SRM 2372 B in 2006.
- ^c N = number of independent results, \bar{x} = mean, s = standard deviation, \bar{u} = pooled standard uncertainty, $u(\bar{x})$ = standard uncertainty of the mean.

Figure 24 compares the upper limit p_0 values estimated from the ratio analysis of Equation 16 to mixture proportions estimated from Equation 13 using two sets of assumptions about the heat denaturation process's efficiency in producing and propensity to damage ssDNA. The p_0 values in subplot A are estimated assuming that heat-denaturation is completely efficient and does no damage: $\chi = 1$ and $\omega = 0$. The mixture estimates use the corresponding limiting values for the proportions of ssDNA in the native and heat-denatured materials, $p_0 = 0.250$ and $p_1 = 1.000$. The values in subplot B are estimated using χ and ω values that provide a best fit to the mixture proportions estimated from the cdPCR staircase analysis in section 3.4: $p_0 = 0.116$ and $p_1 = 0.968$.

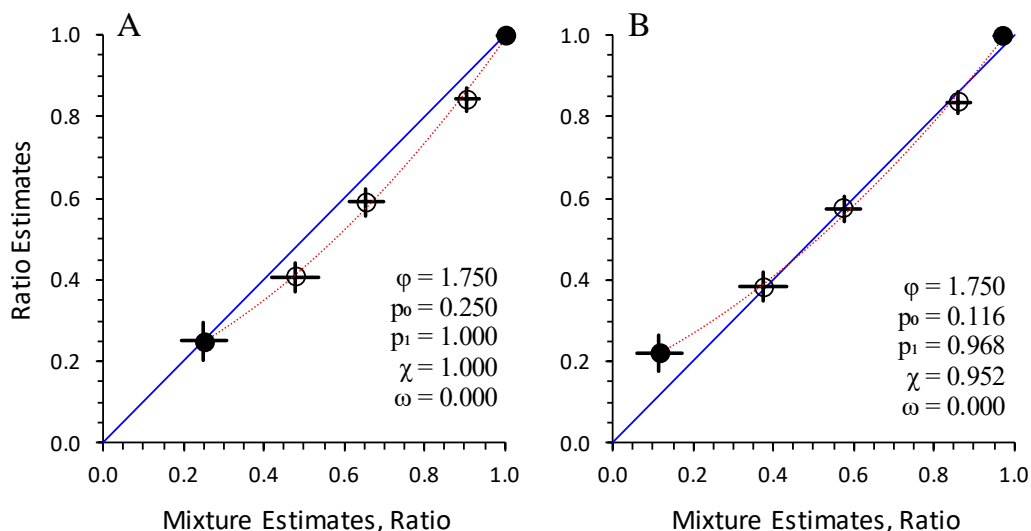


Figure 24. Ratio Measured Vs Estimated Proportions of ssDNA.

The solid black circles represent the mixture and ratio estimates of the ssDNA fraction in the native and heat-denatured SRM 2372 B; the open circles represent estimates for the binary mixtures of the native and heat-denatured materials. The error crosses inside the open circles represent approximate standard uncertainties. The solid diagonal lines represent equality between the mixture and ratio estimates. The dotted lines represent quadratic fits to the data.

The improved agreement between the estimates in subplot B strongly suggests that heat-denaturation is not necessarily completely efficient nor non-damaging. While subplot B displays results ratio analysis parameter values of $\chi = 0.952$ and $\omega = 0$, these values are not unique. Depending on the model used to generate the “best fit” of the ratio estimates to the staircase proportions, many parameter value combinations provide about the same improved agreement.

5. ddPCR Enzyme Analysis

Type II restriction endonucleases (enzymes) digest (“cut”) dsDNA at specific base-pair sequences [27]. If an enzyme can be identified that cuts DNA within the target sequence of a PCR assay such that amplification is prevented and if that enzyme cuts only dsDNA, then comparing ddPCR results for the native sample before and after cutting provides a (naïve) estimate of the fraction ssDNA in a sample:

$$q_0 = \lambda_0(\text{Enzyme})/\lambda_0 \quad [19]$$

where $\lambda_0(\text{Enzyme})$ is the average number of entities per droplet after the native sample has been enzymatically digested.

However, ssDNA can form transient to stable local dsDNA structures through self- and duplex hybridization [28,29]. If the enzyme’s recognition sequence lies within such a structure, the nominally ssDNA may become locally dsDNA and so be cut. The locally duplex structure may not need to perfectly mimic the enzymes’ recognition sequence since some type II enzymes are tolerant of mis-match pairings [30]. In any case the rate of ssDNA cutting is likely to be slower than that for fully dsDNA [26].

While ideally enzyme and assay combinations can be identified that effectively stop amplification of dsDNA entities but do not cut ssDNA, less than ideal combinations may suffice if the rate of ssDNA cutting is slow enough. The fraction ssDNA in the native sample that is rendered non-amplifiable can be estimated by comparing ddPCR results for the heat-denatured sample before and after cutting:

$$\psi = \lambda_1(\text{Enzyme})/\lambda_1 \quad [20]$$

where $\lambda_1(\text{Enzyme})$ is the average number of entities per droplet after the heat-denatured sample has been enzymatically digested. The “true” (or at least less naïve) fraction of ssDNA in the native sample can then be estimated as:

$$p_0 = q_0/\psi . \quad [21]$$

5.1. Enzyme:Assay Combinations

Cutting the template DNA for an assay anywhere within the interval between the 3’-end of the two primer sites should prevent PCR amplification. Cutting the template within the 3’-to-5’ interval of either primer site may not prevent amplification if the residual sequence is long enough to enable even inefficient primer binding. We identified enzymes that had the potential to cut between the primer binding sites of the human nDNA PCR assays described in Table 1 using SeqBuilder Pro software (DNASTAR Inc., Madison, WI USA). Chromosome sequence data were obtained using the “blastn suite” of the U.S. National Library of Medicine’s Standard Nucleotide BLAST system [31].

All readily available enzymes that cut between the primer sites of at least one of the 10 assays were purchased from New England BioLabs, Inc. (Ipswich, MA USA). Table 10 summarizes the 34 enzyme:assay combinations that we investigated, including several combinations that cut within primer sequences.

Table 10. Nuclease Cut Sites for the Human nDNA dPCR Assays

Assay	Sequence (Forward Primer – Probe – Reverse Primer) and Nuclease Cut Sites
NEIF	<p>GC...TCTCATG CAGTTGTCA GAAG CTGCTG...AG CG...AGA GTAC GTCAACAG TCTTC GACGAC...TC</p> <p>▶...▶ ◀...▶ ◀...▶ ◀...▶ ◀...▶</p> <p><i>Nla</i>III <i>Hpy</i>CH4V <i>Hpy</i>188I <i>Alu</i>I</p>
2PR4	<p>CG...TTTACC TTTGTCTACCACTTG CAAAG CT GG CCTTTAG...CAAGACTTCT GAATGTTTTTCATGTAGCA GC...AAATGGAAACAGATGGTGAAC GTTTC GA CC GGAAATC...GTTCTGAAG ACTTACAAAAGTAACATCGT</p> <p>▶...▶ ◀...▶ ◀...▶ ◀...▶ ◀...▶ ◀...▶ ◀...▶</p> <p><i>Hpy</i>CH4V <i>Alu</i>I <i>Hae</i>III <i>Hpy</i>188I <i>Cac</i>8I</p>
POTP	<p>CC...TTTCACCAACTGA AATATGG CCAAGGCCAAAACCCATG T GG...AAAGTGGTTGAC TTTATACC GGTTTCCGTTTTGG GTACA</p> <p>▶...▶ ◀...▶ ◀...▶ ◀...▶</p> <p><i>Xcm</i>I <i>Hae</i>III <i>Nla</i>III</p>
NR4Q	<p>TGGTGGGAATGTTCTTCA GATGATGTATGAGAAACC TGAACGATGGTCT...CAAA...GA ACCACCCCTTACAAGAAG TCTACTACATACTCTTTGGA CTTGCTACCAGA...GTTT...CT</p> <p>▶...▶ ◀...▶ ◀...▶ ◀...▶</p> <p><i>Hpy</i>188I <i>Bcc</i>I</p>
D5	<p>TTCATACAGGCA AGCAATG CATAATAATATCAGGGTAAACAGGG AATCTATTACTG CAAACATTTACCCTTAAG AAGTATGTCGGT TCGTTAC GTATTATTATAGTCCCAATTGTCCCTTA GATAATGAC GTTTGTAATGGGAAATTC</p> <p>▶...▶ ◀...▶ ◀...▶ ◀...▶ ◀...▶ ◀...▶</p> <p><i>Cac</i>8I <i>Hpy</i>CH4V <i>Hinf</i>I <i>Hpy</i>CH4V</p>
ND6	<p>GCATG GCTG AGTCTAAGTCAAAGG CCCAGAAC CA AGGAAGATGGTGA...TTTT...GC C GTACCGACTCA GATTCAGTTTC GGGTCTTGGTTC CTTCTACCCT...AAAA...CG</p> <p>▶...▶ ◀...▶ ◀...▶ ◀...▶ ◀...▶ ◀...▶</p> <p><i>Nla</i>III <i>Hinf</i>I <i>Hae</i>III <i>Bcc</i>I <i>Sty</i>I&<i>Bsa</i>JI</p>
D9	<p>GG...TTGGGCAGGGCACATG AATGAG...CC CC...AACCCGTCCCGT GTACTTACTC...GG</p> <p>▶...▶ ◀...▶ ◀...▶</p> <p><i>Nla</i>III</p>
HBB1	<p>GC...TCCTAAGCCAGTGCCAGAAGAGC CAAGGACAG...CC CG...AGGATTCGGTCACGGTCTTCTCGGTTC CTGTC...GG</p> <p>▶...▶ ◀...▶ ◀...▶</p> <p><i>Sty</i>I&<i>Bsa</i>JI</p>
ND14	<p>TC...TCTC...TTCA G ATTCAG GACTG AATCACACCATCAGTT TTTCT G AGTCTCCAGTTTG CA GGCAGCCGA...CC AG...AGAG...AAG TCTAA G TCTGACTTA GTGTGGTAGTCAA AAG ACTCA GAGGTCAAAC GT CCGTCGGCT...GG</p> <p>▶...▶ ◀...▶ ◀...▶ ◀...▶ ◀...▶ ◀...▶ ◀...▶ ◀...▶ ◀...▶</p> <p><i>Hpy</i>188I <i>Hinf</i>I <i>Hpy</i>188I <i>Hinf</i>I <i>Bcc</i>I <i>Hinf</i>I <i>Hpy</i>188I <i>Cac</i>8I <i>Hinf</i>I <i>Hpy</i>CH4V</p>
22C3	<p>CC...TGCCCAATG TTCTGG CCTTGACCTCAGGTGATTG CAT...CT GG...ACGGG GTACAAGACC GGAAGTGGAGTCCACTAAAC GTA...GA</p> <p>▶...▶ ◀...▶ ◀...▶ ◀...▶</p> <p><i>Nla</i>III <i>Hae</i>III <i>Hpy</i>CH4V</p>

Each row describes one dPCR assay and all restriction enzymes investigated as potentially making its target non-amplifiable. The first and second lines in each row display the forward and reverse strands, where A = adenine, C = cytosine, G = guanine, and T = thymine. Cut sites are marked with “|”, with lines connecting overhanging bases. Forward primer sequences are in red, reverse primers in orange, and probes in green. Bases located in the flanking regions between the primer and probe sequences are in lavender, “...” represents two or more bases that are not pertinent to any cut site. The third line indicates the limits of the forward primer (▶—▶), probe (◀—▶), and reverse primer (◀—◀). Cuts that prevented amplification are marked with “↑”, cuts that did not prevent amplification are marked with “✕”. The bottom line or lines identify the restriction enzymes.

Table 11 provides information on the enzymes used in our studies, including several used to evaluate the impact of enzyme cutting exterior to an assay's amplicon.

Table 11. Restriction Enzymes.

Enzyme	Restriction Mode ^a	Incubation ^b		Units ^c per μ L	Relative Cost ^d
		Temp.	Time		
<i>AluI</i>	5' ...AG CT... 3' 3' ...TC GA... 5'	37 °C	5-15 min	10	5.5
<i>ApoI</i> -HF ^e	5' ...R AATTY... 3' 3' ...YTTAA R... 5'	37 °C	5-15 min	20	5.7
<i>BccI</i>	5' ...CCATC N N N N N... 3' 3' ...GGTAG N N N N N ... 5'	37 °C	60 min	10	5.5
<i>BsaJI</i>	5' ...C C N N G G... 3' 3' ...G G N N C C... 5'	60 °C	60 min	10	5.5
<i>Cac8I</i>	5' ...GCN NGC... 3' 3' ...CGN NCG... 5'	37 °C	5-15 min	5	59.0
<i>HaeIII</i>	5' ...GG CC... 3' 3' ...CC GG... 5'	37 °C	5-15 min	10	1.8
<i>HinfI</i>	5' ...G A N T C... 3' 3' ...C T N A G... 5'	37 °C	5-15 min	10	1.0
<i>Hpy188I</i>	5' ...TCN GA... 3' 3' ...AG NCT... 5'	37 °C	60 min	10	5.5
<i>HpyCH4V</i>	5' ...TG CA... 3' 3' ...AC GT... 5'	37 °C	5-15 min	5	54.9
<i>MseI</i> ^e	5' ...T TAA... 3' 3' ...AAT T... 5'	37 °C	5-15 min	10	11.0
<i>NlaIII</i>	5' ...CATG ... 3' 3' ... GTAC... 5'	37 °C	5-15 min	10	11.0
<i>SacI</i> ^e	5' ...GAGCT C... 3' 3' ...C TCGAG... 5'	37 °C	5-15 min	20	2.4
<i>StyI</i> -HF	5' ...C C W W G G... 3' 3' ...G G W W C C... 5'	37 °C	5-15 min	20	1.9
<i>XcmI</i>	5' ...CCANNNNN NNNNTGG... 3' 3' ...GGTNNNN NNNNNACC... 5'	37 °C	60 min	5	5.5

^a N: can be (A, C, G, T); R: must be (A, G); W: must be (A, T); Y: must be (C, T).

^b Recommended "CutSmart" conditions [32]

^c One unit of enzyme is defined as the quantity that will "completely digest 1 μ g of substrate DNA in a 50 μ L reaction in 60 minutes."

^d 2018 cost per unit of enzyme relative to the cost per unit of *HinfI*, the least expensive of those used.

^e Does not cut within the amplicon of any of the 10 nDNA assays evaluated.

5.1.1. Evolved Method for Preparing Restriction Enzyme Reactions

To fully characterize one material requires ddPCR analysis of four samples: 1) native, 2) enzyme-native, 3) heat-treated, and 4) enzyme-heat-treated. The following method describes the preparation of the enzyme-native and enzyme-heat-treated samples. Since enzyme restriction dilutes stock DNA 1 to 5, the stock native and stock heat-treated samples require a 1 to 5 dilution prior to ddPCR analysis.

While the enzymes are supplied at concentrations ranging from (5 to 20) units per microliter, we use the same 0.5 μL of enzyme and 5 μL of ≈ 50 ng/ μL stock DNA for all reactions. For even the most dilute enzymes, the resulting $(5 \text{ units}/\mu\text{L}) \times (0.5 \mu\text{L}) = 2.5$ units is in 10-fold excess of the nominal quantity needed to digest the $(5 \mu\text{L}) \times (50 \text{ ng}/\mu\text{L}) / (1000 \text{ ng}/\mu\text{g}) = 0.25 \mu\text{g}$ of DNA.

Table 12 details the recipe used to prepare 25 μL of enzyme-treated sample starting with ≈ 50 ng/ μL stock DNA and the minimal useful stock DNA concentration, 11 ng/ μL . For stock DNA concentrations between these values the sum of the water and DNA volumes must equal 22 μL .

Table 12. Recipe for 25 μL Enzyme Reactions

Component	Concentration	Volume
Restriction Buffer	10X	2.5
Restriction Enzyme	5 to 20 units/ μL	0.5
PCR Grade Water		17.0 to 0
DNA	$\approx (50 \text{ to } 11) \text{ ng}/\mu\text{L}$	5.0 to 22.0
Total		25.0

The 25 μL of enzyme-treated sample is enough volume for five technical replicates per sample. Technical replicates are desired to achieve adequate analytical confidence in the ddPCR assay results. We typically use five; three is acceptable as a lower limit.

- 1) Determine how many different materials are to be tested together. Two enzyme-treated samples are required to analyze one material: 1) enzyme-native and 2) enzyme-heat-treated.
- 2) For N materials, prepare a bulk solution by combining $(2N+0.5)$ times the (17 μL water, 2.5 μL 10X buffer, and 0.5 μL enzyme) in a suitably sized PCR tube.
 - a. The additional half-reaction accommodates loss to pipetting and tube-walls.
 - b. Enzyme reactions require use of a proprietary reaction buffer, supplied with each enzyme purchase in 10-fold (10X) concentration.
- 3) Mix the bulk solution gently by finger flicking then microcentrifuge.
- 4) For every enzyme reaction (i.e., native or heat-treated):
 - a. aliquot 20 μL of the bulk solution into labeled PCR tubes,
 - b. add 5 μL of the ≈ 50 ng/ μL stock DNA (native or heat-treated),
 - c. gently mix by finger flicking then microcentrifuge.
- 5) Place all tubes in a well-calibrated thermocycler.
- 6) Incubate for the appropriate time at the appropriate temperature.
 - a. The incubation temperature for all but one of the enzymes studied is 37 $^{\circ}\text{C}$.

- b. While the supplier’s recommended incubation time for many of the enzymes is “5-to-15 minutes”, we adopted 60 min for all enzymes (see below).
- 7) Remove from heat source.
 - a. Mix well by vortexing then microcentrifuge.
 - b. Store on water/ice until use.

5.1.2. Loss of Entities Due to the Restriction Process

Enzyme digestion requires subjecting DNA to conditions that differ from those experienced in ddPCR analysis of native samples, including higher temperature during incubation and higher salt content in the reaction mixture. Any manipulation of extracted DNA has the potential to reduce λ by rendering entities non-amplifiable or relatively inaccessible [7]. The restriction buffer adds 50 mmol/L potassium acetate and 10 mmol/L magnesium acetate to the reaction mixture [32]. If our speculation in section 2.4 is correct, this may be enough to “zip up” not-quite-completely-separated ssDNA, thus reducing the number of independently dispersing entities. Figure 25 describes results from studies that evaluated the magnitude of loss that can be attributed to steps of the restriction process.

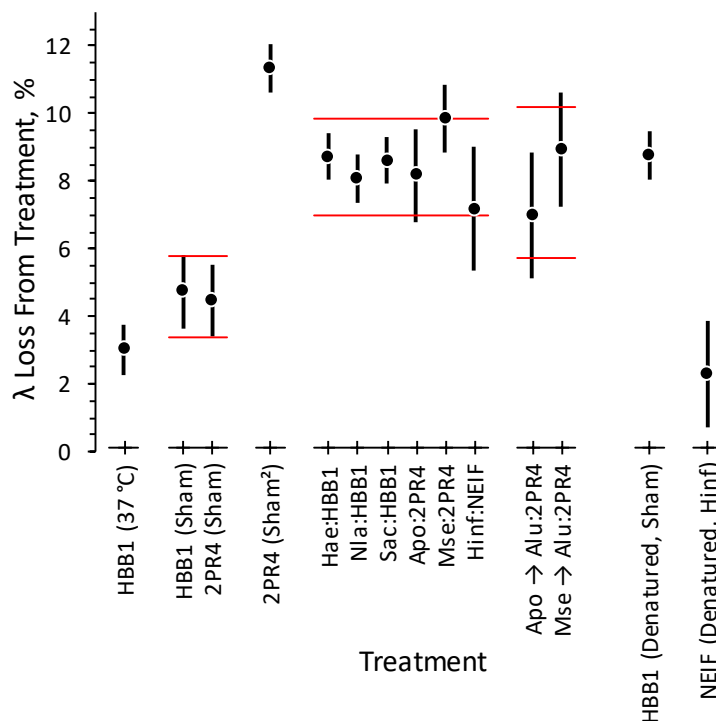


Figure 25. Effect of Restriction Conditions on ddPCR Results

Each symbol represents the mean reduction in the entities per droplet associated with treatments of SRM 2372 B relative to the untreated material. Each bar spans ± 1 standard uncertainty of the mean. The horizontal lines span mean \pm standard uncertainties of groups of related treatments. In order from left to right: one native sample subjected to incubation conditions, two native samples “sham-restricted” (using TE⁴ instead of enzyme in the restriction reaction) in a reaction mixture without enzyme, one native sample sham-restricted twice, six enzyme:assay combinations that cut native samples outside the assay’s amplicon; two two-enzyme:assay combinations where the native samples were initially cut outside the amplicon and then cut within the probe region of the amplicon, one denatured sample sham-restricted in a reaction mixture without enzyme, and one denatured sample cut outside the assay’s amplicon.

Using the HBB1 assay, incubation of a split-sample aliquot of native B at 37 °C for 10 min resulted in a loss in the number of entities per droplet of about 3 % relative to the partner aliquot that was stored on ice. Using both the HBB1 and 2PR4 assays, sham-restricting samples (a type of negative control, using TE⁻⁴ instead of enzyme in the restriction reaction) resulted in a relative loss of about 5 %. These results are compatible with attributing at least some of the loss to renaturation of tenuously connected strands. However, sham-restricting twice increased the relative loss to about 11 %, suggesting that the restriction process actively damages entities, not just promotes renaturation.

Restricting samples with enzymes that do not cut within the amplicon results in 7 % to 10 % relative loss. Since the enzyme:assay combinations used in these studies were chosen to provide a range of sizes and shapes of the fragment containing the target (see Table 13), this relative consistency suggests that fragment length and symmetry have little or no effect on the relative loss of entities during restriction.

Table 13. Size of Restriction Fragments Containing the Target Sequence of the Assay

Enzyme:assay	Fragment Length, bp			
	Cut to 5'	Amplicon	3' to Cut	Total
<i>Hae</i> :HBB1	25	76	30	131
<i>Nla</i> :HBB1	427	76	159	662
<i>Sac</i> :HBB1	9304	76	7039	16419
<i>Apo</i> :2PR4	73	97	15	185
<i>Mse</i> :2PR4	6	97	66	169
<i>Hinf</i> :NEIF	69	67	80	216

Treating the *Apo*- and *Mse*-restricted DNA with the *Alu* enzyme that cuts within the 2PR4 probe sequence yielded a similar 7 % to 10 % relative loss of entities, where the loss is now relative to the λ measured in a sample that was digested only with *Alu*. This suggests that the restriction process causes about the same relative loss of dsDNA and ssDNA entities, which in turn suggests that enzyme assays have the potential for providing useful estimates of the proportion of ssDNA in a mixture despite entity losses from the restriction process.

Sham-restricting a heat-denatured sample caused about a 9 % relative loss. However, cutting a heat-denatured sample with an enzyme that did not cut within the assay's amplicon caused only about a 2 % relative loss. It is plausible that adding the enzyme protein to the reaction mix somehow protected the target DNA from damage or that reducing the size of the ssDNA fragments enclosing the assay's target enhanced amplifiability.

The gel images in Figure 26 provide evidence that the incubation time (10 min) and temperature (37 °C) conditions used in these experiments were sufficient to completely digest the sample DNA. Neither sham-restriction of the sample nor just subjecting it to incubation conditions appreciably fragmented the DNA.

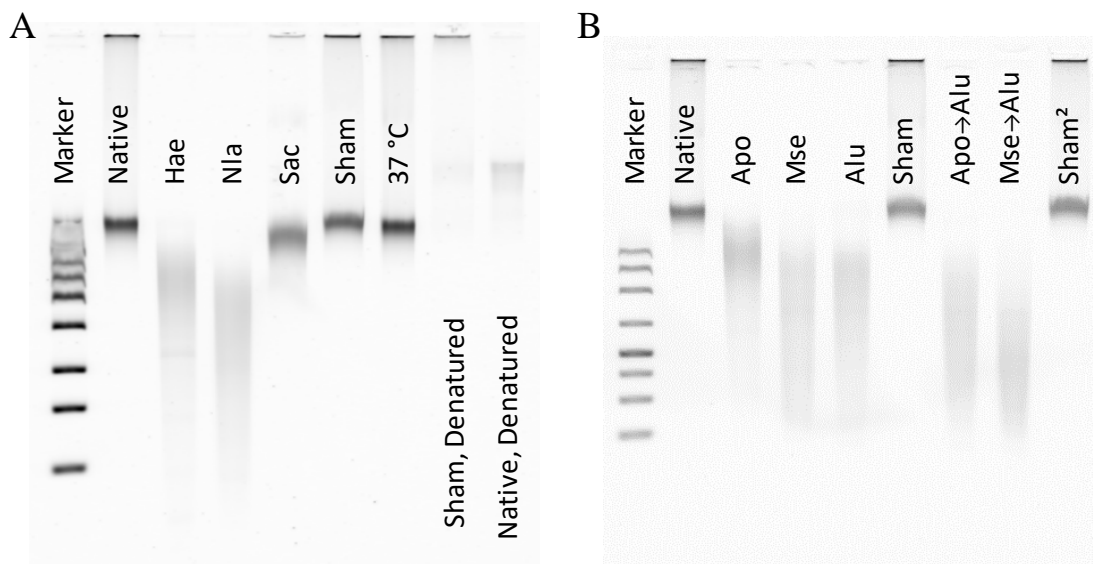


Figure 26. FlashGels of Various Enzyme Treatments of SRM 2372 B

A) Cut with *Hae*, *Nla*, and *Sac*. B) Cut with *Apo*, *Mse*, *Alu*, *Apo* followed by *Alu*, and *Mse* followed by *Alu*. The FlashGel DNA Marker bands, from low to high, are at (100, 200, 300, 500, 800, 1250, 2000, and 4000) bp.

Table 14 lists the numerical results from these studies.

Table 14. Enzyme Treatment Related Loss of Entities

Assay	Treatment	Date ^d	Technical Reps ^a			Independent Replicates ^b				% ^c		
			#	$\bar{\lambda}$	$u(\bar{\lambda})$	#	$\bar{\lambda}$	s	\bar{u}	$u(\bar{\lambda})$	Δ	$u(\Delta)$
HBB1	Native	0628	5	0.2855	0.0017	3	0.2904	0.0009	0.0046	0.0027		
HBB1	Native	0702	5	0.2811	0.0019							
HBB1	Native	0703	5	0.3045	0.0025							
HBB1	<i>Hae</i>	0628	5	0.2793	0.0015	3	0.2651	0.0028	0.0055	0.0036	8.7	1.5
HBB1	<i>Hae</i>	0702	5	0.2583	0.0037							
HBB1	<i>Hae</i>	0703	5	0.2575	0.0016							
HBB1	<i>Nla</i>	0628	5	0.2689	0.0029	3	0.2669	0.0010	0.0061	0.0036	8.1	1.5
HBB1	<i>Nla</i>	0702	5	0.2641	0.0022							
HBB1	<i>Nla</i>	0703	5	0.2678	0.0030							
HBB1	<i>Sac</i>	0628	5	0.2693	0.0008	3	0.2654	0.0034	0.0050	0.0035	8.6	1.5
HBB1	<i>Sac</i>	0702	5	0.2635	0.0036							
HBB1	<i>Sac</i>	0703	4	0.2633	0.0013							
HBB1	Sham	0628	5	0.2793	0.0025	3	0.2766	0.0044	0.0102	0.0064	4.7	2.4
HBB1	Sham	0702	5	0.2809	0.0064							
HBB1	Sham	0703	5	0.2698	0.0039							
HBB1	37 °C	0628	5	0.2719	0.0026	3	0.2816	0.0005	0.0064	0.0037	3.0	1.6
HBB1	37 °C	0702	4	0.2748	0.0031							
HBB1	37 °C	0703	5	0.2982	0.0031							
HBB1	Denatured	0702	5	0.5020	0.0017	2	0.5019	0.0015	0.0051	0.0037		
HBB1	Denatured	0703	5	0.5019	0.0027							
HBB1	Sham, Denatured	0702	5	0.4403	0.0044	2	0.4579	0.0005	0.0101	0.0072	8.8	1.6
HBB1	Sham, Denatured	0703	5	0.4756	0.0047							
2PR4	Native	0705	5	0.2865	0.0015							
2PR4	<i>Apo</i>	0705	5	0.2631	0.0036						8.2	1.4
2PR4	<i>Mse</i>	0705	5	0.2584	0.0025						9.8	1.0
2PR4	Sham	0705	5	0.2737	0.0026						4.5	1.1
2PR4	Sham ²	0705	5	0.2541	0.0014						11.3	0.7
2PR4	<i>Alu</i>	0705	5	0.0219	0.0002							
2PR4	<i>Apo</i> → <i>Alu</i>	0705	5	0.0204	0.0004						7.0	1.9
2PR4	<i>Mse</i> → <i>Alu</i>	0705	5	0.0200	0.0003						8.9	1.7
NEIF	Native	0712	5	0.2946	0.0041							
NEIF	<i>Hinf</i>	0712	5	0.2734	0.0035						7.2	1.8
NEIF	Denatured	0712	3	0.5255	0.0066							
NEIF	<i>Hinf</i> denatured	0712	5	0.5134	0.0050						2.3	1.6

- a Technical replicates, results in entities per droplet: # = number, $\bar{\lambda}$ = mean λ , $u(\bar{\lambda})$ = standard uncertainty of the mean.
- b Independent replicates, results in entities per droplet: # = number, $\bar{\lambda}$ = mean λ , s = standard deviation, \bar{u} = pooled standard uncertainty, $u(\bar{\lambda})$ = standard uncertainty of the mean.
- c Percent relative loss, where $\Delta = 100 (\bar{x}_{\text{reference}} - \bar{x}_{\text{treatment}}) / \bar{x}_{\text{reference}}$. The reference value for each set of related treatments is in *red italic*.
- d Month and day of experiment, all in 2018.

5.1.3. Evolved Method for Preparing Twice-Cut Reactions

To sequentially cut samples with a second enzyme:

- 1) For the first cut, follow the recipe given in section 5.1.1 except
 - a. Double the reaction mixture specified in Table 12 so 50 μL per sample are produced.
 - b. Adjust the thermocycler volume setting for 50 μL solution.
- 2) For each of the sample tubes
 - a. Remove 24 μL and place in a clean labeled PCR tube.
 - b. Add 1 μL of the second cutting enzyme to each tube.
 - c. Mix the tubes gently by finger flicking then microcentrifuge.
- 3) Place all tubes in a well-calibrated thermocycler.
 - a. Adjust the thermocycler volume setting for 25 μL solution.
- 4) Incubate for the appropriate time at the appropriate temperature.
- 5) Remove from heat source.
 - a. Mix well by vortexing then microcentrifuge.
 - b. Store on water/ice until use.

5.1.4. Incubation Time

Our initial studies evaluated enzyme:assay combinations using the enzyme producer's suggested incubation conditions. We incubated the "5 to 15 min" enzymes for 10 min until discovering that the *Alu*:2PR4, *Cac*:2PR4, and *Cac*:ND14 combinations provide much smaller $q_0 = \lambda_0(\text{Enzyme})/\lambda_0$ at 60 min incubation than at 10 min. This suggests that complete restriction of human dsDNA can require more than the suggested incubation time. Incubation for 120 minutes slightly reduced $\psi = \lambda_1(\text{Enzyme})/\lambda_1$ values relative to the values at 60 min for all four combinations tested. This suggests that ssDNA cutting may increase with prolonged incubation. Figure 27 summarizes the q_0 and ψ results for enzyme:assay combinations evaluated at two or three incubation times. Table 15 provides quantitative details.

The *Cac*:2PR4 and *Cac*:ND14 q_0 results are both very high at 10 min incubation relative to the result at 60 min, suggesting that this enzyme may require longer-than-recommended incubation with all human nDNA assays. While the *Alu*:2PR4 result is atypically high at 10 min, the *Alu*:NEIF results at (10, 60, and 120) min are nearly identical. This suggests restriction efficiency is not necessarily related only to the enzyme but rather to the combination of enzyme and the local DNA structure surrounding the restriction recognition sequence.

Ideally, incubation time (and potentially temperature) could be optimized for every enzyme:assay combination. However, for the purposes of this survey the effort required was considered excessive. Since the potential loss of ssDNA entities from prolonged incubation appears small compared to incomplete restriction of dsDNA from too short incubation, we adopted 60 min as our "standard" incubation time for all enzymes. We then investigated incubation conditions only for combinations that gave unusually small or large q_0 results.

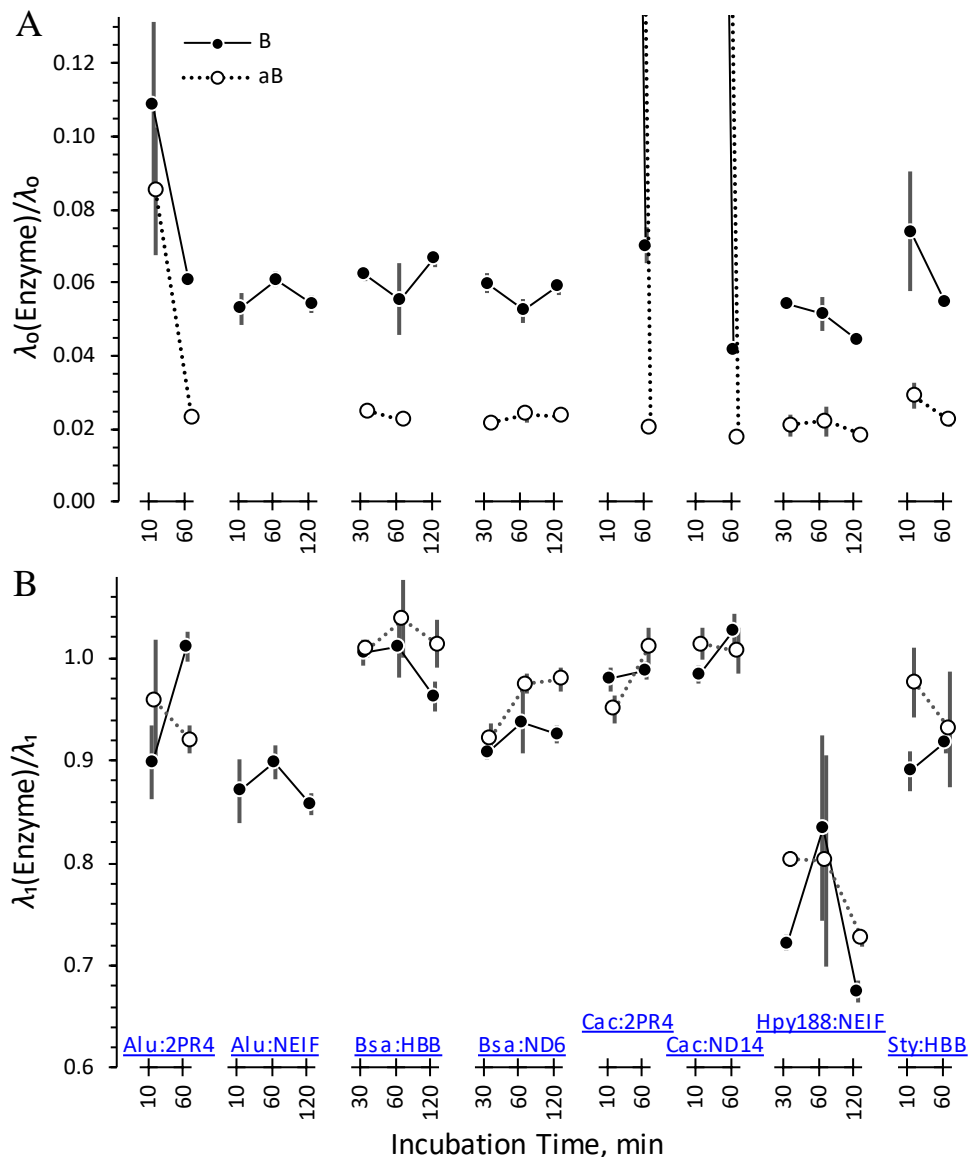


Figure 27. Effect of Incubation Time on Selected Enzyme:Assay Combinations

Subplot A displays $q_0 = \lambda_0(\text{Enzyme})/\lambda_0$, a naïve estimate of the fraction ssDNA entities in the native sample after enzyme digestion, for selected enzyme:assay combinations as functions of incubation time. Subplot B displays $\psi = \lambda_1(\text{Enzyme})/\lambda_1$, an estimate of the fraction of ssDNA entities in a heat-denatured sample that remain after enzyme digestion. The solid black circles connected by solid lines represent results for the SRM 2372 B material; open circles connected by dotted lines represent results for the SRM 2372a material. The bars span ± 1 standard uncertainty.

Table 15. Changes with Enzyme Incubation Time

Enzyme	Assay	Time ^b	SRM 2372 B ^a									SRM 2372a B ^a								
			q_0			ψ			p_0			q_0			ψ			p_0		
			n	\bar{x}	$u(x)$	n	\bar{x}	$u(x)$	n	\bar{x}	$u(x)$	n	\bar{x}	$u(x)$	n	\bar{x}	$u(x)$	n	\bar{x}	$u(x)$
<i>Alu</i>	NEIF	10	3	0.0529	0.0041	3	0.8705	0.0308	3	0.0606	0.0030									
<i>Alu</i>	NEIF	60	1	0.0610	0.0020	1	0.8985	0.0160	1	0.0679	0.0025									
<i>Alu</i>	NEIF	120	1	0.0542	0.0023	1	0.8572	0.0108	1	0.0632	0.0029									
<i>Bsa</i>	HBB1	30	1	0.0626	0.0019	1	1.0049	0.0121	1	0.0623	0.0020	1	0.0250	0.0010	1	1.0091	0.0091	1	0.0248	0.0010
<i>Bsa</i>	HBB1	60	2	0.0554	0.0098	2	1.0117	0.0313	2	0.0545	0.0081	2	0.0224	0.0013	2	1.0383	0.0377	2	0.0216	0.0009
<i>Bsa</i>	HBB1	120	1	0.0667	0.0021	1	0.9626	0.0144	1	0.0693	0.0024	1	1.0134	0.0235						
<i>Bsa</i>	ND6	30	1	0.0598	0.0026	1	0.9079	0.0071	1	0.0659	0.0029	1	0.0215	0.0008	1	0.9219	0.0144	1	0.0233	0.0010
<i>Bsa</i>	ND6	60	2	0.0525	0.0033	2	0.9374	0.0301	2	0.0562	0.0052	2	0.0240	0.0024	2	0.9749	0.0099	2	0.0246	0.0026
<i>Bsa</i>	ND6	120	1	0.0590	0.0022	1	0.9254	0.0088	1	0.0637	0.0025	1	0.0236	0.0010	1	0.9793	0.0122	1	0.0241	0.0010
<i>Cac</i>	2PR4	10	1	0.8309	0.0066	1	0.9794	0.0112	1	0.8484	0.0118	1	0.8522	0.0191	1	0.9506	0.0134	1	0.8965	0.0238
<i>Cac</i>	2PR4	60	2	0.0703	0.0048	2	0.9882	0.0087	2	0.0711	0.0048	2	0.0203	0.0014	1	1.0105	0.0188	1	0.0201	0.0015
<i>Cac</i>	ND14	10	1	0.7590	0.0183	1	0.9840	0.0092	1	0.7713	0.0200	1	0.7292	0.0094	1	1.0138	0.0151	1	0.7193	0.0142
<i>Cac</i>	ND14	60	1	0.0416	0.0015	1	1.0275	0.0150	1	0.0405	0.0016	1	0.0175	0.0007	1	1.0071	0.0228	1	0.0174	0.0008
<i>Hpy1</i>	NEIF	30	1	0.0544	0.0016	1	0.7214	0.0078	1	0.0753	0.0024	1	0.0211	0.0031	1	0.8038	0.0071	1	0.0262	0.0038
<i>Hpy1</i>	NEIF	60	2	0.0515	0.0046	2	0.8346	0.0906	2	0.0630	0.0122	2	0.0222	0.0041	2	0.8024	0.1027	2	0.0275	0.0022
<i>Hpy1</i>	NEIF	120	1	0.0445	0.0009	1	0.6746	0.0112	1	0.0659	0.0018	1	0.0182	0.0008	1	0.7270	0.0075	1	0.0251	0.0012
<i>Sty</i>	HBB1	10	2	0.0741	0.0163	2	0.8901	0.0192	2	0.0829	0.0167	2	0.0290	0.0035	2	0.9762	0.0335	2	0.0298	0.0046
<i>Sty</i>	HBB1	60	1	0.0548	0.0016	1	0.9169	0.0092	1	0.0598	0.0018	3	0.0226	0.0016	3	0.9307	0.0571	3	0.0246	0.0029

^a $q_0 = \lambda_0(\text{Enzyme})/\lambda_0$, 1 - minus fraction dsDNA cut; $\psi = \lambda_1(\text{Enzyme})/\lambda_1$, 1 - fraction ssDNA cut; $p_0 = q_0/\psi$, the fraction of ssDNA in a native material; n = number of independent data sets; \bar{x} = mean value; $u(x)$ = standard uncertainty, combining within- and between-set variability.

^b Length of time that sample was incubated with enzyme.

5.2. Enzyme:Assay Results

Figure 28 summarizes $q_0 = \lambda_0(\text{Enzyme})/\lambda_0$, $\psi = \lambda_1(\text{Enzyme})/\lambda_1$, and $p_0 = q_0/\psi$ results in dot-and-bar format. Each symbol represents the available B or aB results for one enzyme:assay combination. Figure 29 displays the correlations between the B and aB values for the three parameters when the two materials were evaluated in the same ddPCR session.

The q_0 and p_0 values (Figure 28 A and C) are symmetrically distributed about material-specific central locations. The distributions of the p_0 values are more compact and shifted slightly higher than those of q_0 . The correlation between the B and aB results is also sharply reduced by the correction (Figure 29 A and C). With few exceptions, all enzyme:assay combinations tested provide similar estimates of p_0 .

The ψ values (Figure 28 B) are not symmetrically distributed about sample-specific central values. Instead, the ψ range asymmetrically from slightly above 1 to less than 0.3. The correlation between the B and aB results is very high (Figure 29 B). This suggests that the degree of ssDNA cutting is the same regardless of the source material. To the extent that this holds, enzyme:assay combinations that provide ψ close to 1 over a wide incubation time interval may not require independent determination of ψ for every sample.

The ψ values that are greater than 1 may result from the inherent variability of the measurement process for enzyme:assay combinations that do not cut much of the ssDNA. However, with 60 min incubation *Bsa*:HBB1 and *Cac*:ND14 gave $\psi > 1$ for both the B and aB materials. It is plausible that these combinations liberate some ssDNA entities that were rendered inaccessible by heat-denaturing.

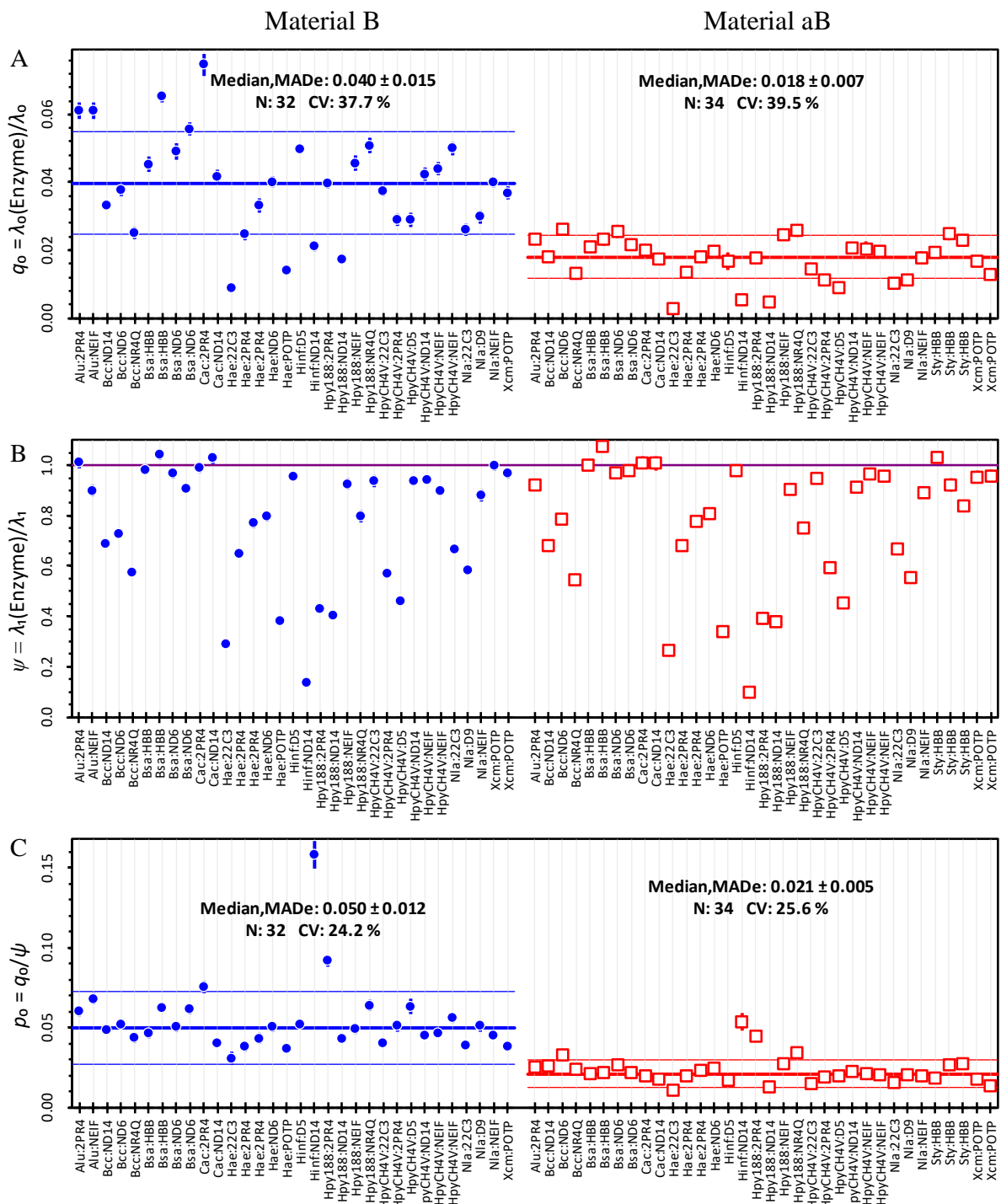


Figure 28. Summary of q_0 , ψ , and p_0 for B and aB

Each dot-and-bar represents the mean \pm 1 standard uncertainty of four to seven technical replicates. The results to the left (blue) of each subplot are SRM 2372 B; those to the right (red) are SRM 2372a B. The horizontal lines in A) and C) represent robust estimates of the average \pm standard uncertainty for each population. The horizontal line in B) denotes a $\psi = \lambda_1(\text{Enzyme})/\lambda_1$ ratio of 1.0.

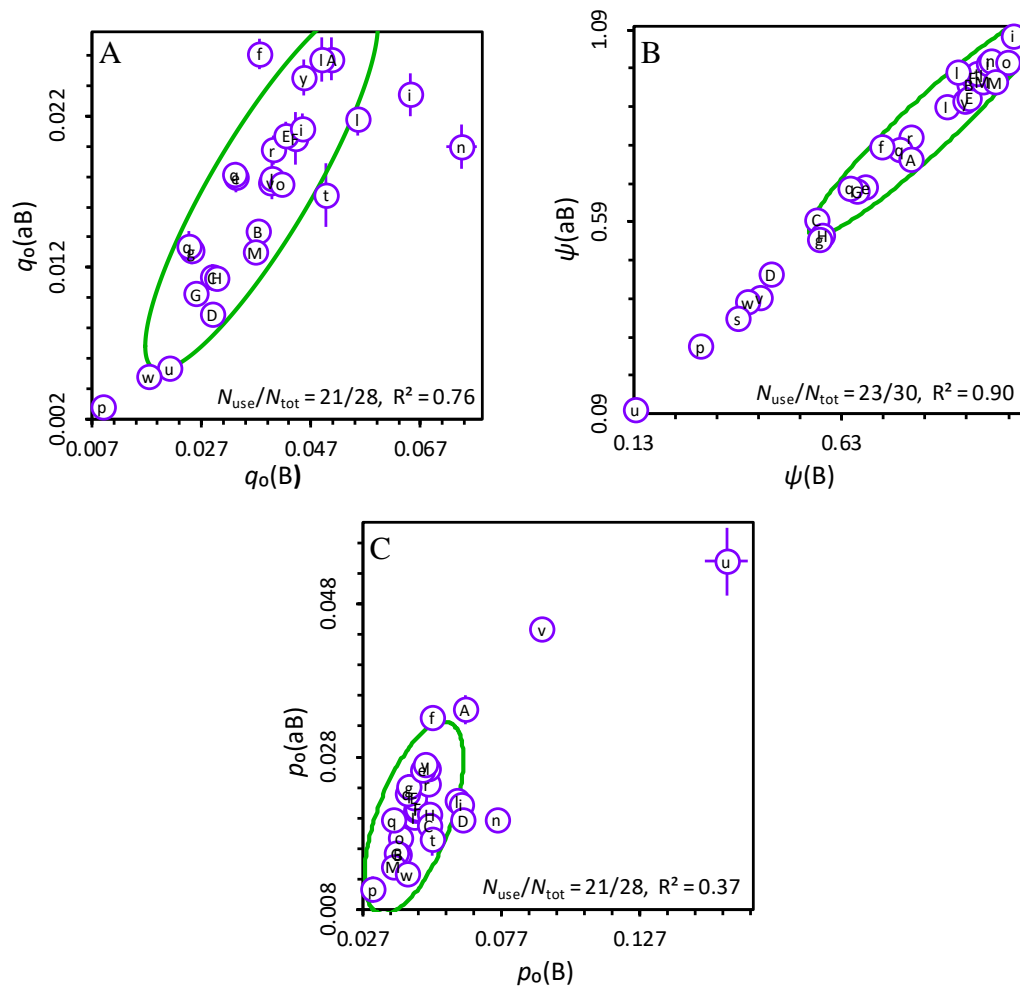


Figure 29. Correlation Between B and aB Values

Each dot-and-cross represents the mean \pm standard uncertainty of the mean of four to seven technical replicates of each material. The ellipse encloses the central 75 % of the bivariate distribution. The legend identifies the total number of (B, aB) pairs, N_{tot} ; the number of pairs in the central 75 %, N_{use} ; and the square of the correlation among the N_{use} pairs. See Table 16 for listing of the codes used to identify the enzyme:assay combinations.

Table 16 lists the summary statistics for all enzyme:assay combinations that successfully cut dsDNA.

Table 16. ddPCR Analysis Results for Native and Heat-Denatured Samples a

Enzyme	Min ^b	Assay	Code	SRM 2372 B ^a						SRM 2372a B ^a											
				q_0			ψ			p_0			q_0			ψ			p_0		
				n	\bar{x}	$u(x)$	n	\bar{x}	$u(x)$	n	\bar{x}	$u(x)$	n	\bar{x}	$u(x)$	n	\bar{x}	$u(x)$	n	\bar{x}	$u(x)$
<i>Alu</i>	10	2PR4	a	3	0.1085	0.0228	3	0.8984	0.0351	3	0.1200	0.0222	2	0.0851	0.0177	2	0.9581	0.0602	2	0.0880	0.0130
<i>Alu</i>	60	2PR4	b	1	0.0610	0.0019	1	1.0107	0.0149	1	0.0604	0.0021	1	0.0233	0.0013	1	0.9204	0.0138	1	0.0253	0.0015
<i>Alu</i>	10	NEIF	c	3	0.0522	0.0040	3	0.8704	0.0308	3	0.0598	0.0028	1	0.0265	0.0015	1	0.8681	0.0169	1	0.0305	0.0018
<i>Alu</i>	60	NEIF	d	1	0.0610	0.0020	1	0.8985	0.0160	1	0.0679	0.0025									
<i>Bcc</i>	60	ND14	e	1	0.0332	0.0008	1	0.6864	0.0080	1	0.0483	0.0013	1	0.0179	0.0010	1	0.6802	0.0122	1	0.0264	0.0015
<i>Bcc</i>	60	ND6	f	1	0.0376	0.0012	1	0.7248	0.0065	1	0.0519	0.0018	1	0.0261	0.0010	1	0.7858	0.0064	1	0.0332	0.0013
<i>Bcc</i>	60	NR4Q	g	1	0.0251	0.0012	1	0.5755	0.0040	1	0.0436	0.0022	1	0.0131	0.0009	1	0.5441	0.0110	1	0.0241	0.0017
<i>Bsa</i>	30	HBB1	h	1	0.0626	0.0019	1	1.0049	0.0121	1	0.0623	0.0020	1	0.0250	0.0010	1	1.0091	0.0091	1	0.0248	0.0010
<i>Bsa</i>	60	HBB1	i	2	0.0552	0.0100	2	1.0117	0.0313	2	0.0544	0.0083	2	0.0223	0.0014	2	1.0383	0.0377	2	0.0214	0.0009
<i>Bsa</i>	120	HBB1	j	1	0.0667	0.0021	1	0.9626	0.0144	1	0.0693	0.0024									
<i>Bsa</i>	30	ND6	k	1	0.0598	0.0026	1	0.9079	0.0071	1	0.0659	0.0029	1	0.0215	0.0008	1	0.9219	0.0144	1	0.0233	0.0010
<i>Bsa</i>	60	ND6	l	2	0.0523	0.0035	2	0.9374	0.0301	2	0.0560	0.0054	2	0.0237	0.0022	2	0.9749	0.0099	2	0.0243	0.0023
<i>Bsa</i>	120	ND6	m	1	0.0590	0.0022	1	0.9254	0.0088	1	0.0637	0.0025	1	0.0236	0.0010	1	0.9793	0.0122	1	0.0241	0.0010
<i>Cac</i>	10	2PR4	NA ^c	1	0.8522	0.0191	1	0.9506	0.0134	1	0.8965	0.0238	1	0.8309	0.0066	1	0.9794	0.0112	1	0.8484	0.0118
<i>Cac</i>	60	2PR4	n	2	0.0702	0.0047	2	0.9882	0.0087	2	0.0710	0.0047	1	0.0200	0.0014	1	1.0105	0.0188	1	0.0198	0.0015
<i>Cac</i>	10	ND14	NA ^c	1	0.7590	0.0183	1	0.9840	0.0092	1	0.7713	0.0200	1	0.7292	0.0094	1	1.0138	0.0151	1	0.7193	0.0142
<i>Cac</i>	60	ND14	o	1	0.0416	0.0015	1	1.0275	0.0150	1	0.0405	0.0016	1	0.0175	0.0007	1	1.0071	0.0228	1	0.0174	0.0008
<i>Hae</i>	10	22C3	p	1	0.0089	0.0009	1	0.2910	0.0048	1	0.0307	0.0031	1	0.0028	0.0004	1	0.2661	0.0038	1	0.0107	0.0017
<i>Hae</i>	10	2PR4	q	2	0.0289	0.0044	2	0.7098	0.0603	2	0.0404	0.0030	2	0.0158	0.0024	2	0.7290	0.0508	2	0.0215	0.0020
<i>Hae</i>	10	ND6	r	1	0.0400	0.0012	1	0.7955	0.0129	1	0.0503	0.0017	1	0.0197	0.0009	1	0.8092	0.0104	1	0.0244	0.0012
<i>Hae</i>	10	POTP	s	1	0.0140	0.0007	1	0.3803	0.0050	1	0.0368	0.0018	0			1	0.3392	0.0035	0		
<i>Hinf</i>	10	D5	t	2	0.0510	0.0014	1	0.9540	0.0101	1	0.0521	0.0010	2	0.0160	0.0016	2	0.9456	0.0327	2	0.0169	0.0015
<i>Hinf</i>	60	ND14	u	1	0.0213	0.0010	1	0.1343	0.0017	1	0.1584	0.0077	1	0.0054	0.0004	1	0.1003	0.0019	1	0.0536	0.0045
<i>Hpy188</i>	60	2PR4	v	1	0.0396	0.0008	1	0.4313	0.0055	1	0.0917	0.0022	1	0.0176	0.0005	1	0.3938	0.0062	1	0.0447	0.0015
<i>Hpy188</i>	10	ND14	w	1	0.0174	0.0006	1	0.4044	0.0047	1	0.0429	0.0016	1	0.0048	0.0003	1	0.3808	0.0077	1	0.0126	0.0008
<i>Hpy188</i>	30	NEIF	x	1	0.0544	0.0016	1	0.7214	0.0078	1	0.0753	0.0024	1	0.0211	0.0031	1	0.8038	0.0071	1	0.0262	0.0038
<i>Hpy188</i>	60	NEIF	y	2	0.0507	0.0053	2	0.8346	0.0906	2	0.0622	0.0129	2	0.0214	0.0033	2	0.8024	0.1027	2	0.0266	0.0018
<i>Hpy188</i>	120	NEIF	z	1	0.0445	0.0009	1	0.6746	0.0112	1	0.0659	0.0018	1	0.0182	0.0008	1	0.7270	0.0075	1	0.0251	0.0012

Enzyme	Min ^b	Assay	Code	SRM 2372 B ^a						SRM 2372a B ^a											
				q_0			ψ			p_0			q_0			ψ			p_0		
				n	\bar{x}	$u(x)$	n	\bar{x}	$u(x)$	n	\bar{x}	$u(x)$	n	\bar{x}	$u(x)$	n	\bar{x}	$u(x)$	n	\bar{x}	$u(x)$
<i>Hpy</i> 188	10	NR4Q	A	1	0.0508	0.0018	1	0.7958	0.0166	1	0.0639	0.0026	1	0.0257	0.0014	1	0.7513	0.0097	1	0.0343	0.0019
<i>Hpy</i> CH4V	10	22C3	B	1	0.0374	0.0011	1	0.9359	0.0170	1	0.0400	0.0014	1	0.0144	0.0006	1	0.9477	0.0146	1	0.0152	0.0007
<i>Hpy</i> CH4V	10	2PR4	C	1	0.0290	0.0013	1	0.5700	0.0075	1	0.0509	0.0024	1	0.0114	0.0009	1	0.5955	0.0113	1	0.0191	0.0015
<i>Hpy</i> CH4V	10	D5	D	1	0.0289	0.0017	1	0.4581	0.0073	1	0.0631	0.0039	1	0.0089	0.0007	1	0.4537	0.0126	1	0.0197	0.0015
<i>Hpy</i> CH4V	10	ND14	E	1	0.0424	0.0015	1	0.9354	0.0067	1	0.0453	0.0016	1	0.0207	0.0008	1	0.9131	0.0150	1	0.0227	0.0010
<i>Hpy</i> CH4V	10	NEIF	F	2	0.0470	0.0031	2	0.9194	0.0249	2	0.0512	0.0047	2	0.0202	0.0011	2	0.9609	0.0093	2	0.0210	0.0011
<i>Nla</i>	10	22C3	G	1	0.0260	0.0012	1	0.6651	0.0064	1	0.0390	0.0019	1	0.0103	0.0004	1	0.6694	0.0105	1	0.0153	0.0007
<i>Nla</i>	10	D9	H	1	0.0298	0.0014	1	0.5829	0.0073	1	0.0511	0.0025	1	0.0113	0.0006	1	0.5541	0.0092	1	0.0205	0.0011
<i>Nla</i>	10	NEIF	I	1	0.0399	0.0009	1	0.8809	0.0182	1	0.0453	0.0014	1	0.0179	0.0014	1	0.8898	0.0137	1	0.0201	0.0016
<i>Sty</i>	10	HBB1	J	2	0.0736	0.0160	2	0.8901	0.0192	2	0.0824	0.0165	2	0.0284	0.0033	2	0.9762	0.0335	2	0.0292	0.0043
<i>Sty</i>	60	HBB1	K	1	0.0538	0.0015	1	0.9169	0.0091	1	0.0587	0.0018	3	0.0224	0.0017	3	0.9307	0.0570	3	0.0244	0.0029
<i>Sty</i>	10	ND6	L	1	0.0519	0.0010	1	0.8954	0.0116	1	0.0579	0.0014	1	0.0242	0.0015	1	0.9071	0.0128	1	0.0266	0.0017
<i>Xcm</i>	60	POTP	M	2	0.0404	0.0037	3	1.0000	0.0203	2	0.0403	0.0025	2	0.0149	0.0019	2	0.9551	0.0131	2	0.0156	0.0021

- a* $q_0 = \lambda_0(\text{Enzyme})/\lambda_0$, 1 - minus the fraction dsDNA cut; $\psi = \lambda_1(\text{Enzyme})/\lambda_1$, 1 - the fraction ssDNA cut; $p_0 = q_0/\psi$, the fraction ssDNA in a native material; n = number of independent data sets; \bar{x} = mean value; $u(x)$ = standard uncertainty, combining within- and between-set variability.
- b* Incubation time, in minutes.
- c* Not assigned due to low activity at 10 min incubation time.

5.2.1. Performance Evaluation

Figure 30 displays p_0 results as a function of ψ for all enzyme:assay combinations evaluated that successfully cut dsDNA. Because the ψ values for B and aB, $\psi(B)$ and $\psi(aB)$, are very strongly correlated and are of similar magnitude, the horizontal axis in the figure displays the mean of the two values:

$$\text{Mean}(\psi) = (\psi(B) + \psi(aB))/2. \quad [22]$$

Although correlated, the p_0 values for B are about twice those of aB. Therefore, the vertical axis displays the mean of the median-normalized p_0 , $p_0(B/\text{Median}(p_0(B)))$ and $p_0(aB/\text{Median}(p_0(aB)))$:

$$\text{Mean}(p_0/\text{Median}) = (p_0(B/\text{Median}(p_0(B))) + p_0(aB/\text{Median}(p_0(aB))))/2. \quad [23]$$

The enzyme:assay combinations that produce p_0 close to the median in both materials therefore have $\text{Mean}(p_0/\text{Median})$ close to 1.

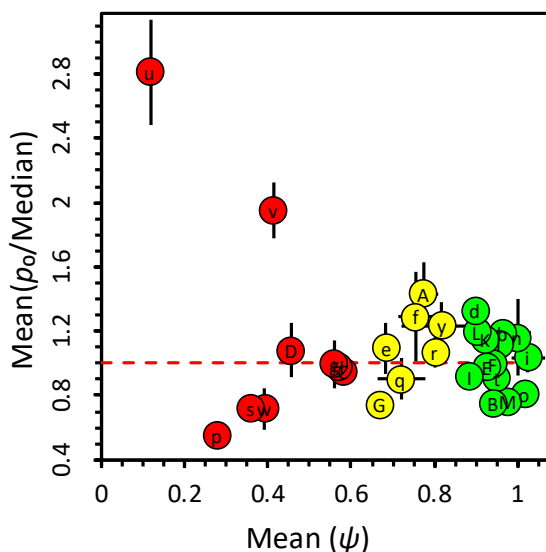


Figure 30. Relationship Between p_0 and ψ

Each dot-and-cross represents $\text{Mean}(p_0/\text{Median}) \pm u(\text{Mean}(p_0/\text{Median}))$ as a function of $\text{Mean}(\psi) \pm au(\text{Mean}(\psi))$. The color-code for the dots is: red = $\text{Mean}(\psi) < 0.6$, yellow = $\text{Mean}(\psi) \geq 0.6$ to 0.85, green = $\text{Mean}(\psi) > 0.85$. The horizontal dashed line represents the composite median. See Table 16 for listing of the codes used to identify the enzyme:assay combinations.

The largest and smallest of the composite p_0 results are for enzyme:assay combinations that have the smallest ψ . This suggests that combinations that severely cut ssDNA may not provide reliable estimates of p_0 , regardless of correction strategies.

Figure 31 displays the composite $\text{Mean}(p_0/\text{Median})$ values ordered from smallest to largest and color-coded by $\text{Mean}(\psi)$. Five of the nine enzyme:assay combinations with $\text{Mean}(\psi) < 0.6$ (red) are at the extreme tails of the distribution. Four of the seven combinations with $\text{Mean}(\psi)$ between 0.6 and 0.85 (yellow) also are in the tails. While there are combinations marked with red or yellow dots near the center of the distribution, we believe it prudent to focus further studies on combinations with $\text{Mean}(\psi) > 0.85$ (green); i.e., that do not cut much of the ssDNA.

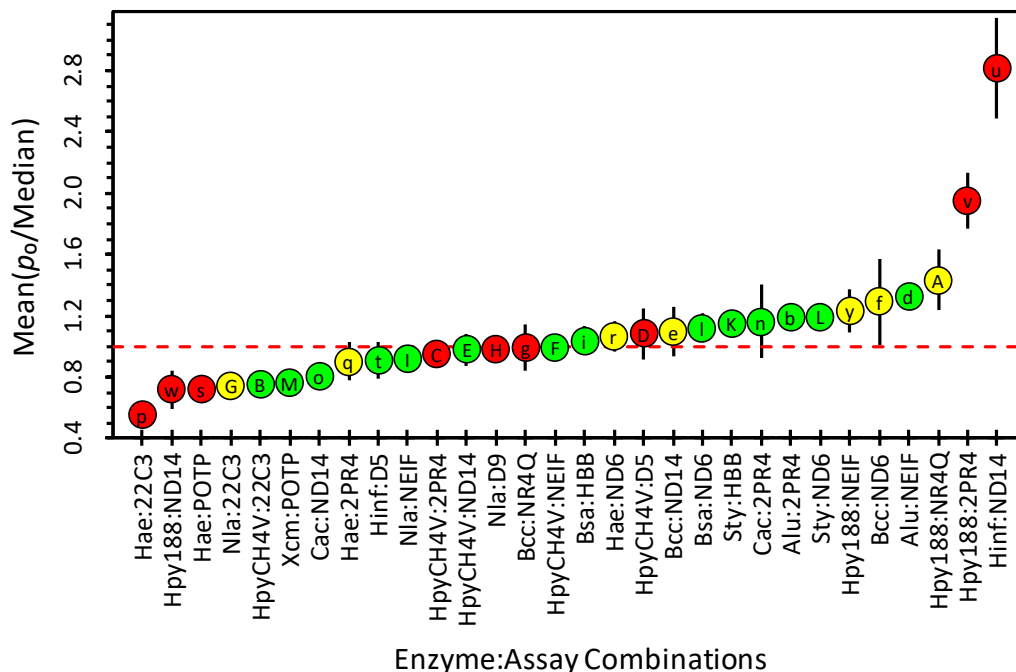


Figure 31. Rank-Ordered Mean(p_0 /Median) Values

Each dot-and-bar represents $\text{Mean}(p_0/\text{Median}) \pm u(\text{Mean}(p_0/\text{Median}))$ sorted from small to large. The color-code for the dots is: red = $\text{Mean}(\psi) < 0.6$, yellow = $\text{Mean}(\psi) \geq 0.6$ to 0.85 , green = $\text{Mean}(\psi) > 0.85$. The horizontal dashed line represents the composite median. See Table 16 for listing of the codes used to identify the enzyme:assay combinations.

The error bars for the “green” *Cac*:2PR4 (n) are large relative to the others in their category. This reflects a fairly large difference in the median-normalized p_0 values for the B and aB materials. Being based on sub-optimal 10 min incubation, it is likely that this difference is an artifact of the measurement process. However, it is plausible that *Cac*:2PR4 behaves differently with different samples. Further measurements are needed to resolve this issue.

5.2.2. Enzyme:Assay Design Considerations

Table 17 displays the 34 enzyme:assay combinations evaluated.

Table 17. Summary of Enzyme:Assay Combinations Evaluated

Enzymes	Human nDNA PCR Assays ^a										# ^b
	22C3	2PR4	D5	D9	HBB1	ND6	ND14	NEIF	NR4Q	POTP	
<i>Alu</i>		b						d			2
<i>Bcc</i>						f ^e	e ^e		g ^d		3
<i>Bsa</i>					i	l					2
<i>Cac</i>		n	c				o				3
<i>Hae</i>	p ^d	q ^e				r ^e				s ^d	4
<i>Hinf</i>			t			c	u ^d				3
<i>Hpy188</i>		v ^d					w ^d	y ^e	A ^e		4
<i>HpyCH4V</i>	B	C ^d	D ^d				E	F			5
<i>Nla</i>	G ^e			H ^d		c		I		c	5
<i>Sty</i>					K	L					2
<i>Xcm</i>										M	1
# ^f	3	5	3	1	2	6	5	4	2	3	34

^a Enzyme:assay combinations are identified as (row header):(column header) and the single-character code provided in Table 16.

^b Number of enzyme:assay combinations involving this enzyme

^c No useful result due to failure to inactivate PCR amplification

^d Result unreliable: Mean(ψ) \leq 0.6

^e Result of questionable reliability: 0.6 < Mean(ψ) \leq 0.85

^f Number of enzyme:assay combinations involving this assay

The four enzyme:assay combinations that do not completely inactivate PCR amplification all cut within either the 5'- or 3'-primer region leaving more than 50 % of the primer sequence intact: *Cac*:D5, *Hinf*:ND6, *Nla*:D6, and *Nla*:POTP. Three other combinations also cut entirely within primer sequences but leave less than 30 % of the primer sequence intact: *Hpy188*:2PR4, *Hpy188*:NR4Q, and *HpyCH4V*:D5 (*HpyCH4V* cuts both the forward and reverse primers of D5). See Table 10 for details.

Some enzymes do appear to cut ssDNA more aggressively than others. Three enzymes have no combinations with Mean(ψ) > 0.85: 1) *Bcc*, 2) *Hae*, and 3) *Hpy188*. Five enzymes have no combinations with Mean(ψ) < 0.85: 1) *Alu*, 2) *Bsa*, 3) *Cac*, 4) *Sty*, and 5) *Xcm*. There are no obvious commonalities in the recognition sequences or type of overhang in these groups (see Table 11 for details). Since the distributions of $q_0(\text{B})$ and $q_0(\text{aB})$ values are (fairly) compact (see Figure 28), it is unlikely that the differences are related to any off-target activity since it would impact dsDNA as well as ssDNA. More plausibly, the differences arise in differential propensity of ssDNA to take on local dsDNA structure that adequately match the various recognition sequences.

There is no obvious systematic pattern to assays having combinations with Mean(ψ) > 0.85. Five of the assays that are cut by two or more enzymes have at least one combination with Mean(ψ) \leq 0.6 and at least one with Mean(ψ) > 0.85: 1) 22C3, 2) 2PR4, 3) D5, 4) ND14, and

5) POTP. Only the HBB1 assay has all combinations with $\text{Mean}(\psi) > 0.85$ – and the two enzymes involved (*Bsa* and *Sty*) have the same cut site although their recognition sequences differ slightly and require different incubation temperatures.

Hinf:ND14 (u) is the enzyme:assay with the largest $\text{Mean}(p_0/\text{Median})$. The q_0 values for this combination are somewhat low, but the ψ values are extremely low. This over-correction causes p_0 for both materials to be atypically high. We believe this atypical result is related to the *Hinf* enzyme cutting the ND14 assay in three places within the probe and flanking regions (see Table 10). Having multiple sites enhances the probability that the ssDNA entities can take on a locally dsDNA structure around at least one of the restriction sites. This suggests that enzyme:assay combinations having more than one restriction site within the amplicon may be less useful than those having a single site. Hyp188:ND14 (w) also has three cut-sites within probe and flanking regions; while the ψ and p_0 values for this combination are low, it should be noted that those for the single cut-site *Hae*:22C3 (p) are lower.

5.3. SRMs 2372 B Mixture

Figure 32 compares the ddPCR enzyme:assay results to the values for $v_m = (0.20 \pm 0.02, 0.40 \pm 0.02, 0.80 \pm 0.02)$ mixtures of native and heat-denatured B estimated using Equation 13. The values are in near-perfect agreement.

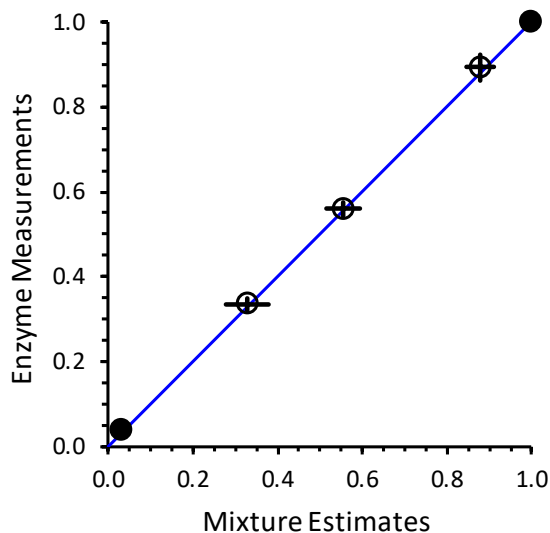


Figure 32. Enzyme:Assay Vs Estimated Proportions of ssDNA.

The solid black circles represent the measured enzyme:assay fraction ssDNA in the native and the ideal fraction in the heat-denatured SRM 2372 B. The open circles represent enzyme-assay estimates of ssDNA in binary mixtures of the native and heat-denatured materials. The error crosses inside the open circles represent approximate standard uncertainties. The solid diagonal line represents equality between the enzyme and mixture estimates.

Table 18 lists the ddPCR p_0 values for native and mixture samples.

Table 18. ddPCR Enzyme:Assay Results for SRM 2372 B Mixtures

				Volume % Heat-Denatured Sample ^a							
				$v_m = 0\%$		$v_m = 20\%$		$v_m = 40\%$		$v_m = 80\%$	
Mtrl ^b	Date	Assay	Enzyme	p_0	$u(p_0)$	p_{20}	$u(p_{20})$	p_{40}	$u(p_{40})$	p_{80}	$u(p_{80})$
UB	08/29/18	HBB1	<i>Sty</i>	3.7	0.5	33.9	1.9	56.7	2.6	89.3	4.0
UB	08/31/18	POTP	<i>Xcm</i>	2.4	0.2	32.6	2.5	55.4	3.6	89.4	4.3
B	09/04/18	POTP	<i>Xcm</i>	4.3	0.3	33.8	1.8	55.6	2.2		
Summaries ^c			N :	3		3		3		2	
			\bar{x} :	3.5		33.4		55.9		89.4	
			s :	0.9		0.7		0.7		0.1	
			\bar{u} :	0.4		2.1		2.9		4.2	
			$u(\bar{x})$:	0.6		1.3		1.7		3.0	

- ^a v_m = mixture by volume of $m\%$ heat-denatured with $(100-m)\%$ native material,
 p_0 = percent ssDNA entities per chamber in native sample,
 p_{20} = percent ssDNA entities per chamber in mixture of 80 % native and 20 % heat-denatured sample,
 p_{40} = percent ssDNA entities per chamber in mixture of 60 % native and 40 % heat-denatured sample,
 p_{80} = percent ssDNA entities per chamber in mixture of 20 % native and 80 % heat-denatured sample,
 $u()$ = standard uncertainty of the quantity “of the quantity within the ()”,
- ^b Material used to prepare mixture. UB is the undiluted stock material used to prepare SRM 2372 B in 2006.
- ^c N = number of independent results, \bar{x} = mean, s = standard deviation, \bar{u} = pooled standard uncertainty, $u(\bar{x})$ = standard uncertainty of the mean.

5.4. Comparison of Enzyme:Assay Combinations

Figure 33 compares the p_0 results obtained using the two enzyme:assay combinations that were used in the mixture studies: *Sty*:HBB1 and *Xcm*:POTP. Because of the 40-fold difference in p_0 between aB and the 20 % native and 80 % heat-denatured mixture of UB, the complete set of six values is displayed using logarithmic axes in subplot A. There is a linear relationship between the \log_{10} -transformed results from the two combinations:

$$\log_{10}(p_0(Xcm:POTP)) = a + b \times \log_{10}(p_0(Sty:HBB1)). \quad [24]$$

While enabling visualization of the empirical relationship between the log-transformed p_0 estimates, the transformation can complicate interpreting the relationship. The results for the three native materials are displayed using linear axes in subplot B, where the log-space linear relationship takes the form of a (non-linear) power curve:

$$p_0(Xcm:POTP) = a \times p_0(Sty:HBB1)^b. \quad [25]$$

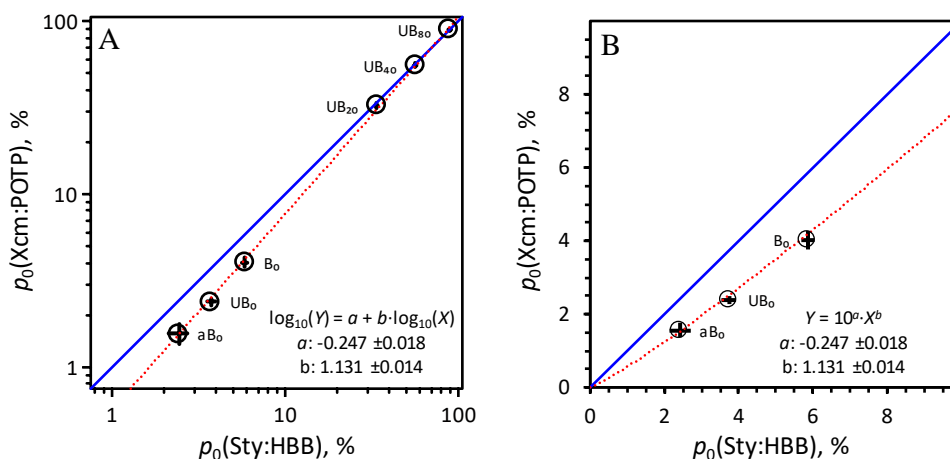


Figure 33. Comparison of two Enzyme:Assay Combinations Used in the Mixture Studies.

The circles compare the percent ssDNA in the native samples as measured with *Xcm*:POTP and *Sty*:HBB1. The labels B₀ and aB₀ denote results for the native 2372 B and 2372a B stock materials. The labels UB₀, UB₂₀, UB₄₀, and UB₈₀ denote results from the 2372 B stock used in the mixture study. The error crosses represent approximate standard uncertainties. The solid diagonal line represents equality between results from the two combinations. A) Data plotted on \log_{10} axes; the dotted line represents the function: $\log_{10}(p_0(Xcm:POTP)) = a + b \times \log_{10}(p_0(Sty:HBB1))$. B) The B₀, UB₀, and aB₀ data plotted on linear axes; the dotted line represents the function $p_0(Xcm:POTP) = 10^a \times p_0(Sty:HBB1)^b$. Note that the coefficients of the functions are identical.

These results are too limited to support asserting that this empirical relationship is more than happenstance. More data involving different enzyme:assay combinations and samples with different proportions of ssDNA are needed before attempting to model these comparisons.

6. Comparison of Staircase with Enzyme Measurements

6.1. SRM 2372 B Mixture

Figure 34 compares the cdPCR staircase and ddPCR enzyme analysis results (listed in Table 6 and Table 18, respectively) for the native, heat-denatured, and $v_m = (0.20 \pm 0.02, 0.40 \pm 0.02, 0.80 \pm 0.02)$ mixtures. The relationship is linear with near-perfect correlation ($R^2 = 0.9998$) but with neither zero intercept nor unit slope. This suggests that the two measurement systems probe different but correlated measurands.

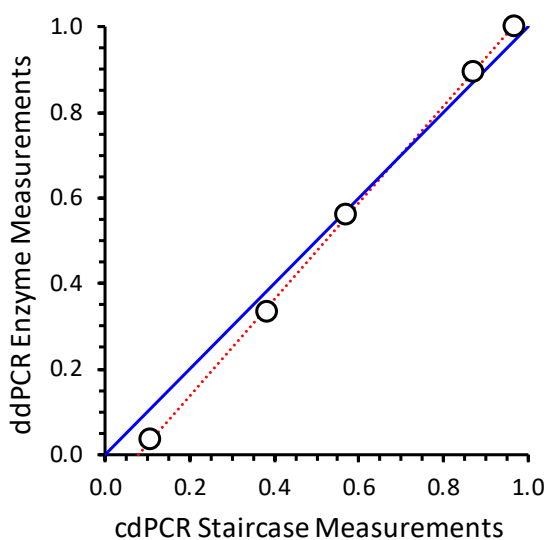


Figure 34. ddPCR Enzyme Vs cdPCR Staircase Estimates

The circles represent the (staircase, enzyme) estimates of fraction ssDNA in the SRM 2372 B mixture samples. The solid diagonal line represents equality between the enzyme and staircase estimates. The dotted line represents an empirical linear fit between the staircase and enzyme estimates:

$$p_0(\text{Enzyme}) = (-0.088 \pm 0.007) + (1.127 \pm 0.010) \times p_0(\text{Staircase}) .$$

While the results from different enzyme:assay combinations are somewhat variable, if the power-curve relationship of Figure 33 B is generally valid then between-combination differences are small at low ssDNA proportions. Since the difference between the staircase and enzyme results in Figure 34 is greatest at low ssDNA, between-enzyme:assay differences are not the primary source of the between-method differences.

As noted in section 3.1, the cdPCR staircase method combines the proportion of chambers containing 1) a single ssDNA that starts amplifying in the first cycle and 2) a single dsDNA entity that starts amplifying on the second cycle. The staircase results thus systematically overestimate ssDNA content, with second-cycle interference most prominent at high dsDNA proportions and declining as the proportion of dsDNA in the sample decreases. This is in at least qualitative agreement with the results displayed in Figure 34.

6.2. Possible Platform Artifact

In section 5.1.2 we noted that the *Hinf*:NEIF combination fragments DNA outside of the assay amplicon, but the ddPCR results for the *Hinf*-restricted sample yielded about a 9 % relative loss for native B and about a 2 % relative loss for heat-denatured B. Figure 35 displays the cdPCR results for these same materials. There are little to no differences between the untreated and *Hinf*-restricted native or denatured material. Based on this limited evidence, it is plausible that the two dPCR platforms estimate somewhat different populations.

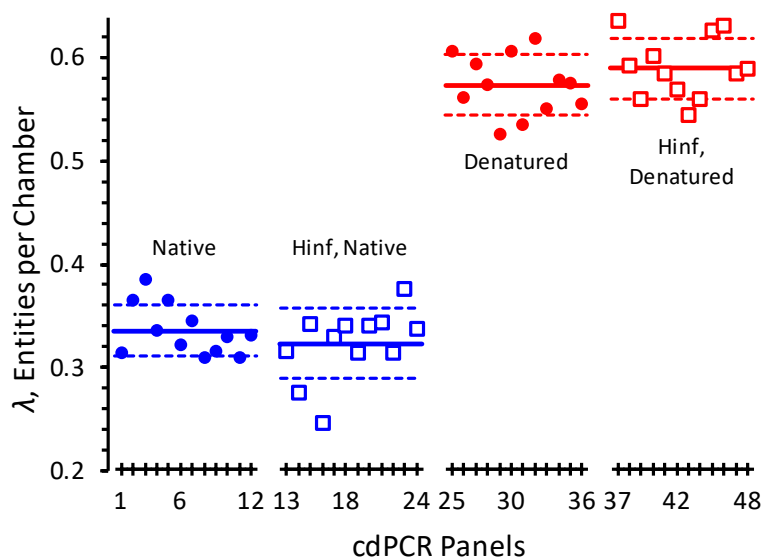


Figure 35. Effect of Restriction Without Cutting on cdPCR Results

The horizontal axis indicates the chamber panel index, 1 to 48. The vertical axis indicates the Poisson-estimate of mean number of entities per chamber, λ . The circles denote results of the NEIF assay for untreated SRM 2372 B samples, squares denote results after *Hinf*-restriction. The blue symbols to the left represent results for the native material, red symbols to the right represent results for the material after heat-denaturation. The solid horizontal lines represent the mean λ for the four sets of replicates. The dotted lines represent $\lambda \pm u(\lambda)$.

The Fluidigm cdPCR platform requires that sample pass through several centimeters of microfluidic piping before being dispersed into chambers, the actual length of the passage depending on panel location. The Bio-Rad ddPCR platform uses much shorter passages, all the same length. We speculate that some incompletely separated fragments may be mechanically converted to completely separated ssDNA during the cdPCR sample loading process.

7. Summary

7.1. Method Evaluation

7.1.1. cdPCR Staircase Analysis

In addition to interference from one-cycle delayed amplification, the staircase results are influenced by the few percent of chambers containing entities that start amplifying erratically later (sometimes much later) than the second cycle. Ideally, these problems could be reduced with further assay optimization. However, improving the model used to interpret somewhat-less-than-ideal staircase ogives is a more general and possibly more practical goal.

Based on the mixture study described in section 3.4, staircase analysis results are linearly related to the proportion of ssDNA in a native sample, p_0 . However, based on the current limited evidence presented in section 6.1 the effective detection limit for staircase analysis is about eight percent.

7.1.2. ddPCR Ratio Analysis

As discussed in section 4.1, the $\varphi = \lambda_1/\lambda_0$ ratio is a function of (at least) two variables besides the proportion of ssDNA in the sample, p_0 : 1) the fraction of dsDNA entities that heat-denaturation converts to ssDNA, χ , and 2) the fraction of ssDNA entities rendered inaccessible or non-amplifiable by denaturing, ω . The relationship between φ and the upper limit values for p_0 is therefore ambiguous unless φ is very close to its 2.0 limiting value.

7.1.3. ddPCR Enzyme Analysis

We believe that the consensus results from the 14 enzyme:assay combinations with $\psi > 0.85$ are metrologically true (i.e., unbiased). The entity fraction of ssDNA in the B and aB materials is 0.0495 ± 0.0094 and 0.0198 ± 0.0034 , respectively, giving a CV for both materials of just less than 20 %. Identifying which one or small subset of these combinations can provide the “best” (precise, true, robust, and cost-effective) estimates will require a better understanding of the sources of their differences.

7.2. Defining the Measurand

We originally considered that human nDNA consisted of two and only two forms: 1) dsDNA and 2) ssDNA. Our studies suggest that incompletely separated intermediate forms exist and may be a source of between-platform and between-treatment bias. Studying the effect of salt concentration in the reaction mixture may help sort out this issue.

7.3. Adapting Methods for Other DNAs

While we believe that ddPCR enzyme analysis is a generally applicable approach to determining the proportion of ssDNA in a nominally dsDNA sample, both ddPCR ratio analysis and cdPCR staircase analysis can provide useful information. We suggest the following evaluation process:

- 1) The “evolved methods” described in this document express concentrations in terms of mass of human nDNA per volume sample, where the relative molecular mass (aka, molecular weight) of haploid human nDNA is about 2×10^{12} g/mol. Further, we use sample dilutions that target 0.3 dsDNA entities per partition to ensure the linearity of our dPCR assays when used with heat-denatured (ssDNA) samples. For other DNAs,

- you will need to characterize the linearity of your assays, identify the mass concentration of your materials that will give an entity concentration of slightly less than one-half of the upper linearity bound, and adapt our methods to this value.
- 2) Develop and optimize at least three PCR assays with different, well-separated target sequences. Regardless of the approach used, assessing potential site-specific bias requires use of multiple assays.
 - 3) Investigate ddPCR ratio analysis. You will need to study $\varphi = \lambda_1/\lambda_0$ as a function of denaturation temperature and exposure time to determine the optimum (largest and least variable) φ conditions. We suggest starting with 95° C for 1 min. If the true proportion of ssDNA in the native sample is very small (and you are very lucky), the optimum φ will be very close to 2 and you will not need to investigate the other methods. In any case, the staircase and enzyme analysis methods require use of optimized denaturation conditions.
 - 4) If a cdPCR system is available, evaluate whether any of your PCR assays provide readily interpretable ogives (ideally, having the profile of a staircase with essentially horizontal treads and vertical risers). If at least one of the assays is sufficiently efficient, evaluate native and heat-denatured versions of the sample on the same chip using a sample dilution that gives λ_0 between 0.25 and 0.5. Comparing the two ogives will enable determining the one-entity tread. If the proportion of late-starters is very small (i.e., there are few chambers with Ct values above the one-entity tread), the relative width of this tread estimates p_0 for the native version and p_1 for the heat-denatured version. When the λ_1/λ_0 ratio is not very close to 2, the p_1 and λ_1 results can help determine whether heat-denaturation is incompletely separating dsDNA into ssDNA or rendering ssDNA entities inaccessible or non-amplifiable. This information can then inform development of a better heat-denaturation process.
 - 5) Identify the type II restriction enzymes that cut your assays once and only once between the primers. Ideally, you should have at least two enzymes for each assay. For each enzyme:assay combination, determine the proportion of ssDNA in the denatured sample that is cut by the enzyme: $\psi = \lambda_1(\text{Enzyme})/\lambda_1$. Identify at least three enzyme:assay combinations that do not cut much of the ssDNA (i.e., ψ close to the ideal 1). Combinations giving ψ less than 0.5 should not be used. Combinations with ψ between 0.5 and 0.85 appear relatively more variable and prone to bias than combinations with ψ greater than 0.85. Determine p_0 with all useful combinations. If the results are in good agreement calculate the consensus value and its uncertainty [33]. If the results are unacceptably different, developing additional enzyme:assay combinations may help identify which (if any) are biased relative to a self-consistent core subset.
 - 6) Regardless of approach, evaluate the linearity of the method for your DNA using mixtures of native and heat-denatured material prepared as described in section 3.4.3. This information will help assess the total measurement uncertainty.

8. Acknowledgements

We thank the following Biomolecular Measurement Division staff: Thomas Cleveland, Biomolecular Structure and Function Group, for suggesting enzyme digestion; Megan Cleveland and Erica Romsos, Applied Genetics Group, for discussions concerning dPCR; and Peter Vallone, Applied Genetics Group, for his suggestions on the influence of salt concentrations on DNA conformation. We thank Katherine E. Sharpless for improving the readability of this document.

9. References

- 1 Pinheiro LB, O'Brien H, Druce J, Do H, Kay P, Daniels M, You J, Burke DG, Griffiths K, Emslie KR. Interlaboratory reproducibility of droplet digital polymerase chain reaction using a new DNA reference material format. *Anal Chem* 2017;89(21):11232-11251. <https://doi.org/10.1021/acs.analchem.6b05032>
- 2 Whale AS, Jones GM, Pavšič J, Dreo T, Redshaw N, Akyürek S, Akgöz M, Divieto C, Sassi MP, He HJ, Cole KD, Bae YK, Park SR, Deprez L, Corbisier P, Garrigou S, Taly V, Larios R, Cowen S, O'Sullivan DM, Bushell CA, Goenaga-Infante H, Foy CA, Woolford AJ, Parkes H, Huggett JF, Devonshire AS. Assessment of Digital PCR as a Primary Reference Measurement Procedure to Support Advances in Precision Medicine. *Clin Chem* 2018;64(9):1296-1307. <https://doi.org/10.1373/clinchem.2017.285478>
- 3 JCGM 200:2012 International vocabulary of metrology –Basic and general concepts and associated terms (VIM). Joint Committee for Guides in Metrology. Sevres, France. 2012, www.bipm.org/en/publications/guides/vim.html
- 4 BIPM, Comité consultatif pour la quantité de matière (CCQM) — 5e session (février 1999) <https://www.bipm.org/utills/en/pdf/CCQM5-EN.pdf>
- 5 De Bièvre P, Dybkaer R, Fajgelj A, Hibbert DB. Metrological traceability of measurement results in chemistry: Concepts and implementation. *Pure Appl Chem* 2011;83(10):1873-1935. <https://doi.org/10.1351/PAC-REP-07-09-39>
- 6 Duewer DL, Kline MC, Romsos EL. Real-time cdPCR opens a window into events occurring in the first few PCR amplification cycles. *Anal Bioanal Chem* 2015;407(30):9061-9069. <https://doi.org/10.1007/s00216-015-9073-8>
Electronic Supplementary Material:
https://static-content.springer.com/esm/art%3A10.1007%2Fs00216-018-0982-1/MediaObjects/216_2018_982_MOESM1_ESM.pdf
- 7 Kline MC, Romsos EL, Duewer DL. Evaluating Digital PCR for the Quantification of Human Genomic DNA: Accessible Amplifiable Targets. *Anal Chem* 2016;88(4):2132-2139. <https://doi.org/10.1021/acs.analchem.5b03692>
- 8 Kline MC, Duewer DL. Evaluating Droplet Digital Polymerase Chain Reaction for the Quantification of Human Genomic DNA: Lifting the Traceability Fog. *Anal Chem* 2017;89(8):4648-4654. <https://doi.org/10.1021/acs.analchem.7b00240>
- 9 Duewer DL, Kline MC, Romsos EL, Toman B. Evaluating droplet digital PCR for the quantification of human genomic DNA: converting copies per nanoliter to nanograms nuclear DNA per microliter. *Anal Bioanal Chem* 2018;410(12): 2879-2887. <https://doi.org/10.1007/s00216-018-0982-1>

- 10 NIST Special Publication 260-189. Certification of Standard Reference Material® 2372a Human DNA Quantitation Standard. 2018. <https://doi.org/10.6028/NIST.SP.260-189>
- 11 SRM 2372a Human DNA Quantitation Standard Certificate of Analysis, March 13, 2018. https://www-s.nist.gov/srmors/view_cert.cfm?srm=2372a
- 12 Wilson PJ, Ellison SLR. Extending digital PCR analysis by modelling quantification cycle data. *BMC Bioinfo* 2016;17:421. <https://doi.org/10.1186/s12859-016-1275-3>
- 13 Wang X, Son A. Effects of pretreatment on the denaturation and fragmentation of genomic DNA for DNA hybridization. *Environ Sci: Processes Impacts* 2013;15:2204-2212. <https://doi.org/10.1039/c3em00457k>
- 14 Volkov SN, Danilov VI. Study of 1st And 2nd Absorption-Band Hypochromism in Natural DNA. *FEBS Letters* 1976;65(1):8-10. [https://doi.org/10.1016/0014-5793\(76\)80609-6](https://doi.org/10.1016/0014-5793(76)80609-6)
- 15 Tinoco I. Hypochromism in Polynucleotides. *J Am Chem Soc* 1960;82(18):4785-4790. <https://doi.org/10.1021/ja01503a007>
- 16 Farkas DH, Kaul KL, Wiedbrauk DL, Kiechle FL. Specimen collection and storage for diagnostic molecular pathology investigation. *Arch Pathol Lab Med* 1996;120(6):591-6.
- 17 Nwokeoji AO, Kilby PM, Portwood DE, Dickman MJ. Accurate Quantification of Nucleic Acids Using Hypochromicity Measurements in Conjunction with UV Spectrophotometry. *Anal Chem* 2017;89(24):13567-13574. <https://10.1021/acs.analchem.7b04000>
- 18 Kypr J, Kejnovská I, Renčičuk D, Vorličková M. Circular dichroism and conformational polymorphism of DNA. *Nucleic Acids Res* 2009;37(6):1713-1725. <https://doi.org/10.1093/nar/gkp026>
- 19 Johnson PH, Grossman LI. Electrophoresis of DNA in Agarose Gels. Optimizing Separations of Conformational Isomers of Double- and Single-Stranded DNAs. *Biochem* 1977;16(19):4217-4225. <https://doi.org/10.1021/bi00638a014>
- 20 Miller SA, Dykes DD, Polesky HF. A simple salting out procedure for extracting DNA from human nucleated cells. *Nucleic Acids Res* 1988;16(3):1215. <https://doi.org/10.1093/nar/16.3.1215>
- 21 Kline MC, Duewer DL, Travis JC, Smith MV, Redman JW, Vallone PM, Decker AE, Butler JM. Production and Certification of Standard Reference material 2372 Human DNA Quantitation Standard. *Anal Bioanal Chem* 2009;394(4):1183-1192. <https://doi.org/10.1007/s00216-009-2782-0>
- 22 Sambrook, J. and Russell D.W. (2001) *Molecular Cloning a Laboratory Manual*, Cold Spring Harbor Laboratory Press. Cold Spring Harbor, New York.
- 23 ISO 21571:2005(E), *Foodstuffs – Methods of analysis for the detection of genetically modified organisms and derived products – Nucleic acid extraction*. Annex B Methods for quantitation of extracted DNA, pp. 34-36
- 24 Dagata JA, Farkas N, Kramer JA. Method for measuring the volume of nominally 100 µm diameter spherical water in oil emulsion droplets. NIST Special Publication 260-184. 2016. <https://doi.org/10.6028/NIST.SP.260-184>

- 25 Thrower KJ, Peacocke AR. Kinetic and spectrophotometric studies on the renaturation of deoxyribonucleic acid. *Biochem J.* 1968;109(4):543-57.
http://www.cellbiol.ru/files/pdfdb/c0t/history/Thrower_1968.pdf
- 26 Niranjani G, Murugan R. Theory on the Mechanism of DNA Renaturation: Stochastic Nucleation and Zipping. *PLoS ONE* 2016;11(4):e0153172.
<https://doi.org/10.1371/journal.pone.0153172>
- 27 Fuchs, R.; Blakesley, R. Guide to the Use of Type II Restriction Endonucleases. *Methods Enzymol* 1983;100:3-38. [https://doi.org/10.1016/0076-6879\(83\)00043-9](https://doi.org/10.1016/0076-6879(83)00043-9)
- 28 Nishigaki K, Kaneko Y, Wakuda H, Husimi Y, Tanaka T. Type II restriction endonucleases cleave single-stranded DNAs in general. *Nucleic Acids Res.* 1985;13(16):5747-60. <https://doi.org/10.1093/nar/13.16.5747>
- 29 Pang-Chu S, Yu-Keung M. XcmI as a universal restriction enzyme for single-stranded DNA. *Gene* 1993;133(1):85-89. [https://doi.org/10.1016/0378-1119\(93\)90228-U](https://doi.org/10.1016/0378-1119(93)90228-U)
- 30 Langhans MT, Palladino MJ. Cleavage of mispaired heteroduplex DNA substrates by numerous restriction enzymes. *Curr Issues Mol Biol* 2009;11:1-12.
<https://doi.org/10.21775/cimb.011.001>
- 31 BLAST. National Center for Biotechnology Information, U.S. National Library of Medicine, National Institutes of Health, U.S. Department of Health and Human Services.
https://blast.ncbi.nlm.nih.gov/Blast.cgi?PAGE_TYPE=BlastSearch
- 32 CutSmart Buffer, B7204S. New England Biolabs, Inc.
<https://www.neb.com/products/b7204-cutsmart-buffer>
- 33 The NIST Consensus Builder. Software freely available at: <https://consensus.nist.gov/>